Contents

Matrix Models and Population Dynamics

J. M. Cushing

IAS/Park City Mathematics Series
Volume XV, 2005

Matrix Models and Population Dynamics

J. M. Cushing

Introduction

These lectures are intended to serve as an introduction to the application of nonlinear matrix models in the study of population dynamics. Matrix models define discrete time (semi) dynamical systems that can be used to project population state variables from time t to $t+1$. They have a long tradition of use in describing the dynamics of so-called structured populations. By a structured population is meant one in which individual members are assigned to classification categories and thereby are not considered identical (as they are in many classical models in population dynamics and theoretical ecology). These categories are most often based on physiological characteristics regarded as important to vital processes driving the dynamics of the population. In their seminal papers, Lewis [**49**] and Leslie [**47, 48**] classified individuals by means of (discrete) chronological age classes, but their methodology is straightforwardly applicable to other kinds of classifications such as body size, gender, life cycle stage, location in a spatial habitat, and so on [**46**]. Individual characteristics can correlate closely with vital rates that effect and determine the dynamics of the population as a whole, including rates of reproduction, mortality, immigration/emigration and dispersal, resource utilization and consumption, and so on.

In these lectures I am interested in discrete time models that describe the dynamics of (a finite number of) discrete classes based on a specified categorization of individuals making up a population. Such matrix models, like all models, have their advantages and disadvantages. They are appropriate under some circumstances and not under others (for example when continuous time and/or continuous structuring variables are more appropriate). Caswell gives a nice discussion of these modeling issues in his book [**1**]. The books [**55**] and [**4**] contain treatments of continuous models for structured populations.

Lecture 1 develops a general framework for the derivation of matrix models that describe the dynamics of a population structured by a finite number of distinct classes. A fundamental question is the extinction or the persistence of the population. In Lecture 1 this question is related to two fundamental quantities, the inherent growth rate r and the inherent net reproductive number n. This is done by means of general theorems implying the loss of stability of the extinction

Department of Mathematics & Interdisciplinary Program in Applied Mathematics, University of Arizona, Tucson, AZ 85721
E-mail address: cushing@math.arizona.edu
The author was supported in part by NSF grant DMS-0414212 .

equilibrium at $r = 1$ (equivalently $n = 1$) and population persistence for $r > 1$ (equivalently $n > 1$).

The bifurcation of viable equilibrium states that occurs at $n = r = 1$ is a main theme of Lecture 2. This primary bifurcation can lead to stable or unstable equilibrium states for the population, depending on the relative roles of negative and positive feedbacks from increased (but low level) population density. (Negative feedback is called density regulation and positive feedback is referred to as an Allee effect.) Stable bifurcating equilibria can undergo further bifurcations, including those that give rise to periodic cycles or quasi-periodic motion on invariant loops. Bifurcation cascades to chaos are a well known property of recursive formulas such as those defined by matrix equations. The most famous is the period doubling route to chaos that commonly occurs for the one dimensional case of unstructured population models. For structured models many other bifurcation sequences are also possible, such as the sequences that arise in the case studies presented in Lecture 3.

The major themes in Lecture 3 include the connection of matrix models to time series data, the evaluation of models (which necessitates stochastic versions of the deterministic matrix models in Lectures 2 and 3), the use of models to study nonlinear phenomena (such as bifurcation routes to chaos) by means of controlled experiments, and a discussion of some issues that arose from these studies (e.g., the importance of habitat size and the effects of discrete state space variables).

Lecture 4 extends the basic theory concerning time autonomous models presented in Lectures 1 and 2 to models with periodically forced model parameters. Experimental observations of a nonlinear resonance phenomenon motivate this extended theory.

Lecture 5 returns to autonomous models, but considers interacting (structured) species. Motivated by the use of discrete models in the early history of competition theory, this lecture focuses on the (interference) competition between two species.

I would like to thank Robert F. Costantino, Brian Dennis, Robert A. Desharnais, Shandelle M. Henson, and Aaron King. My collaborations with this interdisciplinary group of biologists, statisticians, and mathematicians (some of which is reported in these lectures) has been a wonderful adventure into the marvelous world of nonlinear population dynamics.

LECTURE 1

Matrix Models

One of the most important first steps in deriving a mathematical model of a physical or biological system is the choice of the state variables that will be used to describe the system. In the classical logistic differential equation

$$x' = r\left(1 - \frac{x}{K}\right)x, \tag{1.1}$$

as well as many other classic models in population dynamics and theoretical ecology, the state variable is the total population size $x = x(t)$ (e.g., the number, density, or biomass of all individuals), which is assumed to vary with time t according to this equation. Dynamic equations for the time evolution of the state variable(s) derive from specified assumptions, hypotheses, and laws. The resulting models are characterized as much by phenomena they ignore as they are by phenomena they include. In the logistic equation, for example, since the state variable is total population size, all individuals in the population are in effect treated as identical to each other. Thus, the population is assumed homogeneous in its composition, as if the individual organisms were identical billiard balls or molecules. And yet biologists will often point out that there is often more variability among individuals within a biological population or species than there is among populations or species. Even for micro-organisms, for which this homogeneous population structure assumption might be considered appropriate, a close examination usually reveals significant differences among individuals (size, shape, weight, age, gender, etc.). Indeed, the currency of Darwinian evolution is the reproducing individual, among all of whom there are heritable variations on which natural selection can work.

There are other significant homogeneity assumptions in models such as the logistic differential equation (1.1) and many other similar classical differential equation models (e.g., the Lotka-Volterra competition and predator-prey models). The model parameter K is the equilibrium to which all solutions tend asymptotically. If we view this "carrying capacity" as a descriptor of the population's environment, then the assumption that K is a constant means that we ignore all environmental fluctuations. Similarly, the inherent growth rate r (at which the population would exponentially grow if unrestrained by negative effects of large population sizes) is assumed unchanging in time. Certainly some populations live in relatively constant environments, but a great many do not. For many there are variations in innumerable physical and biological environmental factors (temperature, humidity, food resources, etc.), some of which are irregular (random or stochastic) and some of which are approximately periodic (e.g., seasonal or daily or monthly cycles). Autonomous differential equations are convenient for mathematicians (since there are many tools available to analyze them), but they do entail these simplifying homogeneity assumptions which in many cases are biologically unwarranted.

One of the goals of these lectures is to provide an introduction to a theory for the dynamics of structured populations in which individuals are not assumed identical. The modeling methodology uses classes of individuals as state variables (based, for example, on age, body size, life cycle stage, etc.). This is a compromise between, at one extreme, treating all individuals as identical and, at the other extreme, treating each individual as a state variable. I will develop some basic dynamic properties and features of these models in a mathematically general context from the point of view of bifurcation theory.

Another goal of the lectures is to apply the modeling methodology and analysis in some specific biological and ecological contexts. Cases studies involving applications to some controlled and replicated laboratory experiments not only illustrate the effectiveness of matrix models, but provide an investigation into the occurrence of a variety of model predicted nonlinear phenomena in a real biological population. I will address several issues in these case studies. One issue concerns the connection of theoretical models to data for the purpose of calibrating (parameterizing) the model and evaluating its descriptive accuracy. Another aim is to provide examples in which theoretical models are quantitatively predictive of the dynamics of a real biological population. That is to say, the parameterized model is used to create protocols for experiments designed to test (observe) and study model predicted dynamics. This combined modeling and experimental system provides a powerful tool for the study of nonlinear population dynamics. One can use it to corroborate the theoretical predictions of nonlinear theory as they can occur in a real population (e.g., equilibrium destabilization, bifurcation to non-equilibrium dynamics, chaos, etc.). Moreover, the modeling/experimental system often provides explanations for observations that previously had none and in several instances predicts new and sometimes unexpected phenomena that are subsequently corroborated by experiments. It can also provide a means to investigate the extent to which tenets and principles based on classical ecological models can be validated (or contradicted) in a controlled experimental setting.

This and the next lecture develop an autonomous theory for a single population (appropriate for the case of a constant environment and constant vital rates). Lectures 3 and 4 will extend the theory to include both stochastic and regular periodic fluctuations in both environmental and individual characteristics. Lecture 5 contains a brief look at competition between two structured populations.

Broadly speaking, population dynamic models fall into two classes: those in which time t is continuous and those in which time is discrete. Time is continuous in the logistic differential equation (1.1) and the model is based, as is typical in this case, on the consideration of the rate of change of the state variable x. For discrete time models the approach is typically to build a model by prescribing instead the state variable from one time step to the next. The point of view is that given a sequence of population counts

$$x(0),\ x(1),\ x(2),\ \cdots$$

we want a rule that predicts the next census count $x(t+1)$ from the current census count $x(t)$. Here $x(t)$ can be a vector of state variables observable at the census times $t = 0, 1, 2, \cdots$.

For example, if the solution

$$x(t) = Kx(0)\frac{e^{rt}}{K - x(0) + x(0)e^{rt}}$$

of the logistic differential equation (1.1) is sampled at times $t = 0, 1, 2, \cdots$, the resulting sequence of population sizes satisfies the *discrete logistic* difference (or recursive) equation [**47, 48, 59, 60**]

$$x(t+1) = b\frac{1}{1+cx(t)}x(t) \tag{1.2}$$

where $b \triangleq e^r$ and $c \triangleq (b-1)/K$. We can use this difference equation to predict the population size from one census to the next.

Derivations of discrete time models are not best made from continuous time models. The reason is that approximation errors are likely to be introduced in such derivations and the resulting discrete time models can have dynamic properties that are attributable to these errors and not to any biological mechanisms. This is not the case for the discrete logistic (1.2), whose census counts exactly match those obtained from the solution of the differential equation. However, rarely is a solution formula for a differential equation model available. If instead we use an approximating discretization procedure to obtain the prediction $x(t+1)$ from $x(t)$, then the resulting difference equation is no longer exact. For example, the Euler method applied to the logistic differential equation (1.1) yields the approximation scheme $x(t+1) = x(t) + b(1 - x(t)/K)x(t)$ or $x(t+1) = (1 + b - bx(t)/K)\,x(t)$. This quadratic difference equation (often also called the discrete logistic equation) makes dynamic predictions, such as periodic cycles and chaos, that differ drastically from those of the differential equation.

Discrete time models are best derived from first principles as discrete time models. As a warm up example related to models I will use below, consider a population that reproduces at discrete times (which we census just before reproduction). Suppose there are $x(t)$ adult individuals at census time t who then produce $bx(t)$ newborns, where b is the per capita birth rate. If all these newborns survive one unit of time, then they contribute $bx(t)$ individuals to the adult census count at time $t+1$. However, suppose the survival of a newborn depends on the number of adults $x(t)$ present. Suppose that a contact between a newborn and an adult increases the probability that the newborn will die. (One example, relevant to the case studies in Lecture 2, is cannibalism.) Specifically, suppose the probability that a newborn encounters one specific adult, and as a result dies (with a certain probability), is approximately proportional to the length of time that passes. If we divide the time unit t to $t+1$ into $1/\Delta t$ steps and consider encounters during each sub-step as independent probabilities, then the probability that a newborn survives exposure to one adult is approximately $(1 - c\Delta t)^{1/\Delta t}$ where $c > 0$ is the constant of proportionality. If encounters with adults are independent events, then the probability that the newborn will survive in the presence of $x(t)$ adults is approximately $(1 - c\Delta t)^{x(t)/\Delta t}$. Letting $\Delta t \to 0$, we find the probability that a newborn will survive and join the adult population one time unit later is equal to $\exp(-cx(t))$. Thus, the contribution of the newborns to the next adult census is $bx(t)\exp(-cx(t))$. This contribution is added to the surviving adults. The resulting difference equation is

$$x(t+1) = bx(t)e^{-cx(t)} + (1-\mu)x(t)$$

where μ is the adult death rate ($0 \le \mu \le 1$). If $\mu < 1$ the population is *iteroparous* (adults reproduce more than once). If $\mu = 1$ it is *semelparous* (adults reproduce

only once) and the equation reduces to the *Ricker equation* [**62**]

$$x(t+1) = be^{-cx(t)}x(t). \tag{1.3}$$

Over the entire range of the parameter values $b > 0$ and $c > 0$, the Ricker equation makes quite different predictions from those of the discrete logistic (1.2). Both predict population extinction ($x(0) > 0 \Longrightarrow \lim_{t\to+\infty} x(t) = 0$) if $b < 1$ and the existence of a unique positive equilibrium (fixed point) if $b > 1$, namely, $x = c^{-1}(b-1)$ for the discrete logistic and $x = c^{-1}\ln b$ for the Ricker equation. The discrete logistic predicts that when $b > 1$ all populations $x(0) > 0$ tend to the equilibrium as $t \to +\infty$. (We can see this from the way in which the equation was derived from the logistic equation, or we can prove it directly without reference to this derivation.) This is (not necessarily) true for the Ricker equation (1.3). When b is sufficiently large, populations can tend asymptotically to non-equilibrium states, such as periodic cycles or chaotic attractors. This story (which is not easy to analyze rigorously from a mathematical point of view) is summarized in Figure 1 which shows the attractor plotted against the parameter b. This bifurcation diagram, which is perhaps familiar to the reader, has become a virtual icon of chaos theory and illustrates the extraordinary complexity that discrete models of populations dynamics can exhibit. This complexity was first noted by Lord May in several influential papers in the 1970's that served to popularize chaos theory; e.g., see [**28, 52, 53**] (also see [**51**]).

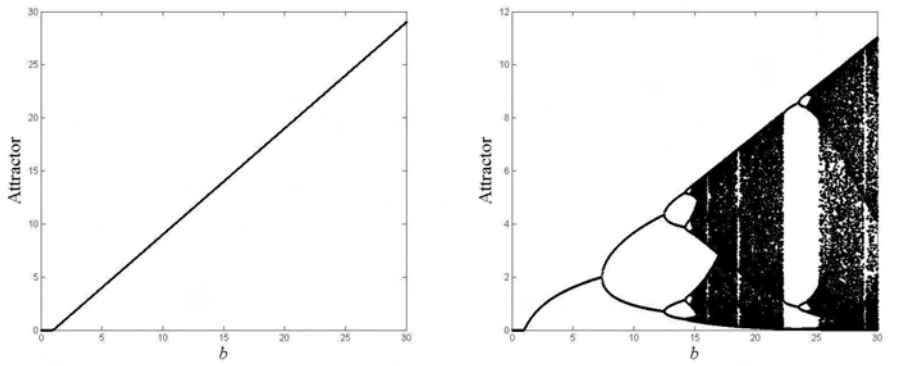

FIGURE 1. (a) The final state (attractor) of all solutions $x(0) > 0$ of the discrete logistic equation (1.2) with $c = 1$ is the equilibrium $x = 0$ for $b < 1$ and the unique positive equilibrium $x = c^{-1}(b-1)$ for $b > 1$. (b) The attractor of solutions $x(0) > 0$ of the Ricker equation (1.3) with $c = 1$ is shown plotted against $b > 0$. For $b < 0$ the attractor is the equilibrium $x = 0$ and for $b > 1$ but less than (approximately) 7.4 the attractor is the unique positive equilibrium $x = c^{-1}\ln(b-1)$. For larger values of b the attractor consists of more than one point. For example, for b between (approximately) 7.4 and 12.5 the attractor consists of the two points of a periodic 2-cycle. For some values of b the attractor apparently consists of a large number of points. The plot was constructed by iterating the Ricker equation 1000 times from the initial condition $x(0) = 1$ and plotting the last 100 points.

The state variable in the discrete time logistic and Ricker difference equations is a single class of homogeneous individuals. To motivate discrete time models that structure the population into more than one class, I consider the classic example of such models in which the structuring classes are based on chronological age. The *Leslie model* age structured model classifies individuals into m age classes x_i of equal length l and tracks the changes in these classes at discrete time intervals of duration l which we take, for notational simplicity, to be $l = 1$. Then $x_{i+1}(t+1) = \tau_{i+1,i}x_i(t)$ where $\tau_{i+1,i}$ is the fraction of individuals of age i that survive one unit of time (and hence move from class i to class $i+1$). The survivors at time $t+1$ are the components of the vector $Tx(t)$ where $x(t) = \text{col}(x_i(t))$ is an m-dimensional column vector (and hence lies in m-dimensional Euclidean space $R^m \triangleq R \times \cdots \times R$) and where

$$T = \begin{pmatrix} 0 & 0 & \cdots & 0 & 0 \\ \tau_{21} & 0 & \cdots & 0 & 0 \\ 0 & \tau_{32} & \cdots & 0 & 0 \\ \vdots & \vdots & & \vdots & \vdots \\ 0 & 0 & \cdots & \tau_{m,m-1} & 0 \end{pmatrix}$$

is the matrix of age class survivorships (or class survival probabilities). This assumes no individual lives more than m time units. Sometimes this assumption is not made and the final class x_m consists of all individuals of age greater than or equal to m, in which case a survival fraction τ_{mm} appears in the lower right hand corner of T. This model also assumes no individuals migrate in or out of the population.

Since by definition newborn individuals are in the first age class x_1, the total number of newborns at time $t+1$ is $x_1(t+1) = \sum_{i=1}^{m} f_{1i}x_i(t)$ where f_{1i} is the number of newborns (i.e., class $i = 1$ individuals), contributed by individuals of age i, who survive to $t+1$. For a non-reproductive age class j, we have $f_{1j} = 0$. The matrix equation

$$\begin{pmatrix} x_1(t+1) \\ x_2(t+1) \\ \vdots \\ x_m(t+1) \end{pmatrix} = \begin{pmatrix} f_{11} & f_{12} & \cdots & f_{1,m-1} & f_{1m} \\ 0 & 0 & \cdots & 0 & 0 \\ 0 & 0 & \cdots & 0 & 0 \\ \vdots & \vdots & & \vdots & \vdots \\ 0 & 0 & \cdots & 0 & 0 \end{pmatrix} \begin{pmatrix} x_1(t) \\ x_2(t) \\ \vdots \\ x_m(t) \end{pmatrix}$$
$$+ \begin{pmatrix} 0 & 0 & \cdots & 0 & 0 \\ \tau_{21} & 0 & \cdots & 0 & 0 \\ 0 & \tau_{32} & \cdots & 0 & 0 \\ \vdots & \vdots & & \vdots & \vdots \\ 0 & 0 & \cdots & \tau_{m,m-1} & 0 \end{pmatrix} \begin{pmatrix} x_1(t) \\ x_2(t) \\ \vdots \\ x_m(t) \end{pmatrix}$$

summarizes the bookkeeping of the census counts in the age categories from one census time to the next. The matrix

$$F = \begin{pmatrix} f_{11} & f_{12} & \cdots & f_{1,m-1} & f_{1m} \\ 0 & 0 & \cdots & 0 & 0 \\ 0 & 0 & \cdots & 0 & 0 \\ \vdots & \vdots & & \vdots & \vdots \\ 0 & 0 & \cdots & 0 & 0 \end{pmatrix}.$$

contains the per capita fertilities of each age class in the first row. The remaining rows of zeros indicate that all newborns belong to the first age class. The *projection matrix* $P = F + T$ in this example is called a *Leslie matrix*.

Other classification schemes for the individuals in a population result in transition and fertility matrices T and F of different forms. (See [**1**] for a detailed treatment of matrix models in population dynamics.) In general, we obtain a recursive matrix (or difference) equation of the form

$$x(t+1) = (F+T)\,x(t). \tag{1.4}$$

The entry τ_{ij} in the *transition matrix* $T = (\tau_{ij})$ is the fraction of j class individuals that survive and become i class individuals in one unit of time. The entry f_{ij} in the *fertility matrix* $F = (f_{ij})$ is the (surviving) number of i class offspring born to a j class individual in one unit of time. Thus,

$$f_{ij} \geq 0, \quad 0 \leq \tau_{ij} \leq 1, \quad \sum_{i=1}^{m} \tau_{ij} \leq 1. \tag{1.5}$$

The reason for the last inequality on the column sums of the transition matrix T is that the number of individuals from class i that get distributed to all classes (including the class i itself) by time $t+1$ cannot exceed the number available in class i at time t. Notice that if newborns cannot arise in class i, then the entire i^{th} row of F consists of zeros. For example if, as in the Leslie age class model, newborns arrive in only one class (usually taken to be the class $i = 1$), then all rows except the first consists entirely of 0's.

A matrix is called *positive (non-negative)* if all its entries are positive (non-negative). In applications to population dynamics positive (non-negative) class distribution vectors $x > 0$ (and $x \geq 0$) are of interest. We call the set of positive (m-dimensional) column vectors $x > 0$ the *positive cone* in R^m and denote this set by R^m_+. The set of non-negative vectors $x \geq 0$ is the non-negative cone $\bar{R}^m_+$.

The entries in the fertility and transition matrices, and hence the projection matrix $P = F + T$, is non-negative. This implies the solution $x(t)$ of (1.4) starting from a non-negative initial condition $x(0) \geq 0$ remains non-negative for all $t = 1, 2, 3 \cdots$. The non-negative cone $\bar{R}^m_+$ is said to be *forward invariant* with respect to the matrix equation (1.4).

A matrix is *reducible* if we can, by reordering the classes, put it in block triangular form

$$\begin{pmatrix} A & 0 \\ C & D \end{pmatrix}$$

where A and D are square matrices. It is *irreducible* if it is not reducible. The projection matrix P is irreducible means that individuals from the i-class contribute to the j-class in a finite number of steps (by transition or by births), for every i and j. (It also means that the directed graph associated with P is strongly connected.) As an example, a Leslie matrix is irreducible if all $\tau_i > 0$ and $f_m > 0$ (the oldest class is fertile).

The eigenvalue of P with the largest absolute value is the *dominant eigenvalue*. The absolute value of the dominant eigenvalue is the *spectral radius* of P, which we denote by r or sometimes by $\rho(P)$.

By iterating the matrix equation (1.4), we obtain the formula $x(t) = P^t x(0)$ for the solution of (1.4) with initial condition $x(0)$.

Theorem 1.1. *([**37**], Theorem 5.612) Consider the matrix equation (1.4) under the assumptions (1.5). If $r = \rho(P) < 1$, then all solutions satisfy $\lim_{t\to+\infty} x(t) = 0$.*

The famous Perron-Frobenius Theorem implies that if the non-negative matrix P is irreducible, then r is an algebraically simple eigenvalue of P. Moreover, r has a positive eigenvector $v > 0$ and no other eigenvector associated with any other eigenvalue is non-negative. An irreducible matrix P is said to be *primitive* if $r = \rho(P)$ is *strictly* dominant (the magnitude of all other eigenvalues are *strictly* less than r). It turns out that P is primitive (hence irreducible by definition) if and only if some integer power of P is positive, i.e., there exists a positive integer k such that $P^k > 0$ ([**26**], p. 80).

Theorem 1.2. *Consider the matrix equation (1.4) under the assumptions (1.5). Assume P is primitive. If $r = \rho(P) > 1$, then all solutions with initial conditions $x(0) \geq 0$, $x(0) \neq 0$ satisfy $\lim_{t\to+\infty} |x(t)| = \infty$.*

The case $r = \rho(P) = 1$ is not covered by Theorems 1.1 and 1.2. In this case, solutions with an initial condition $x(0)$ that is a multiple of an eigenvector of P remain constant: $x(t) = v$ for all $t = 0, 1, 2, \cdots$. Thus, at this (and only at this) one value of $r = \rho(P) = 1$ the population dynamics do not necessarily imply extinction or unlimited growth.

Suppose we view the dynamics of the linear model (1.4) as a function of the spectral radius $r = \rho(P)$. Theorems 1.1 and 1.2 imply that a *bifurcation* occurs at $r = 1$ in the sense that there is a drastic change in the asymptotic dynamics for $r < 1$ and $r > 1$, a change from extinction to unbounded growth. At the *bifurcation point* $r = 1$ there is a branch of equilibria (all scalar multiplies of v) that intersects the equilibrium $x = 0$; that is to say, two equilibrium branches intersect at $r = 1$. Therefore, with regard to the existence of nontrivial equilibria, the linear model (1.4) has a "point spectrum". Feasible asymptotic population dynamics – that is, non-extinction states that are not unbounded – occur only at an isolated value of the bifurcation parameter.

The lowest dimensional case, when the number of classes $m = 1$, is a one dimensional map $x(t+1) = (f+\tau)x(t)$ for which $r = f + \tau$. The conditions $r < 1$, $r = 1$, and $r > 1$ are equivalent to $n < 1$, $n = 1$, $n > 1$ where

$$n \triangleq \frac{f}{1-\tau}.$$

This number, which we can rewrite as

$$n = f + \tau f + \tau^2 f + \cdots + \tau^t f + \cdots,$$

has an important biological interpretation. If a newborn survives for t time steps, then f offspring result. Since the probability of surviving t time steps is τ^t, the expected number of offspring from the newborn at time t is $\tau^t f$. As a result, n is the expected number of offspring (for each newborn) over the course of its entire lifetime. The number n is called the *net reproductive number* (often denoted R_0).

In the $m > 1$ dimensional case we can define the net reproductive number n as follows. Assume that $I - T$ is invertible (i.e., 1 is not an eigenvalue of the transition matrix T). The net reproductive number n is the spectral radius of $F(I-T)^{-1}$, i.e., $n = \rho\left(F(I-T)^{-1}\right)$.

A theorem relating the spectral radius r to n appears in [**50**]. A slightly different version of this result appears in [**15**].

Theorem 1.3. *([**50**], Theorem 3.3) Suppose the projection matrix $P = F + T$, where F and T satisfy (1.5), is primitive. Let $r = \rho(P)$ and $n = \rho\left(F\left(I-T\right)^{-1}\right)$. If $T \neq 0$ and $\rho(T) < 1$, then one and only one of the following holds:*

$$r = n = 1 \qquad or \qquad 1 < r < n \qquad or \qquad 0 < n < r < 1$$

The assumption that $\rho(T) < 1$ means that no individual has an infinite life expectancy. This follows from the fact that iterations of the transition component of the model $T^t x(0)$ tend to 0 if and only if $\rho(T) < 1$ ([**37**], Theorem 5.16). The condition on T appearing in (1.5) implies $\rho(T) \leq 1$, but not necessarily that $\rho(T) < 1$. ($T = I$ is an example.)

It follows from Theorem 1.3 that we can use either quantity r or n to determine the asymptotic fate of a population modeled by (1.4). However, whereas formulas for r (in terms of the matrix entries) are not available except for models of low dimension (m small), formulas for n often are available for models of arbitrary dimension [**4**].

For example, for a Leslie matrix we have

$$n = \sum_{i=1}^{m} f_{1i} \prod_{j=1}^{i} \tau_{j,j-1} \tag{1.6}$$

where, for notational convenience, $\tau_{10} = 1$. The biological interpretation of this formula for n when P is a Leslie matrix is straightforward: $\prod_{j=1}^{i} \tau_{j,j-1}$ is the probability of surviving to age i, $f_{1i} \prod_{j=1}^{i} \tau_{j,j-1}$ is the number of offspring produced when at age i, given survival to age i. Therefore, n is the sum total of all offspring produced during all ages, i.e., is the expected number of offspring per newborn per lifetime.

The general biological interpretation of n is more complicated. The i, j entry in $\left(I-T\right)^{-1}$ is the expected amount of time a j class newborn will spend in the i class during its lifetime. The i, j entry in $F\left(I-T\right)^{-1}$ is the expected number of i class newborns that will be produced by a j class newborn during its lifetime. If (without loss in generality) the classes into which offspring can be born are listed first, then the last $m-k$ rows of the fertility matrix F will consist 0's and, as a result, so will the last $m-k$ rows of $F\left(I-T\right)^{-1}$. The $k \times k$ matrix Q in

$$F\left(I-T\right)^{-1} = \begin{pmatrix} Q & S \\ 0 & 0 \end{pmatrix}$$

is nontrivial, non-negative and irreducible ([**50**], Proposition 4.1) and $n = \rho\left(Q\right)$ is its dominant eigenvalue. If we denote the first k entries in x by z, a well known formula for the dominant eigenvalue of a non-negative irreducible matrix is

$$n = \max_{z \geq 0} \min_{1 \leq i \leq m, z_i \neq 0} \frac{\left(Qz\right)_i}{z_i}$$

where z_i is the i^{th} component of z and $\left(Qz\right)_i$ is the i^{th} component of Qz ([**26**], p. 65). Consider an initial cohort z of newborns. The quantity $\left(Qz\right)_i / z_i$ is the expected number of i class offspring produced by the cohort per member of the i class in the cohort. According to the formula above, the net reproductive number n is found by selecting the smallest of these expected numbers, from among all classes represented in the cohort z ($z_i \neq 0$), and then maximizing this minimum over all possible initial cohorts z of newborns. If there is only one newborn class ($k = 1$),

then the biological interpretation of n is the same as that the Leslie matrix case given above.

Having a formula for the net reproductive number n, in terms of parameters appearing in F and T, means we can study how n depends on any of these model parameters. While Theorem 1.3 provides some comparisons between n and r, it does not provide a functional relationship between r and n. Thus, for example, it is not clear whether an increase in a selected parameter in one of the model matrices F and/or T which results in an increase in n (presumably interpreted as favorable for the population) will result in an increase or decrease in r. Such questions arise in the "sensitivity analysis" of models [**1**].

A linear matrix model (1.4) implies extinction or unbounded growth, except when $n = 1$. Long term sustainable population growth is only possible at the point spectrum $n = 1$. This situation represents a "vertical" bifurcation, by which is meant that a branch of nontrivial equilibria intersects the branch of trivial (extinction) equilibria $x = 0$ at and only at $n = 1$. (By Theorem 1.3 we could also use r.)

Many parameters appear in the projection matrix P (f_{ij} and τ_{ij}) but the asymptotic dynamics of the matrix model (1.4) depends on only one composite parameter, namely, n or equivalently r. These important quantities do not explicitly appear in the matrix model. However, since formulas relating n to model parameters are often available, one can often introduce n explicitly into the model. For example, we can in principle scale the entries in the fertility matrix by n so that $F = n\Phi$ where the dominant eigenvalue of $\Phi\left(I - T\right)^{-1}$ equals 1. Then (1.4) becomes

$$x(t+1) = \left(n\Phi + T\right)x(t).$$

To have long term sustainable population growth, for other than the isolated value $n = 1$, the matrices Φ and T cannot remain constant in time. One important way in which the projection matrix can change in time is through a dependence on $x = x(t)$. In this case, the model is called *density dependent*. As will be seen below, in general such nonlinear models have a branch of nontrivial equilibria that bifurcates from the extinction equilibrium, just as linear models do. However, unlike the case for linear models, the spectrum of n for which unbounded but sustainable growth will, in general, no longer be an isolated point, but instead be an interval. The vertical branch of nontrivial equilibria of a linear model gets "bent" into a nonvertical curve for a density dependent (nonlinear) model, producing a continuous spectrum.

Consider a nonlinear (density dependent) matrix model

$$x(t+1) = \left(F(x(t)) + T(x(t))\right)x(t) \tag{1.7}$$

where now the entries in the fertility and transition matrices $F(x)$ and $T(x)$ are (continuously differentiable) functions of x on some open domain $D \subset R^m$ that contains the non-negative cone $\bar{R}^m_+ \subset D$:

$$f_{ij} \in C^1\left(D, [0, +\infty)\right), \quad \tau_{ij} \in C^1\left(D, [0,1]\right). \tag{1.8}$$

Assume $F(0)$ and $T(0)$ satisfy (1.5), that $F(0)+T(0)$ is primitive, and that $T(0) \neq 0$ satisfies $\rho\left(T(0)\right) < 1$ so that $n > 0$ is defined. Normalize the fertility matrix so that $F(x) = n\Phi(x)$ where $\rho\left(\Phi(0)\left(I - T(0)\right)^{-1}\right) = 1$.

In summary, consider the matrix equation

$$x(t+1) = \left(n\Phi(x(t)) + T(x(t))\right) x(t), \quad x(0) \in \bar{R}_+^m \tag{1.9}$$

under the assumptions

$$\varphi_{ij} \in C^1\left(D, [0, +\infty)\right), \quad \tau_{ij} \in C^1\left(D, [0,1]\right) \tag{1.10}$$

and

$$n\Phi(0) + T(0) \text{ is primitive for } n > 0$$

$$\sum_{i=1}^{m} \tau_{ij}(0) \leq 1, \quad T(0) \neq 0, \quad \rho\left(T(0)\right) < 1 \tag{1.11}$$

$$\rho\left(\Phi(0)\left(I - T(0)\right)^{-1}\right) = 1$$

on the normalized fertility matrix $\Phi = (\varphi_{ij})$ and the transition matrix $T = (\tau_{ij})$. The quantity n is called the *inherent* net reproductive number associated with the nonlinear model (1.9). That is to say, n is the reproductive number when population density is low (mathematically is zero).

Example 1.4. *The $m = 3$ dimensional projection matrix $P(x) = F(x) + T(x)$ with*

$$F(x) = \begin{pmatrix} 0 & 0 & f_{13}\exp\left(-c_{11}x_1 - c_{13}x_3\right) \\ 0 & 0 & 0 \\ 0 & 0 & 0 \end{pmatrix}$$

$$T(x) = \begin{pmatrix} 0 & 0 & 0 \\ \tau_{21} & 0 & 0 \\ 0 & \tau_{32}\exp\left(-c_{33}x_3\right) & \tau_{33} \end{pmatrix}$$

$$f_{13}, c_{ij} > 0, \quad 0 < \tau_{21}, \tau_{32} \leq 1, \quad 0 < \tau_{33} < 1$$

is a nonlinear Leslie matrix that describes a common life cycle that occurs in insect populations. Class $i = 1$ is the (only) newborn class and class $i = 3$ is the only reproducing (adult) class. Class $i = 2$ is an intermediate non-reproductive developmental stage. We can think of class $i = 1$ as a larval stage, after one unit of time in which surviving individuals become pupae. After another unit of time surviving pupae become adults. The component model equations are

$$\begin{aligned} L(t+1) &= bA(t)\exp\left(-\frac{c_{el}}{V}L(t) - \frac{c_{ea}}{V}A(t)\right) \\ P(t+1) &= (1-\mu_l)\,L(t) \\ A(t+1) &= (1-\mu_p)\,P(t)\exp\left(-\frac{c_{pa}}{V}A(t)\right) + (1-\mu_a)\,A(t) \end{aligned}$$

where, in order to conform with the notation used in the literature [**5, 11**]*, some parameters are re-labeled as*

$$\begin{aligned} x &= \mathrm{col}\,(x_1, x_2, x_3) = \mathrm{col}\,(L, P, A) \\ f_{13} &= b, \quad \tau_{21} = 1-\mu_l, \quad \tau_{32} = 1-\mu_p, \quad \tau_{33} = 1-\mu_a \\ c_{11} &= c_{el}/V, \quad c_{13} = c_{ea}/V, \quad c_{33} = c_{pa}/V. \end{aligned}$$

When $x = 0$, the projection matrix $P(0)$ is a Leslie matrix and by (1.6) we find that

$$n = b\frac{(1-\mu_l)\,(1-\mu_p)}{\mu_a}$$

provided $\mu_a > 0$. *This model has the form (1.9) with normalized fertility matrix*

$$\Phi(x) = \begin{pmatrix} 0 & 0 & \frac{\mu_a}{(1-\mu_l)(1-\mu_p)} \exp\left(-\frac{c_{el}}{V}L - \frac{c_{ea}}{V}A\right) \\ 0 & 0 & 0 \\ 0 & 0 & 0 \end{pmatrix}.$$

Calculations show

$$T(0) = \begin{pmatrix} 0 & 0 & 0 \\ 1-\mu_l & 0 & 0 \\ 0 & 1-\mu_p & 1-\mu_a \end{pmatrix}$$

$$n\Phi(0) + T(0) = \begin{pmatrix} 0 & 0 & n\frac{\mu_a}{(1-\mu_l)(1-\mu_p)} \\ 1-\mu_l & 0 & 0 \\ 0 & 1-\mu_p & 1-\mu_a \end{pmatrix}$$

$$\Phi(0)\left(I - T(0)\right)^{-1} = \begin{pmatrix} 1 & (1-\mu_l)^{-1} & (1-\mu_l)^{-1}(1-\mu_p)^{-1} \\ 0 & 0 & 0 \\ 0 & 0 & 0 \end{pmatrix}$$

and $\rho\left(T(0)\right) = 1 - \mu_a < 1$, $\rho\left(\Phi(0)\left(I - T(0)\right)^{-1}\right) = 1$. *Conditions (1.10) and (1.11) are met.*

The nonlinear matrix equation (1.9) has the trivial (extinction) equilibrium $x = 0$ for all values of n. An important question is whether or not the solution of (1.9) tends to $x = \text{col}(0, 0, 0)$ as $t \to +\infty$ or not. For the linear case, according to Theorem 1.3, the solution does so when $n < 1$ and does not do so when $n > 1$. The nonlinear case requires some definitions and theorems.

Let O be an open subset of R^m and $f : O \to R^m$. An equilibrium $x_e \in O$ of the (difference) equation $x(t+1) = f(x(t))$ is a fixed point of f, i.e., $x_e = f(x_e)$. The following definitions are standard in stability theory for dynamical systems.

Definition 1.5. An equilibrium x_e of the equation $x(t+1) = f(x(t))$ is **stable** if $\forall \varepsilon > 0\ \exists\ \delta = \delta(\varepsilon) > 0$ such that $|x(0) - x_e| < \delta \implies |x(t) - x_e| < \varepsilon$ for $t = 0, 1, 2, \cdots$. An equilibrium x_e is a **local attractor** if $\exists\ \delta_0 > 0$ such that $|x(0) - x_e| < \delta_0 \implies \lim_{t\to+\infty} |x(t) - x_e| = 0$ and it is **locally asymptotically stable** if it is a stable local attractor. The set B of all $x(0) \in O$ for which $\lim_{t\to+\infty} |x(t) - x_e| = 0$ is the **basin of attraction** of x_e. An equilibrium is a **global attractor** with respect to a set G if $G \subseteq B$. An equilibrium is **globally asymptotically stable** with respect to a set G if it is both asymptotically stable and a global attractor with respect to G.

For the linear matrix model (1.4) the extinction equilibrium $x_e = 0$ is globally asymptotically stable (with respect to R^m) if $\rho(P) < 1$. If $\rho(P) > 1$ then $x_e = 0$ is unstable (not stable). For nonlinear models local stability of equilibria can be determined by the linearization principle. See [**24**] (chapter 4).

Theorem 1.6. *Assume* x_e *is a fixed point of* $f \in C^1(O, R^m)$ *and* J *is the Jacobian matrix*[1] *evaluated at* x_e. *If* $\rho(J) < 1$, *then* x_e *is locally asymptotically stable. If* $\rho(J) > 1$ *then* x_e *is unstable.*

[1]The Jacobian of f is the matrix $(\partial_i f_j)$ of first order partial derivatives of f, where $\partial_i f_j$ is the derivative of the j^{th} component f_j of f with respect to the i^{th} component x_i of x.

Consider the matrix model (1.9). The Jacobian of $f(x) = (n\Phi(x) + T(x))\,x$ evaluated at the equilibrium $x_e = 0$ is $n\Phi(0) + T(0)$. It follows from Theorem 1.3 and 1.6 that, just as does for the linear model (1.4), the extinction equilibrium of the nonlinear model (1.9) loses stability as n (or r) increases through 1.

Theorem 1.7. *The extinction equilibrium $x_e = 0$ of the matrix model*

$$x(t+1) = (n\Phi(x(t)) + T(x(t)))\,x(t),$$

under the assumptions (1.10)-(1.11), is locally asymptotically stable if $n < 1$ and is unstable if $n > 1$.

This theorem applies, for example, to the three life cycle stage model in Example 1.4.

We will see examples below for which $x_e = 0$ is *not* globally asymptotically stable for $n < 1$. Further restrictions are required on the dependence of Φ and T on x in order to have global stability.

Suppose, for example, that all entries $\varphi_{ij}(x)$ and $\tau_{ij}(x)$ in the matrices $\Phi(x)$ and $T(x)$ satisfy the inequalities

$$\varphi_{ij}(x) \le \varphi_{ij}(0), \qquad \tau_{ij}(x) \le \tau_{ij}(0), \qquad x \in \bar{R}^m_+. \tag{1.12}$$

Then for $x(0) \ge 0$ we have

$$0 \le x(t+1) \le (n\Phi(0) + T(0))\,x(t).$$

By induction $0 \le x(t) \le y(t)$ where $y(t)$ solves the linear initial value problem

$$y(t+1) = (n\Phi(0) + T(0))\,y(t), \qquad y(0) = x(0).$$

If $n < 1$ then, using Theorem 1.1 with $P = n\Phi(0) + T(0)$, we conclude that $\lim_{t\to+\infty} y(t) = 0$ and hence $\lim_{t\to+\infty} x(t) = 0$.

Theorem 1.8. *If $n < 1$, the extinction equilibrium $x_e = 0$ of the matrix model*

$$x(t+1) = (n\Phi(x(t)) + T(x(t)))\,x(t),$$

under the assumptions (1.10)-(1.11) and (1.12), is globally asymptotically stable on the non-negative cone $\bar{R}^m_+$.

The conditions (1.12) describe a strong case of deleterious density dependence (or negative feedback) in the sense that the fertility and transition/survivorship rates of all age classes are decreased in the presence of (stage specific) population densities. These conditions are satisfied by the LPA model in Example 1.4.

What are the dynamics of a nonlinear matrix model (1.9) when $x = 0$ is unstable (for example when $n > 1$)? Two basic questions are: when are solutions bounded (i.e., when is unlimited population growth avoided) and when do solutions not tend to 0 (i.e., when do no populations go extinct)?

Define the vector norm $|x| = \sum_{i=1}^m |x_i|$, which for population models is the *total population size.* For this norm the induced matrix norm[2] is $||M|| = \sup_j \Sigma_i\, |m_{ij}|$, i.e., the largest vector norm from among the columns of M. Assume

$$|F(x)x| \le f_\infty < +\infty, \;\; ||T(x)|| \le \tau_\infty < 1 \text{ for all } x \in \bar{R}^m_+. \tag{1.13}$$

[2]Let $|x|$ be a vector norm on R^m. The *induced (or operator) norm* of a matrix M is $||M|| = \sup_{|x|=1} |Mx| = \sup_{|x|\neq 0} |Mx| \,/\, |x|$. In addition to the defining properties of a norm, the induced norm has the property $||MN|| \le ||M||\,||N||$. By definition, $|Mx| \le ||M||\,|x|$ for all $x \in R^m$.

This assumption on F implies that the total number of newborns (per unit time) in all classes, produced by adults from all classes, is bounded. This is a reasonable biological assumption. The assumption on T implies that there is always some loss in the transitions among classes during a unit of time (due, for example, to mortality). This is also a reasonable biological assumption, although occasionally a model will violate this condition because its transition matrix has a column sum equal to 1.

The matrix model (1.9) is *dissipative* if there exists a constant $\beta > 0$ (that does not depend on the initial state $x(0)$) and a time t^* such that $t \geq t^*$ (which might depend on $x(0)$) implies $|x(t)| \leq \beta$. This means populations are of total size no greater than β after a finite number of time steps.

Theorem 1.9. *Assume (1.8). The conditions (1.13) imply the matrix model (1.7) is dissipative.*

Proof. From the inequalities

$$0 \leq |x(t+1)| \leq f_\infty + ||T(x(t))||\,|x(t)| \leq f_\infty + \tau_\infty\,|x(t)|$$

and an induction we find that $|x(t)| \leq y(t)$ where $y(t) \geq 0$ is the solution of the scalar linear difference equation $y(t+1) = f_\infty + \tau_\infty y(t)$ that satisfies $y(0) = |x(0)|$. The formula $y(t) = \tau_\infty^t\,|x(0)| + f_\infty \sum_{i=0}^{t-1} \tau_\infty^i$ for the solution of this linear recursion equation implies $\lim_{t\to+\infty} y(t) = f_\infty/\left(1-\tau_\infty\right)$. Thus, we can take, for example, $\beta = 1 + f_\infty/\left(1-\tau_\infty\right)$ in the definition of dissipativity. ■

The second question, when $n > 1$ and $x = 0$ is unstable, concerns the possibility that some solutions with $x(0) \geq 0$ tend to 0 (i.e., that some populations will still go extinct). The matrix model (1.9) is *uniformly persistent* (with respect to $x_e = 0$) if there exists an $\alpha > 0$ (that does not depend on $x(0)$) such that $0 \leq x(0) \neq 0$ implies $\liminf_{t\to+\infty} |x(t)| \geq \alpha$. For a uniformly persistent matrix model, the total size of all populations (starting from a nonzero initial class distribution) eventually is no less that α.

The following theorem follows from Theorem 3 in [**45**]. Note: $\bar{R}^m_+/\{0\}$ consists of all nonzero, non-negative $x \in R^m$.

Theorem 1.10. *Assume (1.10), (1.11) and $n > 1$. Assume the matrix model (1.9) is dissipative and that $\bar{R}^m_+/\{0\}$ is forward invariant. Then the matrix model (1.9) is uniformly persistent.*

That $\bar{R}^m_+/\{0\}$ is forward invariant means $x(t) \in \bar{R}^m_+/\{0\}$ implies $x(t+1) \in \bar{R}^m_+/\{0\}$. This is the same thing as saying that no population goes extinct in a finite number of steps. This assumption is necessary in Theorem 1.10, as the $m = 1$ scalar example $x(t+1) = nf(x(t))x(t)$, $f(x) \triangleq (1 - x + |1-x|)/2$, shows. In this example, if $n > 4$ and $x(0) = 1/2$, then $x(2) = 0$.

Example 1.11. *For the LPA model*

$$\begin{aligned}
L(t+1) &= bA(t)\exp\left(-\frac{c_{el}}{V}L(t) - \frac{c_{ea}}{V}A(t)\right)\\
P(t+1) &= (1-\mu_l)\,L(t)\\
A(t+1) &= (1-\mu_p)\,P(t)\exp\left(-\frac{c_{pa}}{V}A(t)\right) + (1-\mu_a)\,A(t)
\end{aligned}$$

we have

$$F(x)x = \begin{pmatrix} bA\exp\left(-\frac{c_{el}}{V}L - \frac{c_{ea}}{V}A\right) \\ 0 \\ 0 \end{pmatrix}, \quad T(x) = \begin{pmatrix} 0 & 0 & 0 \\ 1-\mu_l & 0 & 0 \\ 0 & 1-\mu_p & 1-\mu_a \end{pmatrix}$$

($x = \mathrm{col}\,(L, P, A)$) and hence

$$\begin{aligned} |F(x)x| &= bA\exp\left(-\frac{c_{el}}{V}L - \frac{c_{ea}}{V}A\right) \\ &\le bA\exp\left(-\frac{c_{ea}}{V}A\right) \\ &\le b\frac{V}{c_{ea}}e^{-1} \triangleq f_\infty < +\infty \\ ||T(x)|| &= \sup\{1-\mu_l, 1-\mu_p, 1-\mu_a\}. \end{aligned}$$

The conditions (1.13) are satisfied if μ_l, μ_p, $\mu_a > 0$ and as a result the model is dissipative by Theorem 1.9 for all values of b (and V).

Suppose $x = \mathrm{col}\,(L(t), P(t), A(t)) > 0$. Then it is easy to see from the model equations that $\mathrm{col}\,(L(t+1), P(t+1), A(t+1)) > 0$ and as a result $R^m_+/\{0\}$ is forward invariant.

It follows from Theorem 1.10 that if μ_l, μ_p, $\mu_a > 0$, then the model is uniformly persistent whenever

$$n \triangleq b\frac{(1-\mu_l)(1-\mu_p)}{\mu_a} > 1.$$

EXERCISES

Exercise 1. (a) The discrete logistic (1.2) is called a monotone map because $bx/(1+cx)$ is a monotone function of $x > 0$. Use this fact to prove that $x(0) > 0$ implies $\lim_{t\to+\infty} x(t) = (b-1)/c$. (b) Show that the change of variables $y = 1/x$ transforms (1.2) to a linear difference equation. Use this fact to find a solution formula for $x(t)$ and use the solution formula to prove that $x(0) > 0$ implies $\lim_{t\to+\infty} x(t) = (b-1)/c$.

Exercise 2. Suppose the non-negative matrix P is primitive and diagonalizable in the matrix equation $x(t+1) = Px(t)$. For $x(0) \ge 0$, $x(0) \ne 0$ prove

$$\lim_{t\to+\infty} \frac{x(t)}{|x(t)|} = \frac{v}{|v|}$$

where $v > 0$ is the positive eigenvector associated with the dominant eigenvalue of P. This result (which is also true when P is not diagonalizable) is known as the Strong Ergodic Theorem or the Fundamental Theorem of Demography.

Exercise 3. Prove Theorem 1.2 when P is diagonalizable (i.e., R^m has a basis of eigenvectors of P).

Exercise 4. Consider the fertility and transition matrices

$$F = \begin{pmatrix} f_{11} & f_{12} & \cdots & f_{1,m-1} & f_{1m} \\ 0 & 0 & \cdots & 0 & 0 \\ 0 & 0 & \cdots & 0 & 0 \\ \vdots & \vdots & & \vdots & \vdots \\ 0 & 0 & \cdots & 0 & 0 \end{pmatrix}, \text{and}$$

$$T = \begin{pmatrix} \tau_{11} & 0 & \cdots & 0 & 0 \\ \tau_{21} & \tau_{22} & \cdots & 0 & 0 \\ 0 & \tau_{32} & \cdots & 0 & 0 \\ \vdots & \vdots & & \vdots & \vdots \\ 0 & 0 & \cdots & \tau_{m,m-1} & \tau_{mm} \end{pmatrix}.$$

The matrix $P = F + T$ is sometimes called an Usher matrix and the associated matrix model the "standard size structured model". Here the categories are size classes (weight, volume, length, biomass, etc.) and an individual either remains in the same class or grows into the next class in one unit of time. An individual cannot skip a size class nor shrink in size. All newborns lie in the smallest size class. Derive a formula for the net reproductive number n. Use the formula to obtain a biological interpretation of n.

Exercise 5. Consider a size structured (Usher) matrix with two newborn and two reproducing classes, large and small. (See Exercise 4.) Assume larger size individuals produce larger size offspring while smaller size individuals produce smaller size offspring. A model for this population has projection matrix $P = F + T$ where

$$F = \begin{pmatrix} 0 & 0 & f_{13} & 0 \\ 0 & 0 & 0 & f_{14} \\ 0 & 0 & 0 & 0 \\ 0 & 0 & 0 & 0 \end{pmatrix}, \qquad T = \begin{pmatrix} \tau_{11} & 0 & 0 & 0 \\ \tau_{21} & \tau_{22} & 0 & 0 \\ 0 & \tau_{32} & \tau_{33} & 0 \\ 0 & 0 & \tau_{43} & \tau_{44} \end{pmatrix}.$$

Derive a formula for the net reproductive number n. Use the formula to obtain a biological interpretation of n.

Exercise 6. The matrix model

$$F = \begin{pmatrix} 0 & f_{13} \\ 0 & 0 \end{pmatrix}, \quad T = \begin{pmatrix} \tau_{11} & 0 \\ \tau_{21} & \tau_{22} \end{pmatrix}, \quad 0 \le \tau_{ii} < 1,\ 0 < \tau_{21} \le 1$$

describes a population with a juvenile stage and an adult stable. Find formulas for n and r. Find a functional relationship $r = \phi(n)$ that relates n to r. Show that $\phi(n)$ is an increasing, concave (down) function of n.

Exercise 7. (a) Show all eigenvalues of a 2×2 matrix

$$A = \begin{pmatrix} a & b \\ c & d \end{pmatrix}$$

lie inside the unit complex circle if and only if the "Jury Conditions"

$$|\det A| < 1, \quad |\text{tr } A| < |1 + \det A|$$

hold. (b) Show $\text{tr}A = 1+\det A$ implies $\lambda = 1$ is an eigenvalue and $\text{tr}A = -(1+\det A)$ implies $\lambda = -1$ is an eigenvalue. (c) Show $|\det A| = 1$, $|\text{tr } A| < |1 + \det A|$ imply the eigenvalues are complex conjugates with absolute value equal to 1.

LECTURE 2

Bifurcations

This lecture concerns the bifurcation of positive equilibrium solutions of the nonlinear matrix equation

$$x(t+1) = (n\Phi(x(t)) + T(x(t)))\, x(t). \tag{2.1}$$

In addition to the smoothness assumption (1.10) on the fertility and transition matrices Φ and T, it is assumes for non-negative $x \geq 0$ and $n > 0$ that

$$\begin{gathered} \text{the matrix } n\Phi(x) + T(x) \text{ is primitive,} \\ \sum_{i=1}^{m} \tau_{ij}(x) \leq 1, \quad T(x) \neq 0, \quad \rho\left(T(x)\right) < 1 \text{ and} \\ \rho\left(\Phi(0)\left(I - T(0)\right)^{-1}\right) = 1. \end{gathered} \tag{2.2}$$

Assumptions (2.2) implies (1.11).

Nontrivial equilibria $x \in R^m$, and in particular non-negative or positive equilibria, of the matrix equation satisfy the equilibrium equation

$$x = (n\Phi(x) + T(x))\, x.$$

Using the Taylor expansion

$$n\Phi(x) + T(x) = n\Phi(0) + T(0) + H(n, x),$$

where $\|H(n,x)\| = O\left(|x|\right)$,[1] we can rewrite the equilibrium equation as

$$x = nLx + g(n, x) \tag{2.3}$$

where[2]

$$L \triangleq \left(I - T(0)\right)^{-1} \Phi(0), \quad g(n,x) \triangleq \left(I - T(0)\right)^{-1} H(n,x)x, \quad |g(n,x)| = O\left(|x|^2\right).$$

Those values of n are sought for which there is a non-negative, nontrivial solution of (2.3) (i.e., an equilibrium of (2.1) lying in $\bar{R}^m_+/\{0\}$). We call such a pair (n, x) a *nontrivial, non-negative equilibrium pair* of (2.1). A nontrivial equilibrium pair is a *positive equilibrium pair* when $x > 0$ (i.e., when $x \in R^m_+/\{0\}$).

Define $\mathcal{S}$ to be the set of all nontrivial solution pairs of (2.1). If $(n_c, 0) \in \bar{\mathcal{S}}$ (the closure of $\mathcal{S}$) we say $(n_c, 0)$ is a bifurcation point. A necessary condition that $(n_c, 0)$ is a bifurcation point is that n_c is a characteristic value of L, that is to say, $v = n_c L v$ for some vector $v \neq 0$ in R^m, or in other words n_c is the reciprocal of a nonzero eigenvalue of L. (See Exercise 8.) Note that a characteristic value

[1] This means for any interval $n_1 \leq n \leq n_2$ there are constants $a, b > 0$ such that $\|H(n,x)\| \leq b\,|x|$ for all $|x| \leq a$ and $n_1 \leq n \leq n_2$.

[2] This means for any interval $n_1 \leq n \leq n_2$ there are constants $a, b > 0$ such that $|g(n,x)| \leq b\,|x|^2$ for all $|x| \leq a$ and $n_1 \leq n \leq n_2$.

of $L = (I - T(0))^{-1}\Phi(0)$ is a characteristic value of the matrix $\Phi(0)(I - T(0))^{-1}$ (and vice versa).

The following theorem states that for quite general nonlinear matrix models, $n_c = 1$ is a bifurcation value (just as it is for linear matrix models).

Theorem 2.1. *Consider the nonlinear matrix model (2.1) under assumptions (1.10) and (2.2). There exists a continuum*[3] $\mathcal{C}^+$ *in* $\bar{\mathcal{S}}$ *that contains the bifurcation point* $(n_{cr}, 0) = (1, 0)$ *and such that* $\mathcal{C}^+ / \{(1,0)\}$ *contains only positive equilibrium pairs. The range of the continuum* $\mathcal{C}^+$ *(that is to say, the set* $\{x : (n,x) \in \mathcal{C}^+ / \{(1,0)\}\}$*), is unbounded in* R_+^m *and the spectrum* $\sigma(\mathcal{C}^+) \triangleq \{n : (n,x) \in \mathcal{C}^+ / \{(1,0)\}\}$ *associated with* $\mathcal{C}^+$ *contains only positive* $n > 0$*.*

This theorem follows from Theorem 1.2.7 in [**4**] (which is proved using the global bifurcation theorems of Rabinowitz [**39, 61**]).

Example 2.2. *Consider the matrix model (1.7) with*

$$F(x_1, x_2) = \begin{pmatrix} cbx_2 e^{-x_2} & be^{-x_2} \\ 0 & 0 \end{pmatrix}, \qquad T(x_1, x_2) = \begin{pmatrix} 0 & 0 \\ \tau_{21} & \tau_{22} \end{pmatrix}$$
$$b, c > 0, \qquad 0 < \tau_{21} \leq 1, \qquad 0 \leq \tau_{22} < 1.$$

This describes a population in which newborns lie in class 1*. If* $c = 0$ *then the two classes* $x_1 = J$ *and* $x_2 = A$ *could properly be referred to as juveniles and adults (reproductively immature and mature). With* $c > 0$ *both classes reproduce, with fertility dependent on the population density* x_2 *of class* 2*. In this case we can refer to a population with a younger class and an older class.*

In this model, fertility of the older individuals is negatively affected by increased density of the older class, x_2*. Younger individuals reproduce very little when few older individuals are present (*x_2 *is small), but their reproduction increases as* x_2 *increases, until a maximum is reached (at* $x_2 = 1$*) after which negative density effects reduce their reproduction. This kind of effect, in which increased fertility occurs with increased population density (in this case, adult density) is called an Allee effect. Allee effects have been attributed to a variety of biological mechanisms (e.g., enhanced mating opportunities in denser populations, the care and nurture of young, social behavior, group defense, and many others).*

The model equations are

$$J(t+1) = cbA(t)e^{-A(t)}J(t) + be^{-A(t)}A(t)$$
$$A(t+1) = \tau_{21}J(t) + \tau_{22}A(t). \tag{2.4}$$

The calculation

$$F(0,0)(I - T(0,0))^{-1} = \begin{pmatrix} b\frac{\tau_{21}}{1-\tau_{22}} & b\frac{1}{1-\tau_{22}} \\ 0 & 0 \end{pmatrix}$$

yields the formula $n = b\tau_{21}/(1 - \tau_{22})$ *for the inherent net reproductive number. The solution of the equilibrium equations*

$$J = cbAe^{-A}J + be^{-A}A$$
$$A = \tau_{21}J + \tau_{22}A$$

[3] A continuum is a closed, connected set.

for nontrivial solutions $(J, A) \neq (0, 0)$ *reduces to solving the scalar equation*

$$e^A = \left(c\frac{1-\tau_{22}}{\tau_{21}} A + 1 \right) n$$

for $A \neq 0$ *and letting* $J = (1-\tau_{22})\, A/\tau_{21}$. *This equation for* A *leads to two kinds of bifurcation graphs in the* (n, A)*-plane, as shown in Figure 2. When* $c \leq \tau_{21}\,(1-\tau_{22})^{-1}$ *the spectrum* $\sigma(\mathcal{C}^+) = [1, +\infty)$ *and positive equilibria exist for and only for* $n > 1$. *However, if* $c > \tau_{21}\,(1-\tau_{22})^{-1}$ *then the spectrum is a larger interval and includes the bifurcation value* $n = 1$ *on its interior. In this case, positive equilibria (two of them) also exist for some values of* $n < 1$.

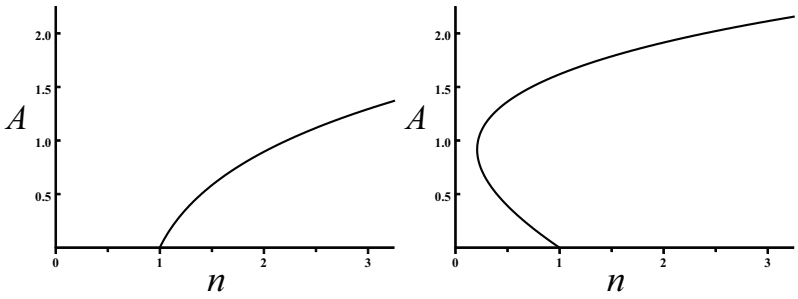

(a) (b)

FIGURE 2. The A components of the positive equilibria of (2.4) are plotted against n. (a) For $c \leq \tau_{21}/(1-\tau_{22})$ the bifurcation is supercritical. (b) For $c > \tau_{21}/(1-\tau_{22})$ it is subcritical.

The two distinct cases that occur in Example 2.2 are distinguished by the *direction of bifurcation* at $n = 1$. When, near the bifurcation point $(1, 0)$, positive equilibrium pairs (n, x) exist for $n > 1$, then the bifurcation is called *supercritical* (or forward). On the other hand, when near the bifurcation point $(1, 0)$ the positive equilibrium pairs (n, x) exist for $n < 1$, then the bifurcation is *subcritical* (or backward). Allee effects typically can lead to a subcritical bifurcation. Models in which fertility and mortality never increase with increases in population density lead to supercritical bifurcations.

One technique that can determine properties of the bifurcating continuum of positive equilibria is based on the *net reproductive number* $n(x)$ at equilibrium x defined as the dominant eigenvalue of $F(x)\,(I - T(x))^{-1}$. This quantity should not be confused with the *inherent* net reproductive number n. We write $n(x) = n\nu(x)$ where $n = n(0)$ is the inherent net reproductive number and where the dominant eigenvalue $\nu(x)$ of $\Phi(x)\,(I - T(x))^{-1}$ satisfies $\nu(x) > 0$, $\nu(0) = 1$. If x is an equilibrium associated with inherent net reproductive number $n(x)$, then

$$n\nu(x) = 1. \tag{2.5}$$

Thus, $n(x) = n\nu(x)$ is an invariant (2.5) along the bifurcating branch $\mathcal{C}^+$ in Theorem 2.1. Properties of $\nu(x)$ can often give information about the direction of bifurcation at $n = 1$ and the spectrum $\sigma(\mathcal{C}^+)$. For example, if $\nu(x) < \nu(0)$ for x near 0 satisfying $0 \leq x \neq 0$, then to maintain the invariance of $n\nu(x)$ the local

bifurcation must be supercritical (i.e., near the bifurcation point n would have to satisfy $n > 1$). For more on this approach see [**4**].

As an example, for the model in Example 2.2 it turns out that

$$\nu(J, A) = \frac{1 - \tau_{22}}{\tau_{21}} cAe^{-A} + e^{-A}.$$

If $c < \tau_{21}(1 - \tau_{22})^{-1}$ then $\partial_A \nu(0, 0) < 0$. It follows in this case that, near $(J, A) = (0, 0)$, the inequality $\nu(J, A) < 0$ for positive equilibria. Thus, near bifurcation the bifurcation point $n = 1$, it must be the case that $n > 1$ and hence the bifurcation is supercritical. Similarly, we deduce that if $c > \tau_{21}(1 - \tau_{22})^{-1}$ then the bifurcation is subcritical (since $\partial_A \nu(0, 0) < 0$). We can also deduce from $\nu(J, A)$ that the spectrum is unbounded. This is because the continuum $\mathcal{C}^+$ is unbounded by Theorem 2.1 and consequently either the spectrum is unbounded or the equilibria on the branch are unbounded. However, even in the latter case the spectrum must be unbounded (as a consequence of the invariant (2.5)) because in this case $\nu(x) = \nu(J, A)$ tends to 0 as A tends to $+\infty$.

An important problem is to determine when the positive equilibria guaranteed by Theorem 2.1 are stable or unstable. It turns out that the stability of the positive equilibria near the bifurcation point usually depends on the direction of bifurcation. The bifurcation $n = 1$ described in Theorem 2.1 is called *stable* if the equilibria from the positive equilibrium pairs near the bifurcation point $(n, x) = (1, 0)$ are (locally asymptotically) stable. If these positive equilibria are unstable then the bifurcation is *unstable.*

Under some additional conditions, the bifurcation at $(n, x) = (1, 0)$ in Theorem 2.1 is stable when it is supercritical and unstable when it is subcritical. This fact is a consequence of the Theorem 1.2.6 in [**4**].

Define γ_{ij} to be the gradient of $\varphi_{ij}(x) + \tau_{ij}(x)$ evaluated at $(n, x) = (1, 0)$:

$$\gamma_{ij} \triangleq \nabla_x \left(\varphi_{ij}(x) + \tau_{ij}(x)\right)\big|_{(n,x)=(1,0)} \in R^m.$$

Let

$$d_{ij} \triangleq \gamma_{ij}^* v$$

(the prime " * " denotes transpose) and form the matrix $D = (d_{ij})$. Let $w > 0$ and $v > 0$ denote the positive left and right eigenvalues of $\Phi(0) + T(0)$ and define

$$\kappa \triangleq -wDv.$$

Theorem 2.3. *Assume*

$$\varphi_{ij} \in C^2(D, [0, +\infty)), \quad \tau_{ij} \in C^2(D, [0, 1])$$

(1.11), and $\kappa \neq 0$. Then the bifurcation of positive equilibrium pairs in Theorem 2.1 is stable if it is supercritical ($\kappa > 0$) and unstable if it is subcritical ($\kappa < 0$).

Since $w > 0$ and $v > 0$, some of the d_{ij} must be positive in order for a subcritical bifurcation to occur, i.e., at least one gradient γ_{ij} must have some positive components. This means Allee effects of some kind are necessary for a subcritical to occur (although they are not necessarily sufficient).

Example 2.4. *For the juvenile/adult model in Example 2.2*

$$\Phi(x_1, x_2) = \begin{pmatrix} c\frac{1-\tau_{22}}{\tau_{21}} x_2 e^{-x_2} & \frac{1-\tau_{22}}{\tau_{21}} e^{-x_2} \\ 0 & 0 \end{pmatrix}, \quad T(x_1, x_2) = \begin{pmatrix} 0 & 0 \\ \tau_{21} & \tau_{22} \end{pmatrix}$$

and $n = b\tau_{21}/(1-\tau_{22})$. *Positive right and left eigenvalues of*

$$\Phi(0,0)+T(0,0) = \begin{pmatrix} 0 & \frac{1-\tau_{22}}{\tau_{21}} \\ \tau_{21} & \tau_{22} \end{pmatrix}$$

associated with eigenvalue 1 *are*

$$w = \begin{pmatrix} \tau_{21} & 1 \end{pmatrix}, \qquad v = \begin{pmatrix} 1-\tau_{22} \\ \tau_{21} \end{pmatrix}.$$

The matrix D *evaluated at* $(n,x) = (1,0)$ *is*

$$D = \begin{pmatrix} c(1-\tau_{22}) & -(1-\tau_{22}) \\ 0 & 0 \end{pmatrix}$$

and

$$\kappa = \tau_{21}(1-\tau_{22})^2\left(\frac{\tau_{21}}{1-\tau_{22}} - c\right).$$

Thus, the bifurcation at $(n,x) = (1,0)$ *is stable (supercritical) if* $c < \tau_{21}/(1-\tau_{22})$ *and unstable (subcritical) if* $c > \tau_{21}/(1-\tau_{22})$.

Even when they contain Allee effects at low population densities[4], most models assume negative density effects for large population densities. The latter assumption is responsible for the "turning around" of the bifurcating branch, at a point (n_{sn}, x_{sn}), as illustrated in Figure 2(b). This creates a sub-interval in the spectrum $\sigma(\mathcal{C}^+)$ on which multiple positive equilibria exist.

Figure 3 shows the basins of attraction[5] of the two stable equilibria (the extinction equilibrium and one of the positive equilibria) when a subcritical bifurcation occurs in Example 2.2. This plot illustrates the commonly occurring situation in which the "smaller" positive equilibria from the "lower" portion of the bifurcating branch of positive equilibria is unstable (consistent with Theorem 2.3), while the "larger" positive equilibrium from the "upper" portion as stable. For those n values less than 1 there are two stable equilibria, the unstable positive equilibrium lies of the boundary of the basins of attraction.

In the typical subcritical bifurcation scenario illustrated in Figure 4, a population can survive for $n < 1$ provided its initial state $x(0)$ is sufficiently far from the extinction equilibrium $x_e = 0$; otherwise it will go extinct. Notice the sudden collapse and extinction of the population as $n < 1$ decreases (and the population follows the stable equilibrium) below the critical value $n_{sn} < 1$ where the bifurcation curve "turns around". If we increase $n < n_{sn}$ (in an attempt to recover the population) the population follows the extinction equilibrium (unless there is also a perturbation so as to move the population sufficiently far from $x_e = 0$) until $n = 1$ is exceeded, at which point the population recovers. This phenomenon where the collapse point n_{sn} is less than the recovery point $n = 1$ is called *hysteresis*.

As we move along the bifurcating branch from the bifurcation point $(n,x) = (1,0)$ in the subcritical case illustrated in Figure 4, equilibrium stability is gained as we move "around" the turn the branch at the point (n_{sn}, x_{sn}) where the lower and upper branches meet. This occurs because the spectral radius of the Jacobian of

[4]Some argue that accurate population models should contain Allee effects [**16**], especially if one is concerned with the possibility of extinction.

[5]The basin of attraction of an equilibrium is the set of initial conditions $x(0)$ that tend to the equilibrium.

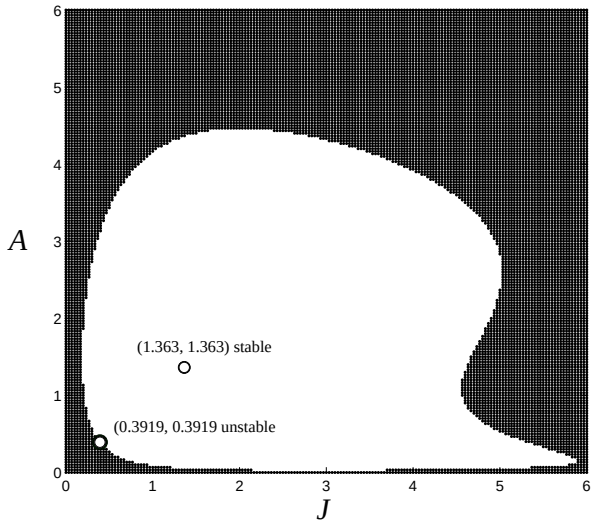

FIGURE 3. The set of initial conditions whose orbits tend to an equilibrium is the equilibrium's basin of attraction. For $c = 2.5$, $\tau_{21} = 0.75$, $\tau_{22} = 0.25$ and $n = 0.5$ ($b = 0.5$) in the juvenile-adult model in Example 2.2 there are two stable equilibria: the extinction equilibrium $(J, A) = (0, 0)$, whose basin of attraction is the dark region, and $(J, A) = (1.363, 1.363)$ whose basin of attraction is the light region. The unstable equilibrium $(J, A) = (0.3919, 0.3919)$ lies on the basin boundary on which orbits tend to this unstable equilibrium. The unstable equilibrium is a *saddle* and the basin boundary is its *stable manifold*.

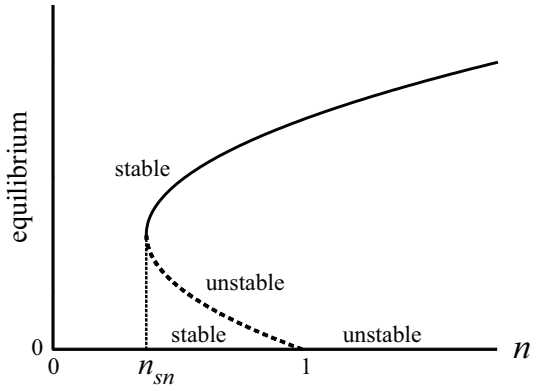

FIGURE 4. A subcritical (unstable) bifurcation caused by Allee effects at low population densities and negative density regulated at high population densities leads to a hysteresis effect.

the model system, evaluated at the equilibrium, changes from greater to less than 1. Thus, an eigenvalue of the Jacobian moves into the unit circle in the complex plane as we move around the turning point, from the lower to the upper branch, and, as

a result, the Jacobian at the point (n_{sn}, x_{sn}) has an eigenvalue of magnitude equal to 1.

We can distinguish three ways in which an eigenvalue λ of the Jacobian can migrate out of (or into) the complex unit circle as a model parameter changes: either λ passes through $+1$ or -1 or $e^{i\theta}$ for some $\theta \neq 0, \pi$. Different kinds of bifurcations result according to which of these three cases occurs.

If λ passes through $+1$ as a parameter in the model is changed, the bifurcation generally involves equilibria. Theorem 2.1 shows that such a bifurcation occurs quite generally in matrix models. When n (or r) increases through 1 two branches of equilibria intersect in what is called a *transcritical bifurcation*[6]. It is characteristic of transcritical bifurcations that one branch losses stability and the other branch gains it, a phenomenon called an *exchange of stability*. Another common bifurcation that can occur when λ leaves the unit circle at $+1$ is that exemplified by the multiple equilibrium case in Figure 4 (as can occur in the subcritical case caused by Allee effects). The bifurcation at $n = n_{sn}$, which occurs as two nontrivial equilibria are created when n increases through n_{sn}, is called a *saddle-node* or (*tangent* or *blue sky*) bifurcation. Other bifurcation scenarios involving equilibria can occur when destabilization results from λ passing through $+1$ (for example, the *pitch fork* bifurcation), but the saddle-node and transcritical are the most common ones to occur in population dynamic models.

When, as a model parameter is changed, an eigenvalue of the Jacobian leaves the unit circle through -1 and an equilibrium thereby loses stability, typically there exists a branch of 2-cycles (periodic solutions of the matrix equation of period 2) that intersects the equilibrium branch at the critical parameter value where $\lambda = -1$. The 2-cycles collapse into an equilibrium at the bifurcation point and so we say small amplitude cycles "bifurcate out of" the equilibrium as it loses stability. Such a *2-cycle* (or *period doubling bifurcation*[7]) can involve stable or unstable cycles and can occur as the model parameter increases or decreases, depending on the circumstances. This famous bifurcation is familiar in maps of dimension $m = 1$ (such as the Ricker map (1.3)).

There are formal theorems to be found in many textbooks that provide conditions under which period doubling and transcritical bifurcations are guaranteed to occur in the cases $\lambda = \pm 1$, and conditions that determine the direction of bifurcation and the stability properties of the equilibria and cycles involved. See for example [**24, 67**].

Transcritical and saddle-node bifurcations commonly occur in population matrix models (1.4) (or 2.1)). Period doubling bifurcations occur commonly in $m = 1$ dimensional models. After all, in $m = 1$ models only two possibilities arise for an eigenvalue λ of the Jacobian (derivative) of the equation, which is necessarily real, to leave the unit circle, namely ± 1. In higher dimensional models, in which eigenvalues can be complex, λ can leave the unit circle at any of infinitely many points $e^{i\theta}$ other than ± 1. (Of course, in the latter case a complex conjugate pair of eigenvalues λ crosses the unit circle.)

---

[6]Although not considered here, the general bifurcation theory for matrix models presented here also implies a bifurcating continuum of negative equilibrium pairs from the point $(n, x) = (1, 0)$. Thus, the set $\mathcal{S}$ contains a continuum of nontrivial equilibrium pairs that transversely crosses the extinction equilibrium branch.

[7]An equilibrium is 1-cycle.

When an equilibrium destabilizes because an eigenvalue λ of the Jacobian crosses the unit circle at a point $e^{i\theta} \neq \pm 1$, a more complicated bifurcation typically occurs. As a warm up for this case, consider the $m = 2$ dimensional linear matrix model $x(t+1) = Px(t)$ with coefficient matrix

$$P = \begin{pmatrix} a\cos\theta & -a\sin\theta \\ a\sin\theta & a\cos\theta \end{pmatrix}$$

where $a > 0$ and $0 < \theta < \pi$ are model parameters. The spectral radius is $\rho(P) = a$ and for $a < 1$ the origin $x_e = 0$ is globally asymptotically stable while for $a > 1$ nontrivial solutions grow exponentially in magnitude. For $a = 1$ orbits remain on the circle $x_1^2 + x_2^2 = x_1^2(0) + x_2^2(0)$ in the x_1, x_2-plane as each successive point is rotated θ radians counter-clockwise. Each circle, centered at the origin, is an invariant loop and the characteristics of an orbit lying on the circle depend on θ. If θ is rationally related to 2π, then the orbits are periodic cycles. If θ is irrationally related to 2π, then the orbits are neither periodic, nor asymptotically periodic, but are dense on the circle and are termed quasi-periodic ([**63**], p. 428). A bifurcation diagram that represents this situation is vertical in that the invariant loops occur only at $a = 1$, where the equilibrium $x_e = 0$ is destabilized.

Branches of invariant loops can also bifurcate from a destabilized equilibrium in nonlinear matrix equations (1.4). In this case, the branch of invariant loops is generally non-vertical and the spectrum is no longer a single point, but instead is an interval of parameter values. This is the subject of the *invariant loop* (or *Sacker/Neimark* or *discrete Hopf*) *bifurcation theorem*. This theorem (see [**24, 67**]) gives rigorous conditions under which a branch of invariant loops bifurcates out of an equilibrium that destabilizes because an eigenvalue λ of the Jacobian passes through the unit circle at a point $e^{i\theta} \neq \pm 1$. The theorem also gives conditions that determine the direction of bifurcation and stability properties of the invariant loops. (One of these conditions, rather unexpectedly, requires that $\theta \neq 2\pi/3$ or $2\pi/4$ or in other words that λ not equal a cube or quartic root of 1. What happens in these exceptional "resonance" cases is apparently still not fully understood.) The motion of orbits on the bifurcating invariant loops can, as in the linear example above, be periodic or tend to a periodic cycle or be quasi-periodic and dense in the loop. As the model (bifurcation) parameter changes, the dynamics on the loop alternates between periodicity (in which case the system is said to be *period locked*) and quasi-periodicity.

Example 2.5. *Figure 5 shows a sample bifurcation diagram for the matrix model*

$$\begin{pmatrix} J(t+1) \\ A(t+1) \end{pmatrix} = \begin{pmatrix} cbA(t)e^{-A(t)} & be^{-A(t)} \\ \tau_{21} & \tau_{22} \end{pmatrix} \begin{pmatrix} J(t) \\ A(t) \end{pmatrix} \tag{2.6}$$

in Example 2.2 using the bifurcation parameter $n = b\tau_{21}/(1-\tau_{22})$. *Plotted against each* n *value are 200 points of the* A *component of the attractor found after first iterating this matrix model 500 times (in order to arrive at an attractor). When the attractor is quasi-periodic 200 different points are plotted, which appear as a nearly solid vertical line segment above the corresponding* n *value. When the attractor is a cycle of period* p, *then only* p *points appear above the value of* n. *For the parameter values indicated in the figure caption, we see an invariant loop bifurcation occurs at a critical value of* $n \approx 8.1$. *A plot of one such invariant loop, for* $n = 9$, *appears in Figure 5(b) and the time series of the* J *component of a dense orbit on the loop in Figure 5(c). It is often difficult to tell the difference between a cycle with a long*

period and a quasi-periodic orbit. Figures 5(d) and (e) show plots of what appear to be a 33*-cycle when* $n = 8.9624$*.*

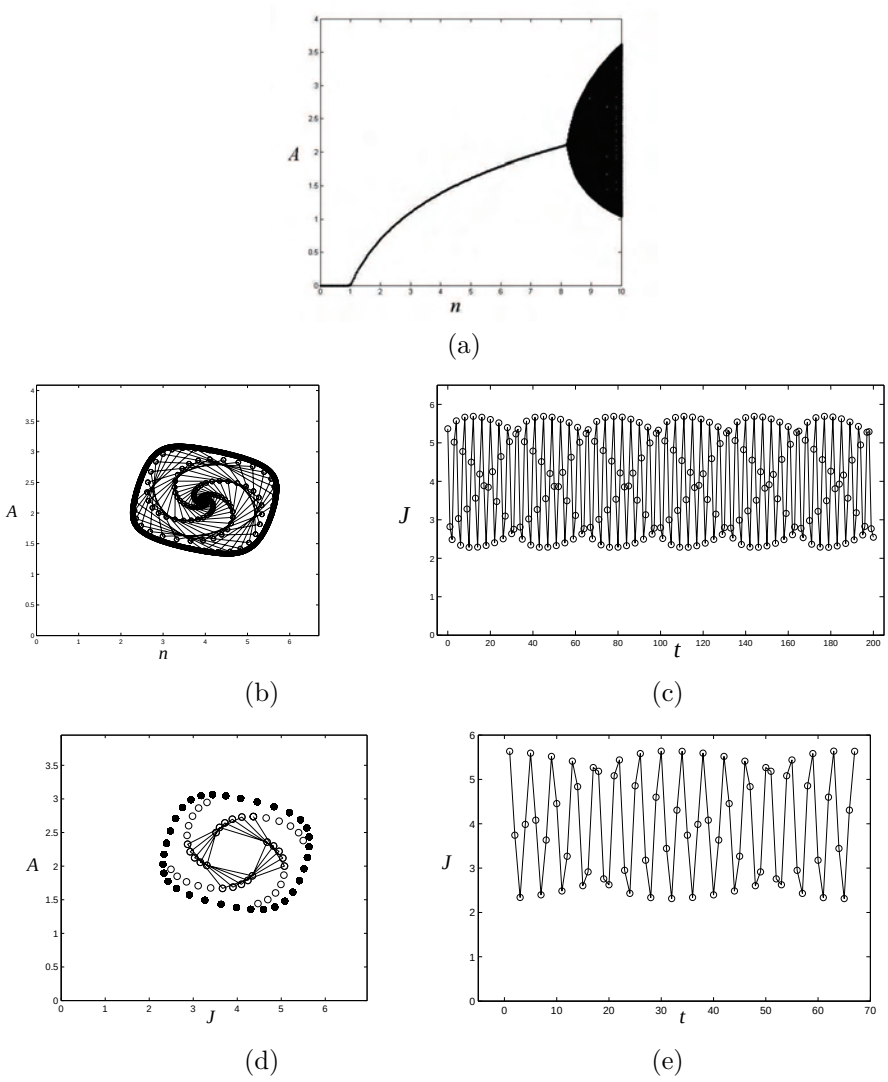

FIGURE 5. Choose $\tau_{21} = 0.5$, $\tau_{22} = 0.1$ and $c = 0$ (no Allee effect) in the juvenile-adult matrix model (2.6). (a) The bifurcation diagram shows the transcritical bifurcation of positive equilibria at $n = 1$ and the destabilization of the positive equilibria with a resulting an invariant loop bifurcation at $n \approx 8.1$. (b) An orbit starting near the unstable equilibrium spirals out to the invariant loop when $n = 9$. (c) The time series for the J component of a quasi-periodic orbit on the invariant loop in (b). A time series plot of the A component exhibits similar oscillations. (d) At $n = 8.9624$ an orbit spirally approaches a 33-cycle (residing on an invariant loop). (e) The J component of the 33-cycle in (d).

While the *primary bifurcation* of positive equilibria from the extinction equilibrium $x_e = 0$ at $n = 1$ is a quite general phenomenon in population models, the occurrence of further bifurcations through the loss of stability of the positive equilibria (or other positive attractors such as cycles or invariant loops) is dependent on the details of specific models. Period doubling and invariant loop bifurcations might or might not occur in a specific model.

In many cases numerous bifurcations occur as n increases, such as the famous period doubling cascade of the Ricker equation. In principle the study of cycles and cycle bifurcations is reducible to the study of equilibrium bifurcations of a composition of the model equations. (A 2-cycle is a fixed point of the first composite, and so forth.) For $m = 1$ dimensional maps, the common occurrence of a $\lambda = -1$ bifurcation can lead to repeated bifurcations of period doublings for higher and higher composites. Therefore, period doubling cascades are common for the $m = 1$ dimensional case. For the higher dimensional cases which arise in the study of structured population dynamics, invariant loop bifurcations often play a significant role.

Cycles also can lose stability through invariant loop bifurcations. For example, a 2-cycle can bifurcate into two disjoint invariant loops (surrounding each point of the cycle). Bifurcations involving invariant loops are more complicated and difficult to study analytically. As n increases invariant loops often suddenly disappear from the bifurcation diagram, yielding to other attractors (e.g. to periodic cycles in what are called period locking windows), or they can become twisted and convoluted or even break into pieces, as the dynamics become more complex and chaotic. Given the complexity of the dynamics in such regions of parameter space, it is not surprising that there are many technical definitions of chaos in the literature and a growing list of exotic bifurcation phenomena identified and classified by mathematicians (usually with the aid of computer simulations). Definitions of a chaotic attractors generally assume (or imply) that such attractors contain infinitely many unstable periodic cycles, bounded orbits that are not periodic and do not tend to a periodic cycle, orbits that are dense in the attractor, phase space directions in which orbits expand and other directions in which orbits contract, and sensitivity to initial conditions. The latter property is perhaps the most famous property of chaotic attractors. It means that orbits initially infinitesimally close diverge exponentially from one another over time, a property that has serious consequences with regard to the ability to predict the future state of a system, even though its dynamics are deterministic.

Needless to say, the study of the complicated dynamics that can occur in some models (e.g., the bifurcation diagram in Figure 6) is usually analytically intractable. Not only can the attractors at selected values of the bifurcation parameter n be chaotic, but the mix of chaotic and tame dynamics throughout in an interval of n values can be complicated. Chaotic and non-chaotic attractors can be densely packed throughout a parameter interval. For this reason, as well as the fact that parameter estimates are not exact and come at best with confidence intervals, in these regions of parameter space the best point of view to take would not be that a particular times series of data has a specific type of model attractor type – chaotic, for example. It might be better to say in such cases that the population's dynamics are "influenced by chaos" [**20**].

Example 2.6. *Figure 6(a) shows the same bifurcation diagram for the juvenile/adult model in Example 2.2 shown in Figure 5, but extended over a larger interval of n values. After the invariant loop bifurcation at $n \approx 8.1$, there occurs a complicated sequence of bifurcations in which periodic cycles play a role as well as other complicated chaotic and strange attractors. In Figure 6(b) we see the break up of an invariant loop into a strange attractor consisting of several distinct pieces.*

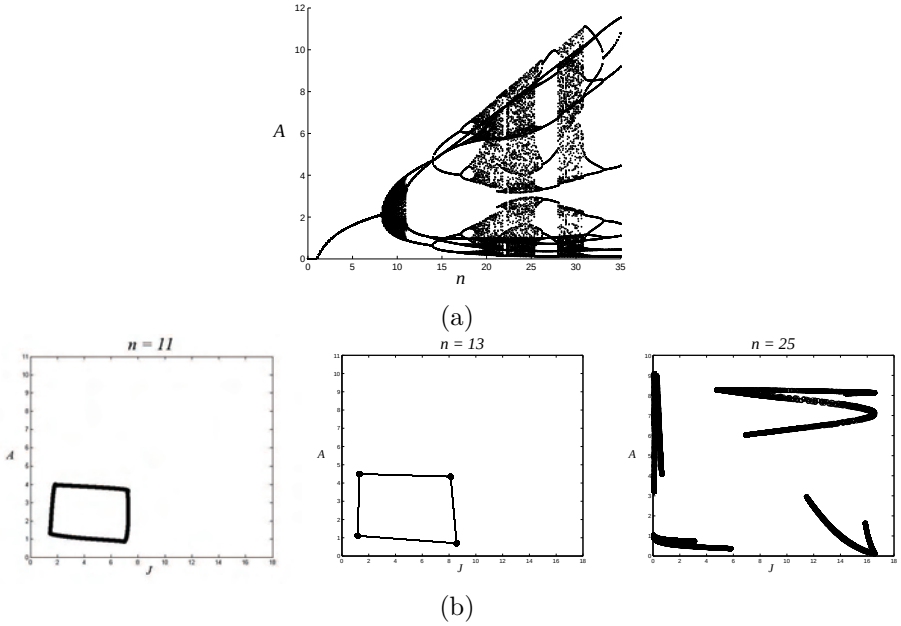

FIGURE 6. Let $\tau_{21} = 0.5$, $\tau_{22} = 0.1$ and $c = 0$ (no Allee effect) in the juvenile-adult matrix model (2.6). (a) The bifurcation diagram shows complicated bifurcations after the invariant loop bifurcation at $n \approx 8.1$. (b) The attractor evolves from an invariant loop at $n = 11$ to a 4-cycle at $n = 13$ to a strange chaotic attractor at $n = 25$.

The parameter n is a convenient parameter to use in the general theory and discussion above. It is well defined in a general setting, there often exists an explicit formula relating it to model parameters, and it has an important biological interpretation (the inherent net reproductive number). In some applications, however, we might want to study the dynamics of a matrix model as a function of a different parameter, one that appears explicitly in the model equations. Theorems generalizing Theorems 2.1 and 2.3 appear in [**4**] (Theorems 1.2.3 - 1.2.6) for matrix models in which $F(0)$ is linear in a parameter μ, that is, for matrix models of the form

$$x(t+1) = (A + \mu B + H(\mu, x))\, x \tag{2.7}$$

where $|H(\mu, x)| = O(|x|)$ near $x = 0$. These theorems provide more alternatives for the bifurcating continuum $\mathcal{C}^+$ than are given in Theorem 2.1 (e.g., see Theorem 4.1 in Lecture 4). Nonetheless, the direction of bifurcation of the positive equilibrium branch still determines the stability of the equilibria, although the relationship

between direction and stability can be reversed. An example using the death rate μ_a in the LPA model of Example 1.4 as the bifurcation parameter appears in [**4**].

Example 2.7. *Figures 7 and 8 show two sample bifurcation diagrams for the LPA model in Example 1.4 using μ_a and c_{pa} as bifurcation parameters. In Figure 7 the $x_1 = A$ component of the attractor is plotted against the bifurcation parameter μ_a. In Figure 7(a) we see a period doubling bifurcation at $\mu_a \approx 0.045$ and an invariant loop bifurcation at $\mu_a \approx 0.83$. There is a re-equilibration that occurs because of a subcritical 2-cycle bifurcation of the equilibrium at $\mu_a \approx 0.565$ and a 2-cycle saddle-node bifurcation at $\mu_a \approx 0.59$; this sequence of bifurcations is seen more clearly in Figure 7(b).*

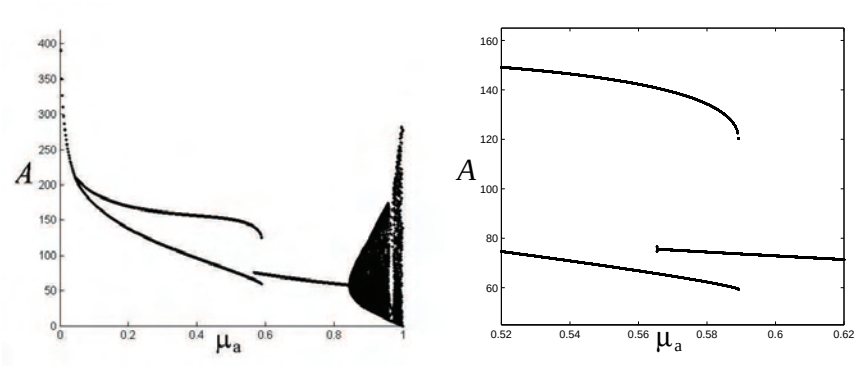

(a) (b)

FIGURE 7. (a) and (b) show bifurcation diagrams for the LPA model in Example 1.4 using the adult stage death rate μ_a as the bifurcation parameter. The $x_1 = A$ component of the attractor is plotted against μ_a. Other parameter values are $b = 10$, $\mu_l = 0.2$ and $c_{ea} = c_{ea} = c_{pa} = 0.01$.

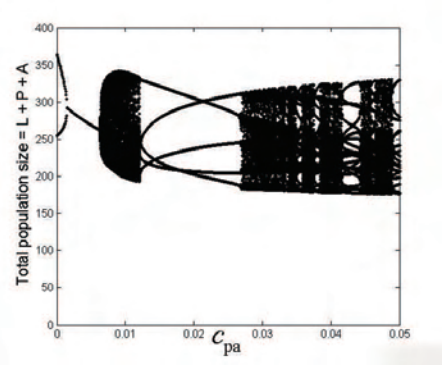

FIGURE 8. In this bifurcation diagram for the LPA model in Example 1.4, the total population size $x_1 + x_2 + x_3 = L + P + A$ of the attractor is plotted against the bifurcation parameter c_{pa}. Other parameter values are $b = 10$, $\mu_l = 0.2$, $\mu_a = 0.95$ and $c_{ea} = c_{ea} = 0.01$.

In Figure 8 the total population size $x_1+x_2+x_3 = L+P+A$ of the attractor is plotted against c_{pa}. A 2-cycle at $c_{pa} = 0$ undergoes a reverse period doubling bifurcation to an equilibrium at $c_{pa} \approx 0.0025$. The equilibrium undergoes an invariant loop bifurcation at $c_{pa} \approx 0.00625$. Further bifurcations occur for large c_{pa} values, bifurcations that lead to period locking windows (such as the large window on the interval $0.012 < \mu_a < 0.03$) interspersed with strange, chaotic attractors.

EXERCISES

Exercise 8. If $(n^*, 0)$ is a bifurcation point of $x = nLx + h(n, x)$, prove that n^* must be a characteristic value of L

Exercise 9. (a) Calculate the quantity κ for the LPA model in Example 1.4. (b) Show that for $n > 1$ there exists exactly one nontrivial equilibrium and it is positive.

Exercise 10. (a) Consider the linear scalar ($m = 1$) difference equation $y(t+1) = ay(t) + b(t)$ where $0 \le a$ is a constant satisfying $0 \le a < 1$ and where $b(t)$ is a bounded sequence: $0 \le b(t) \le b_\infty < \infty$, $t = 0, 1, 2, \cdots$. Show that solutions $y(t)$ with non-negative initial conditions $y(0) = c \ge 0$ are bounded. Specifically, show there exists a constant $\beta > 0$ (independent of c) and an integer $t^*(c)$ such that $0 \le y(t) \le \beta$ for $t \ge t^*(c)$. (b) Consider the linear scalar equation $z(t+1) = \alpha(t)z(t) + \beta(t)$ for which the coefficients $\alpha(t)$, $\beta(t)$ satisfy $|\alpha(t)| \le a < 1$ and $|\beta(t)| \le b(t) \le b_\infty < \infty$, $t = 0, 1, 2, \cdots$. Show that solutions $z(t)$ are bounded. Specifically, show there exists a constant $\beta > 0$ (independent of c) and an integer $t^*(c)$ such that $0 \le |z(t)| \le \beta$ for $t \ge t^*(c)$. (c) Consider the nonlinear scalar ($m = 1$) difference equation $w(t+1) = \alpha(t, w(t)w(t) + \beta(t, w(t))$ for which the coefficients satisfy $|\alpha(t, w)| \le a < 1$ and $|\beta(t, w)| \le b(t) \le b_\infty < \infty$ for $t = 0, 1, 2, \cdots$ and all $w \in R^1$. Show that solutions $w(t)$ with are bounded. Specifically, show there exists a constant $\beta > 0$ (independent of c) and an integer $t^*(c)$ such that $0 \le |w(t)| \le \beta$ for $t \ge t^*(c)$.

Exercise 11. (a) Consider the juvenile/adult model in Example 2.2

$$J(t+1) = cbA(t)e^{-A(t)}J(t) + be^{-A(t)}A(t)$$
$$A(t+1) = \tau_{21}J(t) + \tau_{22}A(t)$$

under the assumption that $c > 0$ satisfies the inequality

$$c < e\frac{\tau_{21}}{1-\tau_{22}}.$$

Recall $n \triangleq b\tau_{21}/(1-\tau_{22})$. Show the model is dissipative when

$$1 < n < \frac{e}{c}\frac{\tau_{21}}{1-\tau_{22}}.$$

(Hint: Use the results in the preceding Exercise 10.) (b) Show the model is uniformly persistent if, in addition, $0 < \tau_{21}, \tau_{22} < 1$.

Exercise 12. Analyze the transcritical bifurcation at $(J, A) = (0, 0)$, $n = 1$ of juvenile/adult model

$$J(t+1) = b_1A(t)\frac{1}{1+A(t)}J(t) + b_2\frac{1}{1+A(t)}A(t)$$
$$A(t+1) = \tau_{21}J(t) + \tau_{22}A(t).$$

Here $n \triangleq b_2\tau_{21}/(1-\tau_{22})$ is the inherent net reproductive number.

Exercise 13. The $m = 2$ dimensional matrix model with fertility and transition matrices

$$F = \begin{pmatrix} 0 & b \\ 0 & 0 \end{pmatrix}, \quad T = \begin{pmatrix} 0 & 0 \\ \tau_{21} & \tau_{22} \end{pmatrix}$$

describes a population classified by juveniles and adults: $x_1 = J$ and $x_2 = A$ respectively. If all three parameters b, τ_{21}, and τ_{22} are constants, the model is linear. Consider the nonlinear model in which τ_{21} is replaced by $\tau_{21} f(J)$ where f models a fractional decrease in juvenile maturation due to the density J of juveniles. Thus, assume $b > 0$, $0 < \tau_{21}, \tau_{22} < 1$ and $f(0) = 1$, $0 < f(J) \leq 1$ for $J \geq 0$. (a) Let $f(J) = 1/(1 + J)$. Show positive equilibria exist for, and only for, $n > 1$ and that they are (locally asymptotically) stable. (b) Let $f(J) = e^{-J}$. Show positive equilibria exist for, and only for, $n > 1$. Show that there exists an $n_{cr} > 1$ such that the positive equilibria are (locally asymptotically) stable for $1 < n < n_{cr}$. What happens at $n = n_{cr}$?

LECTURE 3

Experimental Case Studies

The influential papers of Li and Yorke [**51**] and Lord May [**52, 28, 53**] ignited interest in complex (chaotic) dynamics that can result from simple rules described by difference equations. Ecologists (and other scientists) found this possibility fascinating for several reasons. From a philosophical point of view, there is a paradigm shift away from the long held notion that complex phenomena require complex causes (and, conversely, that only simple phenomena result from simple causes) to one in which extraordinarily complex phenomena can result from simple rules. Indeed, dynamics virtually indistinguishable from randomness or stochasticity can result from simple deterministic rules. From a practical perspective, there arose the possibility that some of the apparent randomness or "noise" that is so common in population and ecosystem data might have a deterministic – indeed a simple (i.e., low dimensional) – component. This opened up new avenues to explore for possible explanations of observed patterns in data and, thereby, to deeper insights that might lead to improved predictability.

Complex sequences of bifurcations and complex/chaotic dynamics are readily found in nonlinear matrix models for the dynamics of a structured population. This is also true for more complicated situations such as multi-species interactions, models with spatial structure, temporally forced models for non-constant environments, and so on. This being the case, we are led to wonder about the role that such bifurcations and chaotic dynamics might play in the ecological world. During the last few decades there have been many studies that examine ecological data for the possibility of chaotic dynamics. Besides the inherent similarity between chaos and stochasticity and the difficulty in distinguishing between the two[1], there are numerous obstacles to carrying out such investigations, including the lack of sufficiently long time series of data, the measurement accuracy (sampling error) of data, and the general lack of quantitatively accurate, mechanistic mathematical models on which to base analyses [**58**].

A study of how a population responds to perturbations in vital parameters is an alternative to the approach of focusing on time series of observations from a population in a specific set of circumstances and trying to identify and classify the dynamic as a particular type or another. This approach is directly based on what a model bifurcation diagram is all about. It is a common approach in science and engineering to disturb, perturb, change, and tweak a system in order to gain an understanding from its responses into how it works. Furthermore, from a practical point of view, the question of how a population or ecosystem responds to certain

[1]Chaos fascinated scientists and mathematics because of the "noise-like" complexity that can arise from deterministic models (especially simple low dimensional models). Of course complicated fluctuations arising from noisy systems are not unexpected or surprising. So, mathematical chaos is of interest because it is deterministic phenomenon.

perturbations is an important one in a world in which hardly any biological system is unperturbed by natural and/or human causes. This is important not only for the purposes of basic scientific understanding, but for the purposes of managing biological resources, preserves, and parks; controlling of invasive species and diseases; insuring the survival of species endangered by resource loss, environmental change, habitat pollution, habitat fragmentation, and so on. Nonlinearity can imply unexpected responses to perturbations. Fluctuations of increasing complexity caused by dynamic bifurcations, for example, can be surprising.

Of course, one usually cannot study an ecosystem by subjecting it to a scheme of perturbations any more that an astrophysicist can subject the solar system or a galaxy to an experimental plan of perturbations to see how it will respond. One can however, like a physicist, study smaller and isolated components of a system in order to gain insight into its workings. Similarly, there can be a role for focused experimental study of population systems in manageable and controllable situations in promoting an understanding how larger communities and ecosystems are put together. To quote E. O. Wilson ([**68**], p.111)

> When observation and theory collide, scientists turn to carefully designed experiments for resolution. Their motivation is especially high in the case of biological systems, which are typically far too complex to be grasped by observation and theory alone. The best procedure, as in the rest of science is first to simplify the system, then to hold it more or less constant while varying the important parameters one or two at a time to see what happens.

The main goal of experimental studies is not always limited to a better understanding of the particular biological species involved (although that results too). Such studies help to develop methods for the study the dynamics of populations in general, to test and corroborate various principles and dogma, to find explanations of observed phenomena that previously had none, and (as inevitably occurs in such studies) discover new phenomena and develop methods to deal with them. Thus, even if a study is specialized to a particular biological organism (as is, of course, necessarily the case in experimental studies) a broader goal is to demonstrate, elucidate, refine, extend, and discover new principles, methods and hypotheses for the dynamics of ecological populations which apply to and aid in the study of other systems.

In order to carry out a study of nonlinear dynamics along the lines discussed above it is necessary to connect mathematical models with data. There is a plethora of mathematical models in theoretical ecology and population dynamics. Precious few, however, have been tied to experimental or observed data to a standard of description and predictability found in the so-called "hard" sciences. This is not to say that mathematical models have not contributed to ecological theory. They have in fact helped establish most of the fundamental principles found today in ecology (exponential growth, logistic growth, carrying capacity, r and K selectors, competitive exclusion, ecological niche, limiting similarity, predator-prey oscillations, and so on). Nonetheless, if mathematical models are to rise above only qualitative accuracy and verbal metaphors, they must be more closely tied to data. This is far easier said than done; ecosystems are notoriously complex.

One approach to the study of biological systems is that advocated by Wilson in the quote above. In that spirit, the focus here will be on some successful case

studies that utilized a manipulatable experimental system. The goal in looking at these selected research projects is to touch (briefly) on several general topics: some methods for connecting models to data; the use of a dynamic model to design experiments for the purpose of testing theoretical predictions and tenets; the ability of models to provide new explanations for dynamic patterns observed in data; how models can predict unexpected and counter-intuitive phenomena that subsequent experiments corroborate; and how the interdisciplinary wedding of mathematical models with controlled experimental studies can lead to the discovery of new phenomena and new general principles.

Any mathematical model is based on assumptions concerning the biological and physical mechanisms to be included in the model and those to be left out. These assumptions might, of course, need re-evaluation when the model predictions are confronted with data. Suppose we have available a time sequence of observations $y(0), y(1), \cdots, y(q)$ of the stage distributions. How well does the model describe this data? How are the model parameters chosen to best describe the data (i.e., how is the model parameterized or calibrated)?

Of course, the model might be so fundamentally inappropriate that it simply cannot describe the data well no matter what parameter values are used. This eventuality should ultimately be revealed in an evaluation of the parameterized model, in which case we take the model back to the drawing board for an overhaul. If the parameterized model is deemed an adequate descriptor of the data, then it can be further evaluated by analyzing how well it describes other data not used in the parametrization procedure. (Perhaps some of the original data is left aside for this purpose, or other data sets are obtained by further experiments.) If the model passes these evaluations, then we gain some confidence in its ability to describe – and more importantly predict – the dynamics of the population under various (possibly changed) circumstances. Experiments based on the model's predictions, whose data bear out the model's predictions, provide further validation of the model's accuracy.

Some model parameters might be known from experiments designed specifically to measure them. Other parameters we can estimate from the data $y(i)$. Given numerical values for its parameters, the model makes a prediction $x(t+1)$ from each data point $y(t)$. We do not expect this prediction to be 100% accurate, of course, and so there is a residual, i.e., there is a nonzero difference between the model prediction $x(t+1)$ and the actual observation $y(t+1)$. Most model parametrization and evaluation procedures are based, in one way or another, on the study of these residuals.

Nonzero residuals arise for many reasons. The model could be perfectly accurate and the data contain measurement errors. Of course, no model perfectly describes a population's dynamics and residuals can also arise because some processes are inaccurately described in the model (or even excluded from the model). Such processes can be deterministic and/or stochastic. Stochastic events (noise) is ubiquitous in ecological data. This point will forcibly be brought home in the case studies below in which experimental results contain significant noise even though they were obtained from highly controlled laboratory experiments with virtually no measurement error.

One way to incorporate stochasticity into a model is include both the deterministic and the stochastic aspects of the population's dynamics into the model's

components. We can use the resulting stochastic model to study residuals, to parametrize and validate the model, to obtain descriptions of data from the validated model, and ultimately to make model predictions.

There are many ways to build a stochastic version of a matrix model (1.7). One class of stochastic models (called nonlinear autoregression models or NLAR models) adds a random term to the deterministic model (the skeleton) on an appropriate scale, i.e., for an appropriate transformation of the data y (say $w = g(y)$) and the model predictions x ($n = g(x)$). "Appropriate" here means that the model is transformed so that additive noise has a stabilized variance. This means in the $m = 1$ dimensional case, for example, that the stochastic model has the form $n(t+1) = f(n(t)) + E(t)$ where for each t the random variable $E(t)$ has mean 0 and a constant variance $v = \sigma^2$ that is independent of t. (It is also assume that $E(0)$, $E(1)$, $E(2), \cdots$ are independent random variables.) For the multi-variate case $m > 1$, $E(t)$ is a vector of random variables with means 0 and a (symmetric) variance-covariance matrix Σ.

Ecologists distinguish two fundamental types of noise in biological systems: environmental noise and demographic noise [**53**]. Roughly speaking, environmental noise arises from random disturbances that effect all individuals in the same way whereas demographic noise is due to random differences among individuals (differences in birth rates, survival rates, etc.).

In [**11**] an instructive example is given that illustrates one way to model environmental and demographic stochasticity. (Also see [**17**].) Consider a simple survival process and let μ denote the fraction of individuals who die during a unit of time. In the case of environmental stochasticity μ is a random variable. The total number of survivors at time $t+1$

$$x(t+1) = (1-\mu)\, x(t) \tag{3.1}$$

is then a random variable that depends on the number of individuals $x(t)$ present at time t. The mean of this random variable is $Mean\,[1-\mu]\, x(t)$ where $Mean\,[1-\mu]$ is the mean of the random variable $1-\mu$ and the variance is

$$Var\,[x(t+1)] = Var\,[1-\mu]\, x^2(t) = Var\,[\mu]\, x^2(t) \tag{3.2}$$

where $Var\,[\mu]$ is the variance of the random variable μ.

In the case of demographic stochasticity each individual in the population has an independent random chance of dying with probability μ. In this case the number of survivors $x(t+1)$ at time $t+1$ is a binomial random variable of $x(t)$ trials with success probability $1-\mu$. The mean of this random variable is $(1-\mu)\, x(t)$ and the variance is

$$Var\,[x(t+1)] = (1-\mu)\, \mu x(t)\ . \tag{3.3}$$

Many statistical techniques are available for stochastic processes of the (nonlinear autoregressive or NLAR) form

$$n(t+1) = f(n(t)) + E(t) \tag{3.4}$$

where $E(t)$ is a normal random variable with mean 0 and a constant variance σ^2 and $E(0)$, $E(1)$, $E(2)$, ... are uncorrelated. The nonlinear function f defines the deterministic skeleton $n(t+1) = f(n(t))$, i.e., the the nonlinear model that describes the model dynamics in the absence of noise [**65**]. The stochastic survival processes

derived in the motivational illustrations above for environmental and demographic stochasticity do not have the additive form (3.4).

One approach to take is to transform the state variable $x(t)$ in such a way that the stochastic process for the resulting transformed random variable $n(t)$ does have (at least approximately) the NLAR form (3.4). Toward this end, define a transformation $n(t) = g(x(t))$ by means of a function g satisfying

$$n = g(x), \qquad \frac{dg(x)}{dx} > 0.$$

Consider the first order Taylor polynomial approximation

$$n(t+1) = g(x(t+1)) \approx g(x(t)) + g'(x(t))(x(t+1) - x(t))$$

in which $x(t+1)$ is a random variable conditioned on a given value of $x(t)$. Then, from basic facts about the variance of a random variable, we find that

$$\begin{aligned} Var(n(t+1)) &\approx Var[g(x(t)) + g'(x(t))(x(t+1) - x(t))] \\ &= Var[g'(x(t))(x(t+1) - x(t))] \\ &= Var[x(t+1) - x(t)](g'(x(t)))^2 \\ &= Var[x(t+1)](g'(x(t)))^2. \end{aligned}$$

If the (conditional) variance of $x(t+1)$ is a function of $x(t)$, so that

$$Var[x(t+1)] = v(x(t)), \tag{3.5}$$

then

$$Var[x(t+1)] \approx v(x(t))(g'(x(t)))^2 \ .$$

The goal is to find a transformation $g(x)$ so that $Var[x(t+1)]$ is approximately constant. That is to say, we need to solve the differential equation

$$v(x)(g'(x))^2 = c_0$$

for $g(x)$, where c_0 is a (yet to be specified) constant. The general solution of this equation is

$$g(x) = \int \left(\frac{c_0}{v(x)}\right)^{1/2} dx + c_1 \tag{3.6}$$

where c_1 is another arbitrary constant.

For a stochastic model for which the variance of $x(t+1)$ is a function $v(x(t))$ of $x(t)$ as in (3.5), the function $g(x)$ defined by (3.6) transforms the model (approximately) to an NLAR of the form (3.4) for the transformed state variable $n(t) = g(x(t))$. The arbitrary constants c_0, c_1 of integration in (3.6) are free to be used to simplify $g(x)$ in any convenient way. Here are two fundamental examples.

For environmental stochasticity, from (3.2) we found above that

$$v(x) = Var[\mu]\, x^2$$

which by (3.6) leads to the transformation

$$g(x) = \left(\frac{c_0}{Var[\mu]}\right)^{1/2} \ln x + c_1.$$

For demographic stochasticity, from (3.3) we have

$$v(x) = \mu(1-\mu)\, x.$$

which by (3.6) leads to the transformation

$$g(x) = \left(\frac{c_0}{Var\,[\mu]}\right)^{1/2} \ln x + c_1.$$

In these expressions c_0 and c_1 are arbitrary constants. If $c_0 = Var\,[\mu]$ and $c_1 = 0$ in the environmental case and $c_0 = (1-\mu)\mu/4$ and $c_1 = 0$ in the demographic case, then transformations simplify to log and square root transformations $g(x) = \ln x$ and $\sqrt{x}$ respectively.

Thus, one way to model environmental stochasticity for a $m = 1$ dimensional model with deterministic skeleton

$$x(t+1) = f(x(t))$$

is to add noise on the logarithm scale or, equivalently, by means of the stochastic equation

$$x(t+1) = f(x(t))e^{E(t)}. \tag{3.7}$$

Here we proceed by analogy with the survivorship model and assumes that the variance of $x(t+1)$ conditioned on $x(t)$ is approximately constant on the logarithmic scale. (In a higher dimensional case $m > 1$, random exponential factors appear in each component of the skeleton model.)

Similarly, a model for demographic stochasticity utilizes a square root transformation of the state variables. Thus, in the $m = 1$ case, a demographic stochastic version of the model is $x(t+1) = \left(\sqrt{f(x(t)} + E(t)\right)^2$, although $\sqrt{f(x(t)} + E(t)$ should be replaced by 0 if it turns out to be negative:

$$x(t+1) = \left(\frac{\phi(t) + |\phi(t)|}{2}\right)^2 \text{ where } \phi(t) \triangleq \sqrt{f(x(t))} + E(t).$$

Example 3.1. *An environmental stochastic version of the Ricker equation (1.3) adds a random variable $E(t)$ (of mean 0) to the equation on the log scale:*

$$x(t) = be^{-cx(t)}x(t)e^{E(t)}.$$

A demographic stochastic version of the discrete logistic equation (1.2) adds a random variable $E(t)$ on the square root scale:

$$x(t+1) = \left(\frac{\phi(t) + |\phi(t)|}{2}\right)^2, \quad \phi(t) \triangleq \sqrt{b\frac{1}{1+cx(t)}x(t)} + E(t).$$

A stochastic version of the juvenile/adult model in Example (2.2) in which both life cycle stages are subject to environmental noise is

$$J(t+1) = \left[cbA(t)e^{-A(t)}J(t) + be^{-A(t)}A(t)\right]e^{E_1(t)}$$

$$A(t+1) = \left[\tau_{21}J(t) + \tau_{22}A(t)\right]e^{E_2(t)}$$

where $E(t) = (E_1(t), E_2(t))$ is a vector of random variables $E_i(t)$.

Given $q+1$ observations $y(0), y(1), \cdots, y(q)$ what is the probability that these stage vectors could be produced by a stochastic version of a matrix model (1.7), for some choice of the model parameters? A formula that relates this probability to model parameters is the *likelihood function*, and parameters that maximize this function are *maximum likelihood parameter (ML) estimates*.

A maximum likelihood function is basic to statistical inference and analysis, e.g., for estimation of parameters, the calculation of confidence intervals, and hypothesis testing. (For more about maximum likelihood methods and comparisons with other methods see [**18**].) A requirement for deriving an explicit formula for a ML function is a distributional assumption about the random variable $E(t)$. A mathematical formula for the *pdf* (probability distribution function) of $E(t)$ permits a formula for the ML function and to maximize it as a function of the model parameters. This maximization calculation can rarely be done analytically and usually must be done numerically with the aid of a computer.

Consider the $m = 1$ dimensional case. Suppose $w(0), w(1), \cdots, w(q)$ are transformed observations of a population's transformed state variable. Let $n(t+1) = f(n(t), \theta) + E(t)$ be the model equations for the transformed variable, where θ is the vector of model parameters appearing in the deterministic skeleton f. If the random variables $E(t)$ are normally distributed with mean 0 and variance $v = \sigma^2$ (and uncorrelated in time), then the probability of observing $w(t)$ given the observation $w(t-1)$ is

$$\frac{1}{\sqrt{2\pi v}} \exp\left(-\frac{(w(t) - f(w(t-1), \theta)^2}{2v}\right)$$

and the probability of observing the q data points $w(1), \cdots, w(q)$ is the product

$$\Lambda \triangleq \prod_{t=1}^{q} \frac{1}{\sqrt{2\pi v}} \exp\left(-\frac{(w(t) - f(w(t-1), \theta)^2}{2v}\right).$$

$\Lambda = \Lambda(\theta, v)$ is a function of the parameters θ and v. The maximum likelihood parameter estimates for θ and v are those that maximize $\Lambda(\theta, v)$.

In practice one often maximizes instead the log likelihood function

$$l(\theta, v) \triangleq \ln \Lambda(\theta, v) = -\frac{1}{2} q \ln 2\pi - \frac{1}{2} q \ln v - \frac{1}{2v} S(\theta)$$

where

$$S(\theta) \triangleq \sum_{t=1}^{q} (w(t) - f(w(t-1), \theta))^2 \tag{3.8}$$

is the *sum of squared (transformed) one-step residuals*. It is possible to show that the maximum occurs for

$$v = \frac{1}{q} S(\theta) \tag{3.9}$$

where θ maximizes

$$l(\theta, S(\theta)/q) = -\frac{1}{2} q \ln(2\pi) - \frac{1}{2} q \ln\left(\frac{1}{q} S(\theta)\right) - \frac{q}{2}.$$

Thus, in the $m = 1$ case, the maximum likelihood estimates of the parameters in the vector θ are those that minimize the sum of squared residuals $S(\theta)$ together

with v defined by (3.9).[2] (For $m > 1$ the ML estimates for the parameters in θ do not necessarily minimize $S(\theta)$.)

Example 3.2. *Consider the time sequence of* 101 ($q = 100$) *data points plotted in Figure 9. To calculate the ML parameter estimates of the environmental stochastic version (3.7) of the discrete logistic (1.2) we transform the data to the log scale and minimizes $S(\theta)$, given by (3.8) with $f(w, \theta) = \ln b + w - \ln(1 + ce^w)$, with respect to b and c (with the help of a computer program). The results are (recall (3.0))*

$$b \approx 13.14, \quad c \approx 0.06059, \quad v \approx 0.08163.$$

For the environmental stochastic version of the Ricker model (1.3) the ML estimates are, obtained , using the same minimization procedure with $f(w, \theta) = \ln b + w - ce^w$, are

$$b \approx 7.591, \quad c \approx 0.009751, \quad v \approx 0.009702.$$

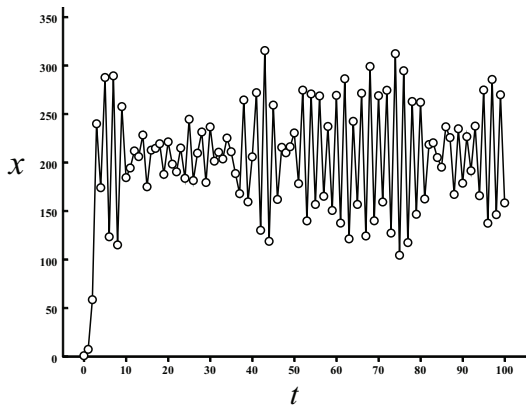

FIGURE 9. This plot shows the data points used to calculate ML parameter estimates for the environmental stochastic versions of the logistic and the Ricker models in Example 3.2.

All solutions of the discrete logistic (1.2) model equilibrate for $b > 1$. If we were to accept the parameterized version of this model in Example 3.2, then we would conclude that the data in Figure 9 is a noisy equilibrium $x_e = (b-1)/c \approx 200.4$. On the other hand, if we were to accept the parameterized Ricker model in Example 3.2 then, because the Ricker model (1.3) predicts a 2-cycle (that oscillates between $x_1 \approx 166.6$ and $x_2 \approx 249.2$) when $b = 7.591$, we would conclude that the data in Figure 9 is a noisy 2-cycle. Which of these different conclusions should we accept?

One of the fundamental issues with regard to connecting models to data is the assessment or validation of a model. This is not usually an easy problem. It can involve, among other things, a considerable amount of sophisticated statistical analyses and careful considerations of the model's assumptions (both the deterministic and the stochastic portions) with regard to the biological mechanisms thought to most predominant in the application. In the end we reject a model as inadequate or

[2]Note that the one-step residuals in $S(\theta)$ are not those calculated from points on an orbit of the model. This method does not fit an orbit to the data.

accept it (at least tentatively) as reasonably accurate. There is no clear cut, algorithmic path to arrive at such decisions and there will always be room for criticism and improvement.

One way to confront a model with data is to think in terms of two aspects: an analysis of fit and an analysis of prediction. So, in Example 3.2 we ask "how well does the environmental stochastic logistic" fit the data in Figure 9? We can also ask that question of the environmental stochastic Ricker, and then ask "which does a better job"? Answers help us choose between these two models, but it must be remembered that there are other (infinitely many other) models. Having made a choice, we then ask how well the chosen model predicts, in the sense that it also adequately describes other data not used in the parametrization estimation procedure. This other data might be subset of a given data set deliberately set aside for this purpose. Or it might be another data set collected as a replicate or from a different experiment or set of observations. A strong test of the model is to test its ability to make accurate predictions (perhaps even unusual or unexpected predictions) that are subsequently corroborated by controlled experiments or observations. This is perhaps the ultimate goal in modeling building and validation. Accurate and trustworthy predictions not only serve scientific and engineering purposes, but serve to further validate the model and add confidence in its accuracy. This prediction aspect of a model will be a an important component of the case studies described below.

Returning to Example 3.2, we consider only a couple of basic ways to quantify an assessment of the two models. We want more than a plot of a model orbit superimposed on the data that visually looks good. For example, if we plot the solution of the parameterized logistic starting from the initial data point $x(0) = 1$ in Example 3.2, we obtain an orbit that rather convincingly "goes through the middle of the data". Similarly, however, the orbit of the parameterized Ricker also looks visually reasonable when superimposed on the original data time series. See Figure 10. We need quantifiable ways to assess the results of these two parameterized models.

One way to proceed is to recall that the stochastic version of the model claims that the one-step residuals are normally distributed with a mean 0 and with the estimated variance v. The residuals constitute a data set that we can test for normality using a number of normality tests from statistics. We will not dwell on these statistical issues here, but simply be content with a visual inspection histogram plots the residuals shown in Figure 11. The residuals from the ML parameterized Ricker model appear more normally distributed than those of the ML parameterized logistic model.

Moreover, the residuals of the parameterized Ricker model have a smaller variance (by an order of magnitude) than those of the parameterized logistic model. That is to say, a one-step prediction of the deterministic Ricker model, made from the data point at time t, is more often closer to the next data point at time $t+1$ than is the one-step prediction of the deterministic logistic model. One way researchers quantify this observation is by means of an "R-squared" value:

$$R^2 \triangleq 1 - \frac{v}{v_0}$$

where $v = S/q$ (see (3.8)) and v_0 is the variance of the transformed data $w(t)$:

$$v_0 \triangleq \frac{1}{q}\sum_{t=1}^{q}\left(w(t) - w_0\right)^2, \qquad w_0 \triangleq \frac{1}{q}\sum_{t=1}^{q} w(t).$$

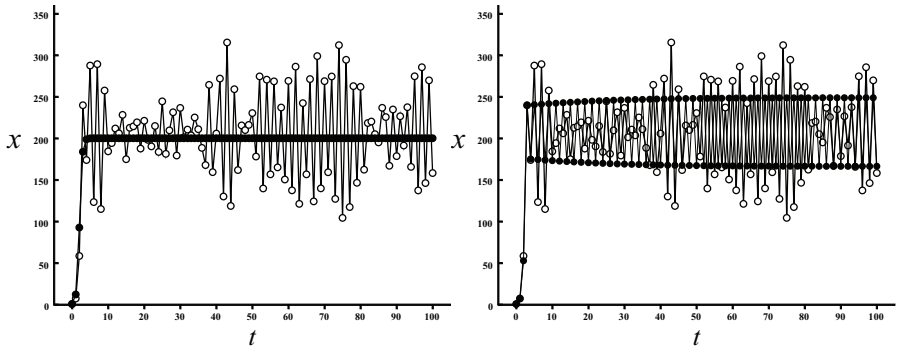

(a) (b)

FIGURE 10. (a) and (b) show plots of the orbits of the discrete logistic and the Ricker models (1.2) and (1.3), respectively, superimposed on the data from Figure 9 used to parametrize the models. The initial condition is the first data point $x(0) = 1$ and the parameters are the ML parameters estimated in Example 3.2. It should be pointed out that the ML parameter estimates in, for example (a), were not obtained by minimizing the residuals between the data and this orbit (as in a regression analysis). This common procedure does not calculate the maximum likelihood estimates of any obvious model and almost certainly not the one being parameterized. The ML parameter estimates, which minimize the residuals from the conditional one-step predictions (i.e., the residual at $t + 1$ conditioned on starting from the data point at t), are not explicitly designed to "optimally fit an orbit through the data".

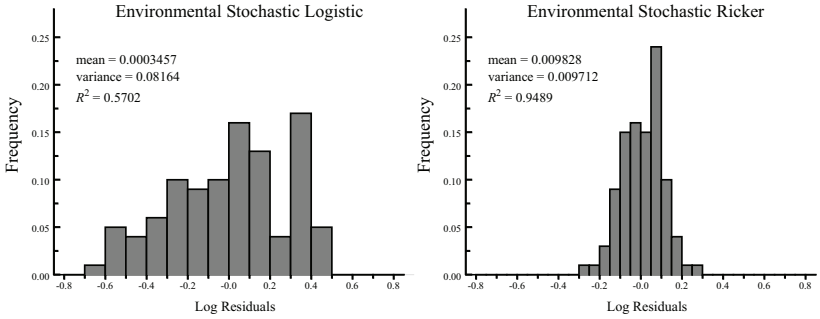

(a) (b)

FIGURE 11. These plots show frequency histograms of the one-step conditional log residuals of the ML parameterized logistic and Ricker, using the data in Figure 9. For the data in Figure 9, $v_0 = 0.1899$ and $w_0 = 5.258179$.

One says that R^2 is "the fraction of the variability in the data that is explained by the model". So, if $R^2 = 0.75$, then one says that the model "explains 75%" of the variability in the data. R^2 values reported in Figure 11 show that the ML parameterized logistic model explains 57% of the variability in the data in Figure 9, while the ML parameterized Ricker model explains 95%. On this basis, it is

reasonable to conclude that the Ricker model is the more accurate model for this data set.[3]

Figure 12 shows histograms of the log residuals of both parameterized models applied to another data set from the same source – a replicate data set. The *predictive* accuracy of the Ricker model is reflected in a virtually unchanged R^2 value from that of the Ricker model fit shown in Figure 11, even though these data were not used to estimate the ML parameters for the model. In contrast, the R^2 value of the parameterized logistic drops over 50% in going from the fitted data to the predicted data sets.

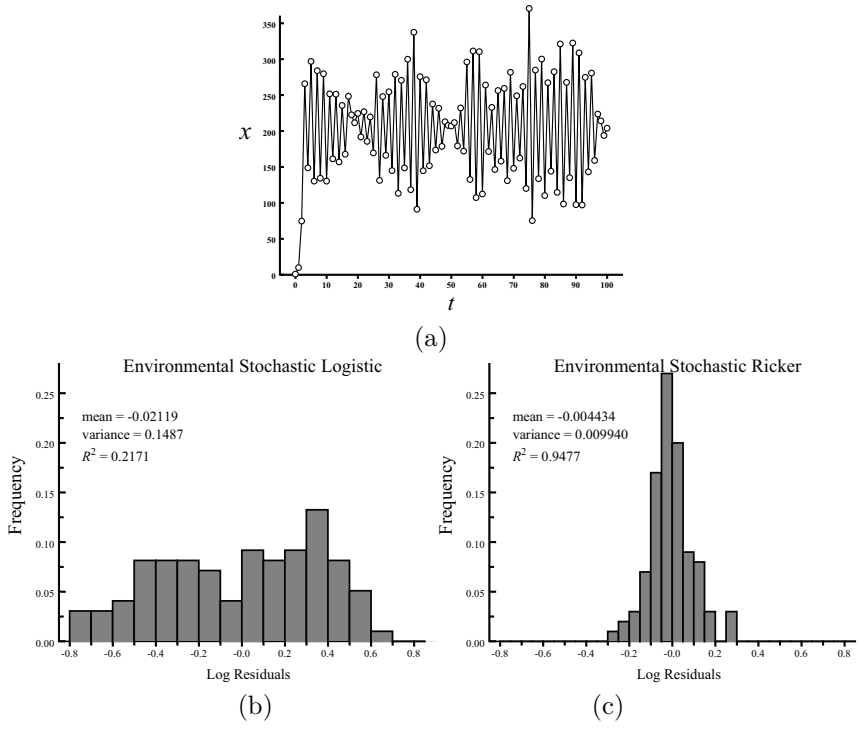

FIGURE 12. The plot in (a) shows data from a replicate of the experiment that produced the data in Figure 9 used for the ML parametrization of the logistic and the Ricker models in Example 3.2. Frequency histograms of the one-step log residuals of the parameterized logistic and Ricker appear in (b) and (c). Note that the data in (a) was not used to obtain the ML parameter estimates. The R^2 value of the logistic model drops over 50% while that of the logistic remains nearly unchanged.

[3]To compare models one shouldn't always simply compare their variances or R^2 values. Such a comparison is reasonable if both models have the same number of estimated parameters. However, if one model has more parameters than the other, then its smaller R^2 value might be due more to its extra parameters than to its superior structure as a model. When two models have a different number of parameters, one should use statistics that compensate, or penalize, for the number of parameters when making comparisons. One example is the *Akaike information criterion* (AIC) which quantifies the relative goodness-of-fit of statistical models, given a sample of data. The model is preferred that has the smallest quantity $A \triangleq 2k + q\ln(S/q)$ where k is the number of estimated parameters.

Figure 13(a) shows a data set taken from a laboratory experiment. The data show the adult numbers in an insect population (the beetle *Tribolium castaneum*) obtained from census counts taken at two week intervals. The ML parameter estimates for the environmental stochastic Ricker model turn out to be

$$b \approx 3.5733, \qquad c \approx 0.03026, \qquad v \approx 7.756. \tag{3.10}$$

The histogram of one step log residuals in Figure 13(b) shows a marked departure from a normal distribution, a fact that leads us to reject this model as a description of this data set. Indeed, if we were to accept the model as accurate then we would conclude that the data in Figure 13(a) is a (very) noisy equilibrium. (The Ricker map as an equilibrium $x_e = c^{-1} \ln b \approx 42.09$ for the parameter estimates of b and c above.) Yet the data in Figure 13(a) seems to have distinctive non-equilibrium patterns that we might reasonably expect to be amenable to model description and explanation. We can critique the rejected environmental Ricker in two ways. Its deterministic skeleton (the Ricker equation) could be ill formulated for the data in Figure 13(a) and/or the environmental stochastic version might be a poor description of the noise present in the system. We can, of course, modify either of these model components in any of innumerable ways.

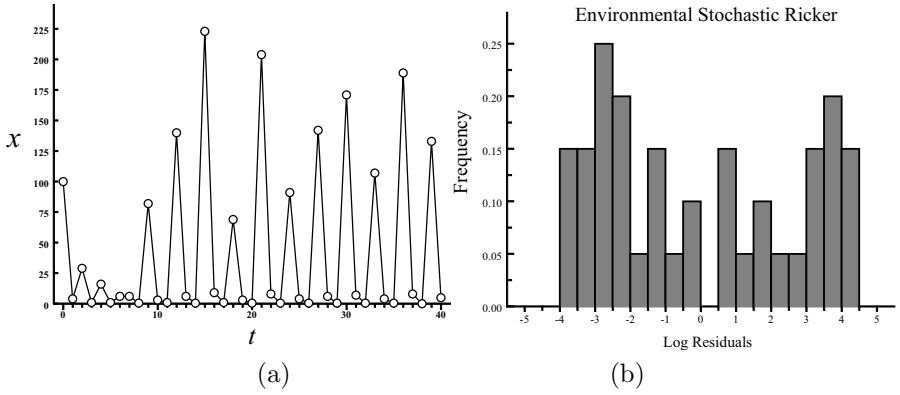

FIGURE 13. If we use the data time series in (a) to estimate the parameters in the environmental stochastic Ricker model (using the maximum likelihood parameter estimation procedure), we obtain the estimates (3.10). However, the histogram of one-step log residuals in (b) show a significant departure from a normal distribution.

To obtain guidance in the construction of an improved model, one should consider the important features of the population's biology and the physical features of its environment. A good model is based on mechanisms that are known, or thought to be, significantly important in determining the population's dynamics. Biologists who study a particular species generally have a very good idea what such mechanisms are. Indeed, biologists (by the nature of their training) generally know a formidable number of details about a species, and it is often a challenge for a modeler, when collaborating with a biologist, is to determine which of a plethora of facts and details known to the biologist are to be incorporated into the model. Mathematicians (by their training) tend to be generalists and the contrast with the focused attention to a complexity of details that is characteristic of a biologist's

understanding of a biological system can make for lively (and frustrating) conversations in this regard. Keeping in mind that a model with enough parameters can fit virtually any data set, whether it is a reasonable model or not (after all, one can find a high degree polynomial that passes through any number of given data points, with all residuals equal to 0!), we try to find a few mechanisms that dominate the dynamics of the population and build from them a model with as few parameters as possible.

The data in Figure 13 are adult population numbers of an insect species, the beetle *T. castaneum*. This beetle is a significant agricultural pest, and as a result researchers have extensively studied this species (and others from the genus *Tribolium*) since the early 20th century. Grown in a finite volume of medium[4], which is regularly renewed, sustainable populations must regulate their numbers in some manner. The species *T. castaneum* regulates its population growth by means of cannibalism.

T. castaneum has four main life cycle stages, egg, larval, pupal, and adult, and the moving stages cannibalize the non-moving stages (although larvae cannibalism of pupae is rare). This suggests a model with at least four state variables. However, the egg stage is relatively short (2 to 3 days) compared to the census time (which is taken to be the length of the larval stage, namely 2 week). We can utilize this fact to construct a model with three state variables: larvae, pupae, and adults. In this way, by using a stage structured model we are able to account for interstage cannibalistic interactions, the mechanisms known to drive the dynamics of this species.

It turns out that the pupal stage in *T. castaneum* is very nearly of the same duration as the larval stage (two weeks). As a result a matrix model for the population density distribution vector $x = \text{col}\,(L, P, A)$ has the form of a Leslie age-structured model with only the third stage fertile, i.e., a projection matrix $P = F + T$ with

$$F = \begin{pmatrix} 0 & 0 & b \\ 0 & 0 & 0 \\ 0 & 0 & 0 \end{pmatrix}, \quad T = \begin{pmatrix} 0 & 0 & 0 \\ 1-\mu_l & 0 & 0 \\ 0 & 1-\mu_p & 1-\mu_a \end{pmatrix}.$$

Here the μ_i are the stage mortality fractions and b is the larval recruitment per adult per unit time.

The cannibalism of eggs by larvae and adults decrease larval recruitment b by a fraction dependent on the density of larvae and adults L and A. Cannibalism of pupae by adults decreases adult recruitment fraction $1 - \mu_p$ by an additional fraction dependent on A (but not on L since observation has shown that for *T. castaneum* pupal cannibalism by larvae is negligible). In this model Ricker type exponential nonlinearities account for the cannibalistic interactions. The rationale for this is as follows.

Cannibalism in *T. castaneum* occurs, as far as careful observation has revealed, because of random encounters among individual adult or larvae (as they continually move and feed in the medium) with eggs or pupae (which are stationary). If we begin with the assumption that the probability of an encounter between one larva, say, with an egg during Δt time units is proportional to Δt and inversely proportional to the volume V of the culture medium [**2**], then the probability that

[4]For many species of *Tribolium* growing in a finite container of medium is not far removed from their "natural" habitat, since they have grown in containers of grain products stored by humans for centuries. For example, evidence of *Tribolium* has been found in ancient Egyptian urns.

the egg is not encountered by the larva is $1 - c_{el}\Delta t/V$ where $c_{el} > 0$ is a constant of proportionality (the cannibalism coefficient). The probability that the egg will not encounter the larva during one full unit of time is $(1 - c_{el}\Delta t/V)^{1/\Delta t}$. If L larvae are present, then the egg's survivorship probability is the product

$$\Pi_{i=1}^{L} (1 - c_{el}\Delta t/V)^{1/\Delta t} = (1 - c_{el}\Delta t/V)^{L/\Delta t}.$$

As $\Delta t \to 0$, the probability approaches $\exp(-c_{el}L/V)$. A similar argument holds for adult/egg and hence the probability that an egg survives cannibalism by both larvae and adults is $\exp(-c_{el}L/V)\exp(-c_{ea}A/V)$. As a result larval recruitment is reduced from bA in the absence of cannibalism to $bA\exp(-c_{el}L - c_{ea}A)$ when cannibalism is taken into account. A similar argument introduces a fractional reduction term $\exp(-c_{pa}A)$ in the survivorship of pupae to the adult stage.

The result of introducing exponential nonlinearities into the transition matrix T is the LPA model in Example 1.4, namely

$$\begin{aligned} L(t+1) &= bA(t)\exp\left(-\frac{c_{el}}{V}L(t) - \frac{c_{ea}}{V}A(t)\right) \\ P(t+1) &= (1-\mu_l)\,L(t) \\ A(t+1) &= (1-\mu_p)\,P(t)\exp\left(-\frac{c_{pa}}{V}A(t)\right) + (1-\mu_a)\,A(t). \end{aligned} \tag{3.11}$$

This $m = 3$ dimensional matrix model has eight parameters. The medium volume V is known in experimental situations. Moreover, extensive observations have shown that pupal survivorship of *T. castaneum* (and for the species in the genus *Tribolium* in general) in the absence of cannibalism is virtually 100% and therefore we can safely assume $\mu_p = 0$. This leaves six parameters to be estimated, unless of course some are controlled as part of an experimental protocol.

The three life cycle stages of *Tribolium* are easily recognized and can be routinely counted. (The example data in Figure 13(a) is, in fact, the $x = A$ stage component from a time series of all three life cycles L, P and A.) We can estimate the model parameters from a time series of L, P, A data by using the maximum likelihood procedure described above extended to the multivariate case when x is a vector. (Sometimes we can instead estimate a parameter another ways. For example, if dead adults are counted then we can estimate μ_a from the results.)

Suppose $w(0), w(1), \cdots, w(q)$ are transformed observations of a population's transformed ($m > 1$ dimensional vector) state variable. Let $n(t+1) = f(n(t), \theta) + E(t)$ be the model equations for the transformed (vector) variable, where θ is the vector of model parameters appearing in the deterministic skeleton f. Here we assume that $E(t)$ is a vector of normal distributions (a multivariate normal distribution) with mean 0 and (symmetric) variance-covariance matrix Σ. The variances of the components of $E(t)$ appear on the diagonal and covariances among the components appear in the off diagonal elements. In situations in which a disturbance that occurs in one stage is unlikely to effect other stages then the covariances can be assumed equation to 0 and Σ is diagonal. The likelihood function is

$$\Lambda \triangleq$$

$$\prod_{t=1}^{q} \frac{1}{\sqrt{(2\pi)^m \det\Sigma}} \exp\left(-\frac{(w(t) - f(w(t-1),\theta))^* \Sigma^{-1} (w(t) - f(w(t-1),\theta))}{2}\right)$$

and the log likelihood function is

$$l \triangleq \ln L = -\frac{m}{2} q \ln(2\pi) - \frac{1}{2} q \ln\left(\det \Sigma\right) - \frac{1}{2} \sum_{t=1}^{q} \left(w(t) - f(w(t-1),\theta)\right)^* \Sigma^{-1} \left(w(t) - f(w(t-1),\theta)\right).$$

(The asterisk denotes the transpose of a vector or matrix.) The log likelihood function l is a function of the skeleton's parameters in the vector θ and of the entries in the (symmetric) variance-covariance matrix Σ. The ML parameter estimates are those values of θ and the entries in Σ that maximize l.

It turns out that the maximum occurs when $\Sigma = RR^*/q$ where R is the matrix with the residuals $w(t) - f(w(t-1),\theta)$ as columns. If this expression for Σ is substituted into l, then the problem becomes to maximize the resulting formula for l as a function of θ only (and calculate Σ from R, in which the residuals are calculated using the calculated ML estimate for θ).

Stochastic versions of the LPA model (3.11), and various modifications of the model, constitute the basis for over fifteen years of experimental and theoretical investigations of a long list of nonlinear phenomena in population dynamics[5]. Reports on these studies appear in [**1, 3, 11, 56**]. I will give here only a summary report of some of these studies.

There are several levels on which we can view the results of the studies. First of all, we can consider them to be illustrative examples of the modeling methodology discussed above. Second, the studies will demonstrate that a mathematical model can "work" in population dynamics; that is to say, a mathematical model can make accurate quantitative descriptions of the dynamics of a biological organism and, importantly, can make predictions that are later born out by controlled experiments. Thus, we can go beyond the statement that a model is only "qualitatively correct", as is found so often in the literature, and make a small contribution towards raising population dynamics and theoretical ecology above verbal metaphors. Third, these studies often provide explanations for observations that had no previous explanation. Fourth, an accurately validated model can make surprising predictions, sometimes counter-intuitive, that are subsequently corroborated by experimental observations. This leads to a deeper understanding of the population's dynamics and provides an ability to predict the outcome of disturbances and altered circumstances (environmental perturbations, generic changes, application of control policies, etc.). Fifth, new phenomena are discovered and new mathematical methodologies are developed to handle them. And finally, going beyond the particular experimental system used, the studies often elucidate, confirm, and sometimes challenge accepted ecological principles and tenets. This provides some guidance to the study of nonlinear dynamics of other systems, both laboratory and field systems. Each of these aspects have played, and continue to play, a role in the application of the LPA model to experimental cultures of *Tribolium* [**3**].

[5]The senior researchers involved are R. F. Costantino (University of Arizona), R. A. Desharnais (California State University at Los Angeles), Brian Dennis (University of Idaho), Shandelle M. Henson (Andrews University), Aaron A. King (University of Michigan) and J. M. Cushing (University of Arizona). Many undergraduate and graduate students have also made significant contributions over the years. A list of contributors can be found in [**11**].

In the experiments described below, all three life cycle stages are counted every two weeks, and the cultures returned to their habitats with refreshed medium[6]. In some experiments manipulations are performed at this time in order to force certain values for selected parameters in the model. Many studies, particularly those in which demographic stochasticity predominate, have shown that the covariances (off diagonal entries in Σ) are quite small compared to the variances (diagonal entries) and as a result these covariances are assumed equal to 0 in the stochastic model. These details, which can change from one experimental protocol to another, reflect on the number of parameters in the model that need to be estimated.

Details of a preliminary parametrization of the LPA model using historical data for *T. castaneum* and an environmental stochastic version of the LPA model appear in [**18**]. This initial study used an environmental stochastic model because population sizes were large and demographic stochasticity is generally less of a factor in large populations [**53**]. In subsequent studies and experiments, in which large oscillations resulted in numbers in individual life cycle stages being small (but not total population size), it was found that a demographic stochastic version of the LPA model was a more accurate model [**19, 20**]. Details of the statistical analyses that validates the model are found in [**18**] (also see [**11, 20**]).

The goal of one study was to demonstrate that a biological population would traverse a model predicted bifurcation route-to-chaos. A preliminary experiment tested the predictive capability of the parameterized LPA model for cultures of *T. castaneum* on the basis of a relatively simple bifurcation diagram. In that experiment the bifurcation sequence results by varying the adult death rate μ_a from its parameterized value (holding all other parameters fixed). Varying μ_a between its allowable limits of 0 and 1, we obtain a bifurcation diagram similar to the that in Figure 7(a). An experiment placed replicated cultures of *T. castaneum* at selected positions in the bifurcation diagram, in order to corroborate that the predicted bifurcations would indeed occur in the dynamics of beetle cultures. (There were also unmanipulated and replicated control cultures.) The historical data used to obtain the preliminary parameter estimates for the LPA model came from a strain of *T. castaneum* that was no longer available for experiments. As a result, the preliminary bifurcation experiment used different strains. The experiment was conducted twice, once for two *T. castaneum* strains called SS and RR. For this reason, the data obtained from the experimental treatments were used to re-parametrize the LPA model and re-calculate the bifurcation diagram (which, as it turned out, did not significantly change from the original bifurcation diagram). The result for the SS strain appears in Figure 14 (taken from [**11**]).

The arrows in Figure 14 indicate where experimental cultures of *T. castaneum* (strain SS) were placed by experimental manipulation of the adult survival fraction μ_a. The model predictions for these treatments, for increasing μ_a, were: an equilibrium at $\mu_a = 0.04$, a 2-cycle at both $\mu_a = 0.27$ and 0.50, another equilibrium at $\mu_a = 0.7$, and quasi-periodic fluctuations at $\mu_a = 0.96$. The state space plots of the data shown in Figure 15 visually show how these predictions were born out by the experimental data. Model evaluations using a variety of tests and analyses provide

[6]R. F. Costantino and R. A. Desharnais carried out the experiments in laboratories at the University of Rhode Island and University of Arizona. Details of the experimental protocols can be found in [**11**] and the research papers cited therein.

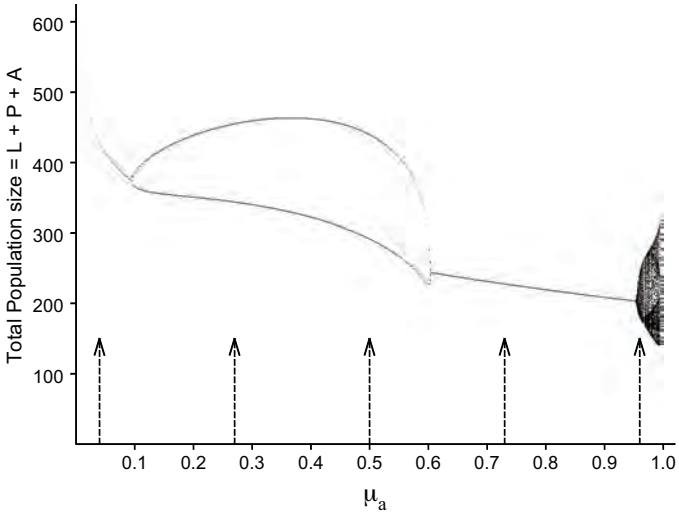

FIGURE 14. The bifurcation diagram for the LPA model (3.11) using the adult death rate μ_a as a bifurcation parameter and plotting total population size $L+P+A$ for the attractor. Other ML parameter values, obtained from the environmental stochastic LPA model and data for the SS strain, are $b = 7.483$, $\mu_p = 0$, $\mu_l = 0.2670$, $c_{ea} = 0.009170$, $c_{el} = 0.01200$, $c_{pa} = 0.004139$. (Confidence intervals for these parameters and the estimates for Σ appear in [**11, 20**].) [Reprinted from [**11**], with the permission of Academic Press.]

statistical support for the accuracy of the model predictions [**19**]. (The experiment was duplicated with similar results using the RR strain of *T. castaneum*. See [**11**].)

It is interesting to note that the bifurcation diagram in Figure 14 makes predictions that are perhaps counter-intuitive to what one might expect if the adults in an insect population are subjected to increasing mortality (as part of, say, a pest control procedure). It is probably not intuitive that increasing adult mortality can lead to the crash boom outbreaks of a 2-cycle, followed by a re-equilibration, with very little drop in infestation level, and ultimately at very high mortality rates to quasi-periodic (and hence difficult to predict) outbreaks.

The success in the predictive capability of the LPA model parameterized for the flour beetle *T. Castaneum* in the preliminary bifurcation experiment reported in Figures 14 and 15 was sufficient to encourage an investment into a longer term experiment (which ultimately lasted over 8 years or over 100 generations of beetles). A considerably more complicated LPA model predicted bifurcation diagram – one that involved a route-to-chaos – formed the basis of a more elaborate experiment using *T. Castaneum*. The ML parameter estimates for the RR strain produce the bifurcation diagram in Figure 16 when two parameters are manipulated. Specifically, the adult death rate is held fixed at $\mu_a = 0.96$ and the adult-on-pupae cannibalism rate c_{pa} is varied as a bifurcation parameter[7]. The arrows in Figure 16 show the locations in the bifurcation diagram where replicated treatments were placed in the experiment. These locations were chosen in order to determine if the

[7]See [**11, 20**] for a description of how c_{pa} was experimentally manipulated.

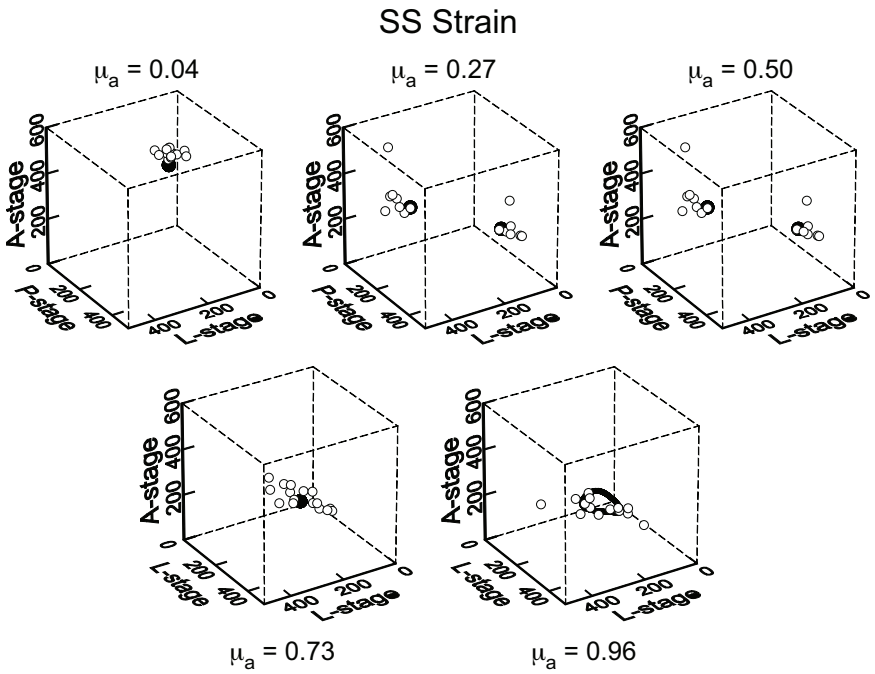

FIGURE 15. Open circles are experimental data points plotted in $m = 3$ dimensional (L, P, A) phase space. Transients are removed in order to emphasize the predicted attractors, which appear as solid points and lines. These results are for the *SS* strain of *T. Castaneum*. A duplicate experiment, with similar results, was carried out for the *RR* strain. [Reprinted from [**11**], with the permission of Academic Press.]

beetle populations would exhibit the distinctively different attractors predicted by the LPA model for these parameter values. Figure 17 shows four examples of the attractors that are possible: equilibria, cycles, quasi-periodic oscillations (invariant loops), and chaotic strange attractors.

The state space plots of the experimental data displayed in Figures 18 and 19 show how the data bear out the model predictions. Model evaluations using a variety of tests and analyses provide statistical support for the accuracy of the model predictions [**20**]. Also note in Figures 18 and 19 how closely simulations from the demographic stochastic LPA model resembles the data.

Of particular interest in Figures 18 and 19 is the treatment at $c_{pa} = 0.35$ which lies in a parameter interval that contains chaotic dynamics. Indeed, for the point estimates of the parameters in this treatment, the model predicted attractor is chaotic. (This has not been proved rigorously in a mathematical sense, but is indicated by computer simulations and the calculation of Liapunov exponents, which measure sensitivity to initial conditions.) As is typical in models with chaotic dynamics, non-chaotic dynamics can be found for nearby parameter values lying within the confidence intervals for the estimated parameters. Nonetheless, for such parameter values it is typical that transients still exhibit chaotic-like dynamics in their approach to the attractor. Moreover, the bifurcation diagram in Figure 20 is quite robust throughout the confidence intervals [**11, 20**]. We could reasonably

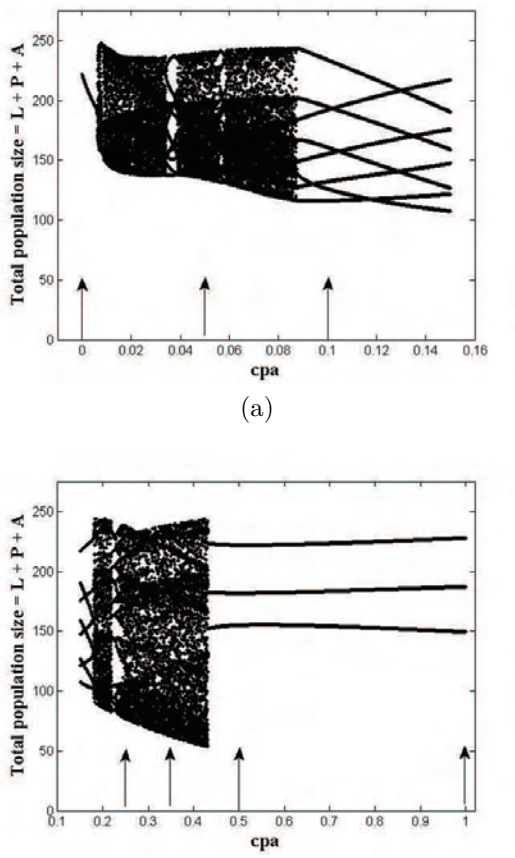

FIGURE 16. Two plots show bifurcation diagrams for the LPA model (3.11) using the adult-on-pupa cannibalism rate c_{pa} as a bifurcation parameter and plotting total population size $L + P + A$ for the attractor. Other ML parameter values for the RR strain (calculated with the environmental stochastic version of the LPA model) are $b = 7.876$, $\mu_p = 0$, $\mu_l = 0.1613$, $c_{el} = 0.01385$, $c_{ea} = 0.01114$, $\mu_a = 0.96$. (Confidence intervals for these parameters and the estimates for Σ appear in [**11, 20**].) In (a) c_{pa} ranges from 0 to 0.15 and in (b) c_{pa} ranges from 0.15 to 1. A post-experiment re-parametrization using the demographic stochastic LPA model forms the basis of detailed statistical analyses of the data, which show slightly better validation results. The bifurcation diagram changes little, however. For a robustness study of the bifurcation diagram see [**11, 20**]. [Reprinted from [**11**], with the permission of Academic Press.]

refer to the data from this treatment as chaotic, even though it is perhaps better to say that the data (i.e., the beetle population's dynamics) are "influenced" by the chaotic dynamics present through the confidence intervals for the parameters.

A study of chaotic dynamics requires a long time series of data and for that reason the three replicates of the $c_{pa} = 0.35$ treatment were continued for over

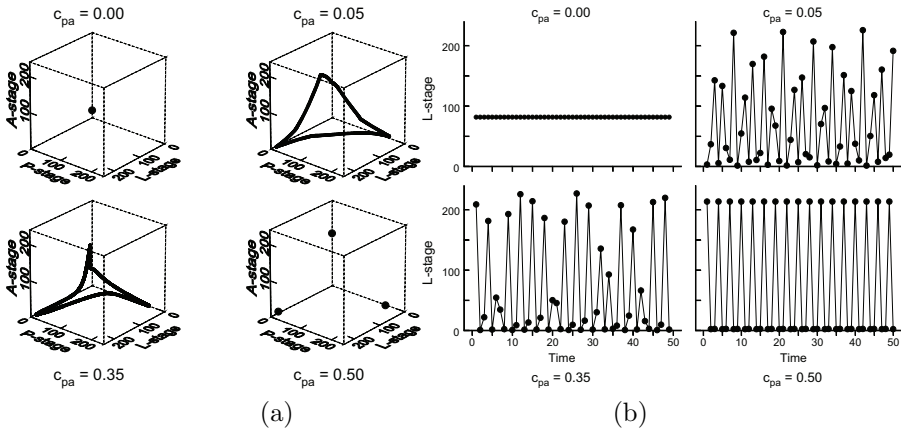

FIGURE 17. (a) These plots show the attractors in phase space at four locations in the bifurcation diagram of Figure 16. At $c_{pa} = 0$ the attractor is an equilibrium. At $c_{pa} = 0.05$ the attractor is an invariant loop. At $c_{pa} = 0.25$ the attractor is an chaotic strange attractor. At $c_{pa} = 1$ the attractor is a 3-cycle. (b) The L stage components of the attractors in (a) appear plotted against time t. [Reprinted from [**11**], with the permission of Academic Press.]

eight years (100 generations). The resulting data provide an opportunity to study various issues concerning chaos as realized in a biological population. I will briefly discuss only three such topics: transients, state space lattice effects, and habitat size.

One way to view the effects of demographic or environmental noise is that such disturbances continually produce transient dynamics. Even should the trajectory of a population reach the vicinity of a deterministic attractor such perturbations will move it away and cause it to follow a transient path back to the attractor. Such perturbations might even be sufficient to place the population far from an attractor in which case the influence of other deterministic entities might come into play, such as the stable and unstable manifolds of non-attracting invariant sets. Such events are frequently observed in the experimental data shown in Figures 18 and 19.

An example appears in Figure 21 which shows the time series from one replicate taken from the treatment at $c_{pa} = 0.05$ in the bifurcation diagram Figure 16. The deterministic model predicted attractor for this treatment is an invariant loop. At the sixteenth week of the experiment a random perturbation placed the data orbit, which until then (for four generations) had been reasonably close to the predicted invariant loop, near the model predicted equilibrium. After residing near this unstable equilibrium for two months (two generations) the data orbit moves away from the equilibrium. This transitory pattern, which lasts 10 weeks until the data orbit returns to the attractor, has a rotational pattern that is remarkably well predicted by the linearization of the model at the equilibrium. Details are explained in the caption of Figure 21.

See [**11**] for other examples of "saddle flybys" and of random visitations near other kinds of unstable invariant sets of the LPA model observed in the data from

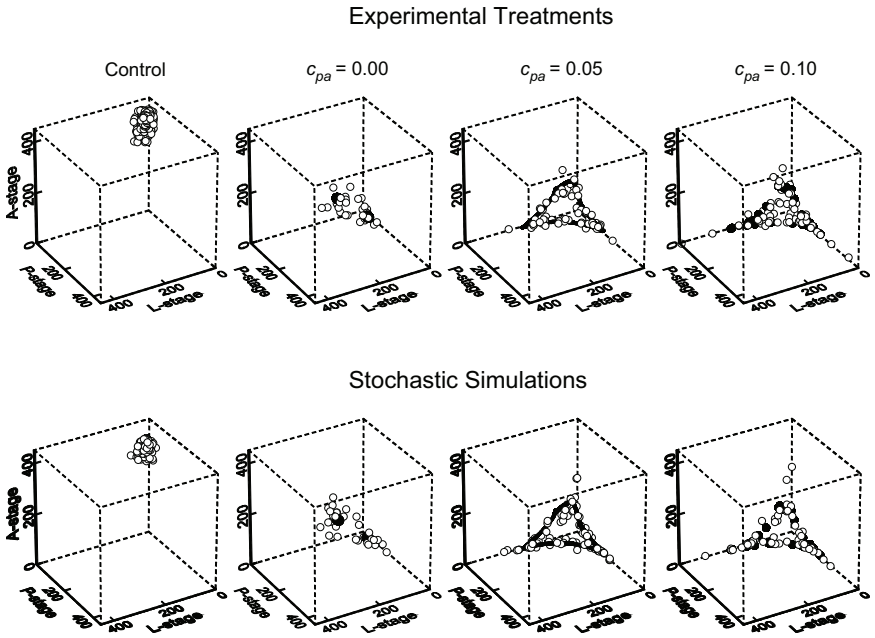

FIGURE 18. The top row of plots shows the experimental data obtained from cultures placed at the selected values of c_{pa} indicated in the bifurcation diagram in Figure 16(a) and from a control culture (which the model predicts should equilibrate). The bottom row of plots shows simulations from the demographic (square root scale) LPA model. [Reprinted from [**11**], with the permission of Academic Press.]

the route-to-chaos experiment. Of course, if the initial condition is not close to the attractor, and especially if it is near an unstable saddle or its stable manifold, then the model would predict such a transient saddle flyby. However, as Figure 21 shows, occasionally a data orbit will exhibit a flyby later in an experiment, after the vicinity of the attractor has been reached. A dramatic case of this is seen in Figure 22 where a saddle equilibrium flyby is observed in one replicate of the chaotic $c_{pa} = 0.35$ treatment during weeks 358 to 380 of the 424 week (106 generation long) experiment. Moreover, a data orbit will occasionally experience several flybys during the course of the experiment. Stochastically caused flybys of unstable invariant sets of other kinds of attractors, such as cycles, are also observed. See [**11**] for examples.

Another effect of random perturbations in populations with oscillatory dynamics can be a change in the phase of the oscillation. For example, the 3-cycle attractor in the $c_{pa} = 1.0$ treatment has three different phases. The three replicates in the treatment, by the end of the experiment, were all out of phase because each had suffered a perturbation that adjusted the phase and, as it happened, all three phases were represented in the three replicates at the end of the experiment. See Figure 23. Other examples of phase shifts are given in [**11**]. One way of explaining these shifts is to view the dynamics in composite phase space, where each point of a cycle is a different equilibrium, and study the stochastic hops from one basin of attraction to another. See [**32**] for several applications of this approach. One take

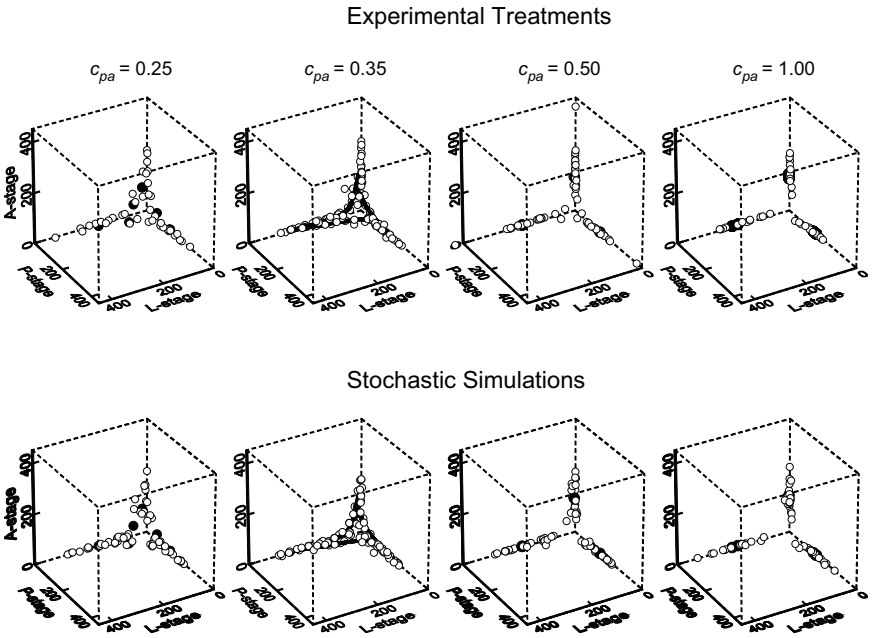

FIGURE 19. The top row of plots shows the experimental data obtained from cultures placed at the selected values of c_{pa} indicated in the bifurcation diagram in Figure 16(b). The bottom row of plots shows simulations from the demographic (square root scale) LPA model. The solid circles and lines are the model predicted attractors using a re-parametrization based on the route-to-chaos data itself (rather than the parameter estimates used Figure 16 for the a priori bifurcation sequence obtained from historical data): $b = 10.45$, $\mu_p = 0$, $\mu l = 0.2000$, $c_{el} = 0.01731$, $c_{ea} = 0.01310$, $\mu_a = 0.96$. [Reprinted from [**11**], with the permission of Academic Press.]

home message here is the erroneous view of a population's dynamics that might result from the common practice of averaging over replicates. For example, out of phase cycles, when averaged, will result in a time series that will likely look like an equilibrium.

A close look at the data from the chaotic treatment $c_{pa} = 0.35$ reveals several distinctive cyclic patterns. Figure 24 shows one cyclic pattern, with period 11 (22 weeks, or 5.5 generations). Chaotic attractors typically contain infinitely many unstable (saddle) cycles and it turns out that a saddle 11-cycle is located on the chaotic attractor predicted for this treatment. Moreover, this 11-cycle has a strong influence on the dynamics of the chaotic attractor (as, for example, a spectral analysis shows) [**11**]. Thus, the attractor of the deterministic LPA model offers an explanation of this particular pattern observed in the data.

Another cyclic pattern – a near 6-cycle pattern – also appears prominently in data from the chaotic treatment $c_{pa} = 0.35$. Examples appear in Figure 25(a). The LPA model does not, however, provide an explanation for this period 6 pattern. Although there is yet no rigorous proof, extensive computer searchers suggest that a 6-cycle solution (stable or unstable) of the LPA model does not exist for the

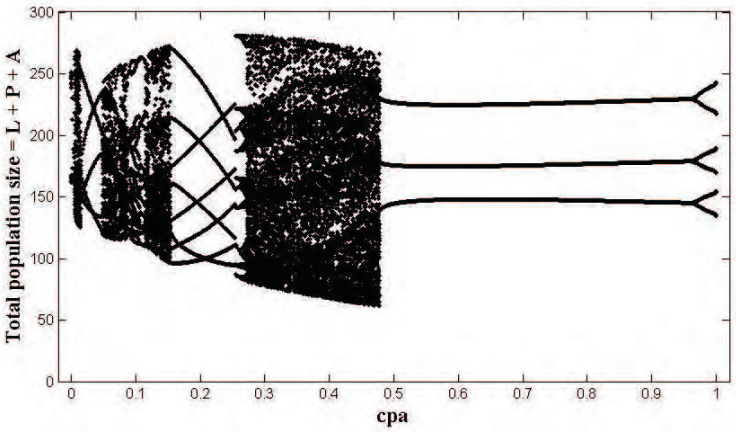

FIGURE 20. The re-calibrated bifurcation diagram the attractors are: an invariant loop at $c_{pa} = 0.00$ (two disjoint loops that appear nearly as a 2-cycle); chaos at $c_{pa} = 0.05$; a 26-cycle at $c_{pa} = 0.10$; an 8-cycle at $c_{pa} = 0.25$; chaos at $c_{pa} = 0.35$; a 3-cycle at $c_{pa} = 0.50$; a 6-cycle at $c_{pa} = 1.00$. [Reprinted from [**11**], with the permission of Academic Press.]

parameter values associated with this experimental treatment. We can, however, find a model explanation for these 6-cycle patterns in an unexpected way.

The census counts of individuals in each life cycle state are, of course, whole integers. The predictions of the LPA model (3.11), on the other hand, are not whole integers; the state space for the LPA model is continuous. A simple mathematical way to get integer predictions from the LPA model is to round the right hand sides of the three model equations. The "integerized" LPA model obtained in this manner, namely

$$\begin{aligned} L(t+1) &= \text{round}\left[bA(t)\exp\left(-\frac{c_{el}}{V}L(t) - \frac{c_{ea}}{V}A(t)\right)\right] \\ P(t+1) &= \text{round}\left[(1-\mu_l)\,L(t)\right] \\ A(t+1) &= \text{round}\left[(1-\mu_p)\,P(t)\exp\left(-\frac{c_{pa}}{V}A(t)\right)\right] \\ &\quad + \text{round}\left[(1-\mu_a)\,A(t)\right], \end{aligned} \tag{3.12}$$

predicts the 6-cycle shown in Figure 25(b), when the model parameters and the initial conditions of the $c_{pa} = 0.35$ treatment are used[8]. The 6-cycle in Figure 25(b) is strikingly similar to the cyclic patterns often observed in the data (such as the examples in Figure 25(a)). Therefore, we can attribute the observed period 6-cycle pattern to the fact that the data reside on a integer lattice in state space, not the continuous state space of the LPA model (3.11). A comparison of Figures 24 and 25 shows intermittent episodes when the data from a portion of one replicate were close to the 11-cycle (the chaotic attractor) and the lattice model predicted 6-cycle.

[8]The same is true if in the third equation the sum is rounded instead of the individual terms.

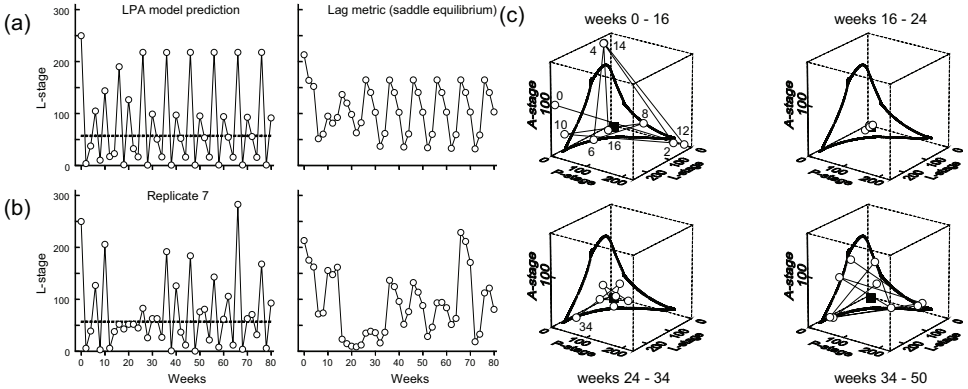

FIGURE 21. [**11, 10**] (a) The LPA model (3.11) does not predict a flyby of the saddle equilibrium for the treatment $c_{pa} = 0.05$ in the bifurcation diagram of Figure 16 when the orbit is started at the experimental initial conditions $(L(0), P(0), A(0)) = (250, 5, 100)$. The lag metric plotted here is the Euclidean distance in $m = 3$ dimensional phase space between data points and the model predicted equilibrium $(L, P, A) = (22.41, 4.625, 334.77)$, as a function of time. (b) Data from one from of the replicates for the $c_{pa} = 0.05$ treatment shows a remarkable visitation near the model predicted equilibrium (which is an unstable saddle). A random perturbation occurs at week sixteen that places the population near this equilibrium. (c) The flyby of the saddle equilibrium by the data orbit is strikingly apparent in state space. Note the star-like rotational motion in state space that occurs during weeks twenty-four through thirty-four when the data orbit leaves the vicinity of the saddle equilibrium. This geometrically distinctive path is in fact predicted by the deterministic LPA model. The linearization at the equilibrium has a conjugate pair of complex eigenvalues $re^{\pm i\theta}$ of magnitude $r \approx 1.265 > 1$ and polar angle $\theta \approx 2.576$ (and a third real positive eigenvalue $\lambda \approx 0.3945 < 1$). This complex eigenvalue implies a rotational motion away from the saddle of approximately $2\pi/\theta \approx 2.439$ radians (139.8 degrees) degrees per step, the motion occurring approximately in a plane parallel to that spanned by the eigenvectors $(L, P, A) \approx (1, -1.166, 0.4860)$ and $(1, -0.3526, -0.2817)$. These characteristics are seen in the orbit data during weeks 24 to 34. [Reprinted from [**10**] with the permission of Elsevier]

Lattice effects (i.e., patterns in data, or in stochastic model simulations, attributed to the fact that data lies on a finite lattice in phase space) in the chaotic treatment $c_{pa} = 0.35$ are the object of study in [**41**]. The take home message from that study is that in order to explain the observed patterns in the dynamics of a biological population it might be necessary to use both a continuous state space model and a discrete state space model (based on whole integer numbers or on fractions as densities obtained from integers divided by an area or volume). What we expect to observe are episodes of lattice cycle attractors (there are generally more than one) randomly mixed by stochastic events with transient dynamics that resemble the continuous state space attractors (and unstable invariant sets, such as saddle

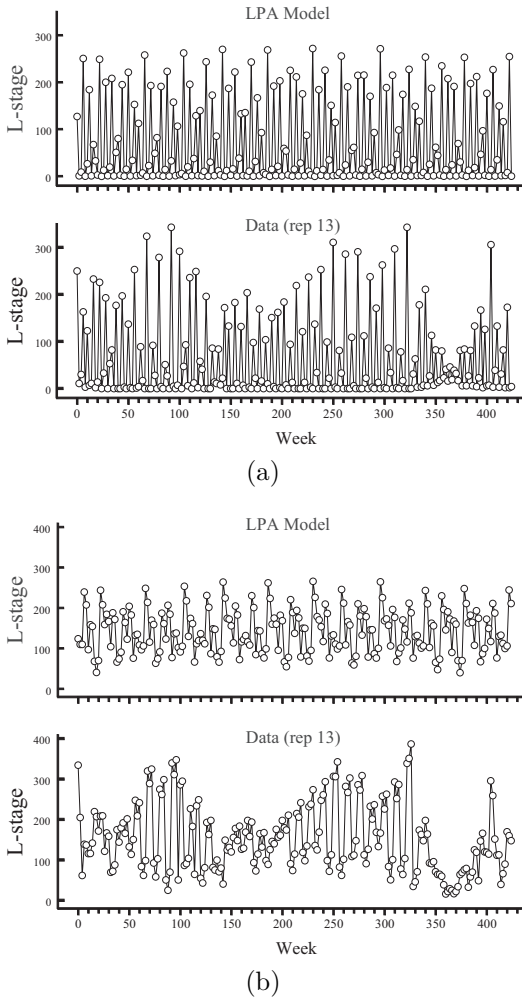

FIGURE 22. (a) A comparison of the L-stage components of one replicate of the chaotic $c_{pa} = 0.35$ treatment to those of the chaotic attractor. Notice the damped oscillations in the replicate's L-stage during weeks 358 to 380. The lag metric plots (distance to model predicted equilibrium in phase space) shown in (b) indicate that this damping is caused by a flyby of the equilibrium.

equilibria and cycles). Figure 26 shows an example of lattice effect phenomena in a stochastic, integerized version of the Ricker model [**11, 34, 40**].

Henson et al. [**35**] give one way to provide a unifying point of view for this conclusion about discrete state space lattice effects and continuous state space attractors. From an probabilistic model that describes the prediction of state variables on a lattice from time t to time $t + 1$ as random variables, we can derive a

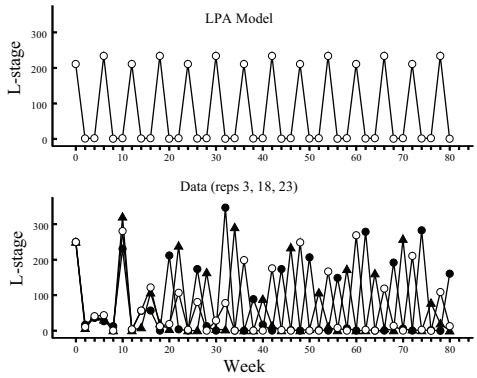

FIGURE 23. The three replicate cultures of the treatment $c_{pa} = 0.1$ whose predicted attractor is a 3-cycle are all out of phase by the end of the experiment.

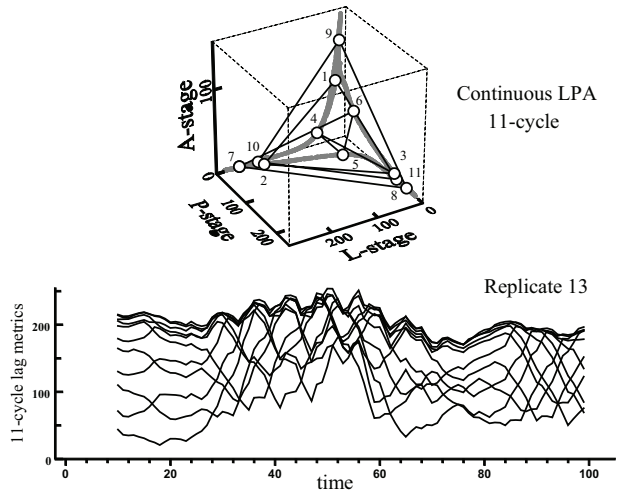

FIGURE 24. An unstable (saddle) 11-cycle is located on the chaotic attractor predicted for the treatment $c_{pa} = 0.35$ in Figure 16(b). This saddle cycle has a significant influence on the dynamics of orbits on and near the chaotic attractor [**11**]. We can view this 11-cycle as a signature of the chaotic attractor. The lag metric for the 11-cycle is the (average) distance that 11 consecutive data points are from the 11-cycle. Since there are 11 phases of the 11-cycle, there are 11 lag metrics associated with the 11-cycle, as shown in the lower plot for a portion of one replicate of data. Low lag metric values and an "unbraiding" of the lag metric plots indicate episodes when the data are near a phase of 11-cycle. Note that 11 time steps in the LPA model span nearly 3 generations of *T. castaneum*.

deterministic prediction in different ways. If the expectation (mean) of the random variable is taken as the prediction at $t + 1$, then the resulting deterministic model has a continuous state space. If instead we take the mode as the prediction at $t+1$, the resulting deterministic model still lies on the lattice.

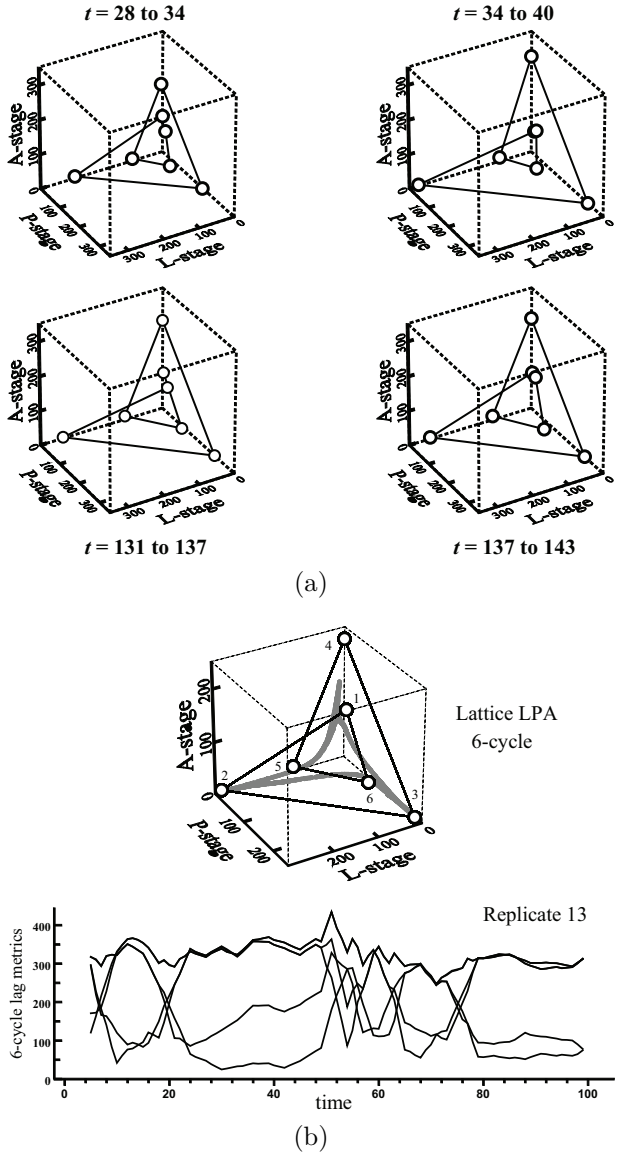

FIGURE 25. (a) Sample temporal 6-cycle patterns appearing in the data from the chaotic treatment $c_{pa} = 0.35$. (b) The upper plot shows the lattice 6-cycle predicted by the integerized LPA model (3.12) for the chaos treatment $c_{pa} = 0.35$ in Figure 16(b). The lower plot shows the lag metrics for the phases of this 6-cycle for a portion of one replicate of data. Low lag metric values and an "unbraiding" of the lag metric plots indicate episodes when the data are near a phase of the 6-cycle.

For example, consider the following probabilistic model for the dynamics of a population with three life cycle stages (such as *Tribolium*) subject to demographic

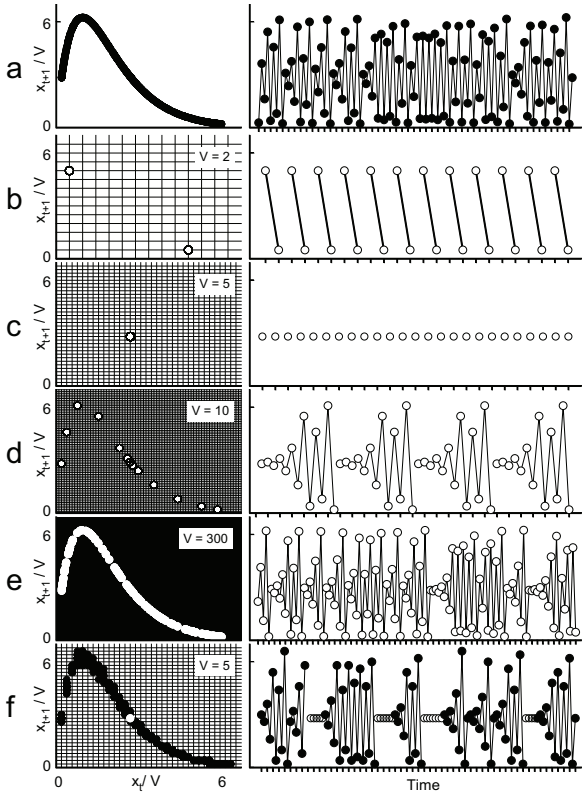

FIGURE 26. Lattice effects are illustrated in these plots using the Ricker model and its integerized version $x(t+1) = \text{round}\left[bx(t)e^{-cx(t)/V}\right]$. As V (habitat volume) increases, the mesh size of the lattice of densities x/V is refined. The plot (a) shows that continuous state space chaotic attractor for the Ricker model with $b = 17$ and $c = 1$. Plots (b)-(d) show the (density) lattice attractor of the integerized Ricker model obtained (in finite time) from the initial condition $x(0) = 5V$ for a sequence of habitat volumes V. The attractor in each case is a periodic cycle (case (c) is a 1-cycle or an equilibrium). On the lattice in plot (e) the 117-cycle lattice cycle resembles the chaotic attractor of the continuous state space in (a). Plot (f) shows a typical simulation of the environmental stochastic version of the lattice Ricker model in volume $V = 5$ when the lattice attractor is an equilibrium. In that plot we see episodes that resemble the equilibrium randomly interspersed with episodes that resemble the chaotic attractor. [From [**34**]. Reprinted with permission from AAAS]

stochasticity [**20, 35**] :

$$\begin{array}{lll} \text{(a)} & L_{t+1} & \sim \text{ Poisson}\left(ba_t \exp\left(-\frac{c_{el}}{V} l_t - \frac{c_{ea}}{V} a_t\right)\right) \\ \text{(b)} & P_{t+1} & \sim \text{ binomial}\left(l_t, 1-\mu_l\right) \\ \text{(c)} & A_{t+1} & \sim \text{ binomial}\left(p_t, \exp\left(-\frac{c_{pa}}{V} a_t\right)\right) + \text{ binomial}\left(a_t, 1-\mu_a\right). \end{array} \tag{3.13}$$

Here "$\sim$" means "is a random variable distributed as". This model assumes mortality is described by a binomial random variable and fertility is described by a

Poisson random variable. (The first equation involving larval recruitment involves both adult fertility and survivorship. The composition of a Poisson and a binomial random variable is a Poisson random variable.) If we extract a deterministic model from the Poisson-binomial LPA model (3.13) by choosing the means of each life cycle stage as the "most likely" observations at time $t+1$, then we obtain the deterministic, continuous state space LPA model (3.11). If instead we choose the modes as the most likely observations, then we obtain a deterministic, integer state space model

$$
\begin{aligned}
L_{t+1} &= \text{floor}\ \left[bA_t \exp\left(-\frac{c_{ea}}{V}A_t - \frac{c_{el}}{V}L_t\right)\right] \\
P_{t+1} &= \text{floor}\ \left[(1-\mu_l)\,(L_t+1)\right] \\
A_{t+1} &= \text{floor}\ \left[(P_t+1)\exp\left(-\frac{c_{pa}}{V}A_t\right)\right] + \text{floor}\ \left[(1-\mu_a)\,(A_t+1)\right],
\end{aligned}
\tag{3.14}
$$

which we call the mode-LPA model. It turns out that this integerized version of the LPA model also predicts a 6-cycle for the chaos treatment $c_{pa} = 0.35$, and simulations of the Poisson-binomial LPA model (3.13) typically exhibit randomly interspersed patterns of the chaotic attractor predicted by the continuous state space LPA model and this discrete state space 6-cycle.

A final point concerning the analysis of the chaotic treatment $c_{pa} = 0.35$ has to do with the dependency of the model predictions on the habitat size V. Notice first that in the continuous state space LPA model (3.11), V is simply a scaling factor. That is to say, if $(L(t), P(t), A(t))$ is an orbit for $V = 1$, then $(L(t)/V, P(t)/V, A(t)/V)$ is an orbit for any $V > 0$. As a result, orbits and attractors remain unchanged when plotted in density phase space $(L/V, P/V, A/V)$. This fact is not true of the mode-LPA model (3.14) or the Poisson/binomial LPA model (3.13).

If L, P, and A are integers, then the points $(L/V, P/V, A/V)$ in density phase space constitute a finite lattice on which densities orbits of the mode and Poisson/binomial LPA models reside. As V increases, the lattice becomes finer. For each value of V orbits of the mode-LPA model (3.14) attain a periodic cycle in finite time. As $V \to \infty$ we might expect that these lattice cycles converge to an attractor of the continuous state space model (3.11). This can be proved true when the attractor is a hyperbolic cycle. For a chaotic attractor, such as in the treatment $c_{pa} = 0.35$ of the route-to-chaos experiment, this fact has not been proved rigorously, although the numerical simulations in Figure 27 suggest it is true for the LPA model. These simulations suggest that as the habitat size increases lattice effects become less pronounced and the continuous state space attractor should becomes more visible. This suggests that a clearer view of the chaotic attractor in the $c_{pa} = 0.35$ treatment would be obtained if the experiment were conducted in larger volumes of media. ($V = 1$ corresponds to the experimental conditions in which 20g of flour media were used.)

There is another phenomena that also implies a clearer view of the chaotic attractor occurs in larger habitats. Consider the Poisson/binomial model (3.13). Each stage variable L, P and A are random variables. The coefficient of variation κ of a random variable measures the amount of variation relative to the mean; namely, $\kappa = s/m$ is the ratio of the standard deviation $s = \sqrt{v}$ to the mean m. For a Poisson random variable, the mean and variance are equal and hence $\kappa = 1/\sqrt{m}$. Consider the larval stage variable L in the Poisson-binomial LPA model. A comparison of

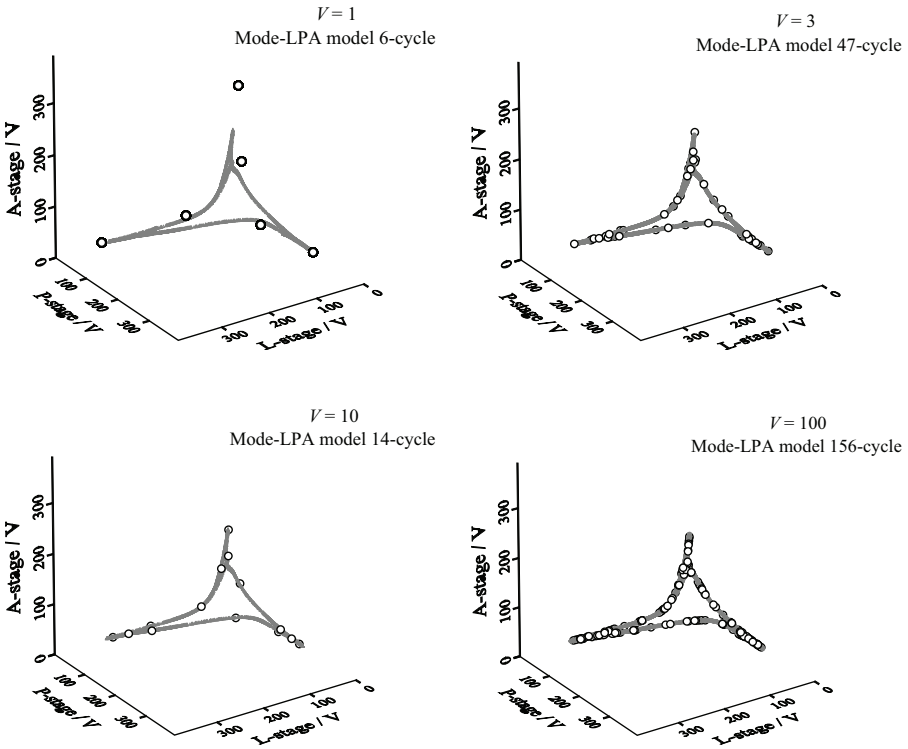

FIGURE 27. From the experimental initial conditions the orbit of the mode-LPA model (3.14) tends to different cycles for different habitat volumes V. Namely, for $V = 1$ the lattice attractor is a 6-cycle, whose points are shown in phase space in relation to the continuous state space chaotic attractor in the upper left plot. For $V = 3$ the lattice attractor is a 47-cycle; for $V = 10$ it is a 14-cycle; and for $V = 100$ it is a 156-cycle. Notice how the lattice cycle attractor seems to converge to the chaotic attractor as V increases.

the coefficient of variation κ_1 of the L component at a point (L, P, A) in volume $V = 1$ with that κ_V of the L component of the corresponding point (LV, PV, AV) in volume V follows from the relationship

$$\begin{aligned} Vm_1 &= VbA \exp\left[-c_{el}L - c_{ea}A\right] \\ &= b\,(AV) \exp\left[-\frac{c_{el}}{V}\,(VL) - \frac{c_{ea}}{V}\,(VA)\right] \\ &= m_V \end{aligned}$$

between the means m_1 and m_V and the calculation

$$\kappa_V = \frac{1}{\sqrt{m_V}} = \frac{1}{\sqrt{V}}\kappa_1.$$

It follows that the coefficient of variation decreases inversely with the square root of habitat volume. Similar calculations show that the same is true for the binomial random variables P and A.

Thus, as habitat volume V increases we expect the demographic noise in model (3.13) to decrease in the sense that the coefficient of variation decreases. This rule

for demographic stochasticity is a familiar one to ecologists [**54**]. (It does not hold for environmental stochasticity.) The rule is usually expressed in terms of increased population size (carrying capacity) rather than habitat size, but, as we have observed, for our system population size scales with habitat size V.

For two reasons, namely decreased lattice effects and decreased demographic noise, the Poisson-binomial LPA model (3.13) predicts clearer deterministic signals in larger habitat sizes V. In particular, experimental data obtained from larger habitat volumes should more closely resemble the chaotic attractor in the $c_{pa} = 0.35$ treatment of the route-to-chaos experiment. See Figure 28. A recently conducted experiment [**21**] tested this prediction by repeating the treatment $c_{pa} = 0.35$ of

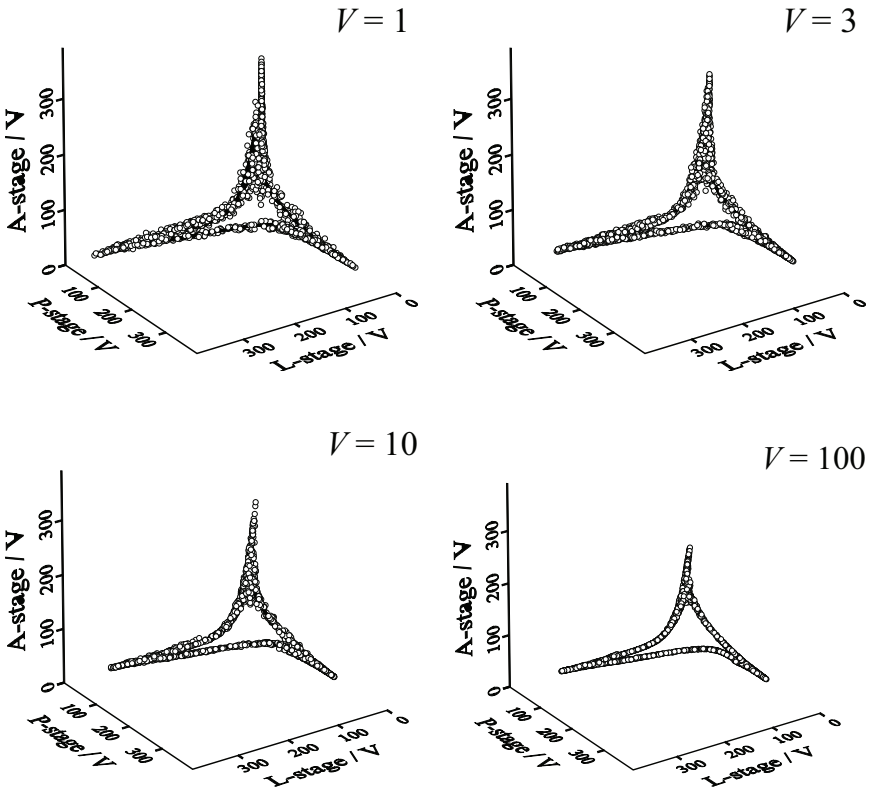

FIGURE 28. Sample simulations of the Poisson-binomial LPA model of length 2,000 show a convergence around the deterministic, continuous state space chaotic attractor predicted by the LPA model for the $c_{pa} = 0.35$ treatment as habitat volume V Increases.

the hunt-for-chaos experiment in a habitat of $60g$, i.e., $V = 3$. Figure 29 shows the data obtained from the experiment in habitat size $V = 3$ together with that from habitat size $V = 1$ and compares both with the LPA model predicted chaotic attractor. The data from the larger habitat is clearly more tightly clustered around the chaotic attractor than the data from the smaller habitat. This observation can be quantified by calculating the mean distance δ_c of the data points from the chaotic attractor. This distance decreased from $\delta_c = 18.39$ in $V = 1$ to $\delta_c = 5.504$ in $V = 3$. We can also quantify the strengthening of the deterministic signal of

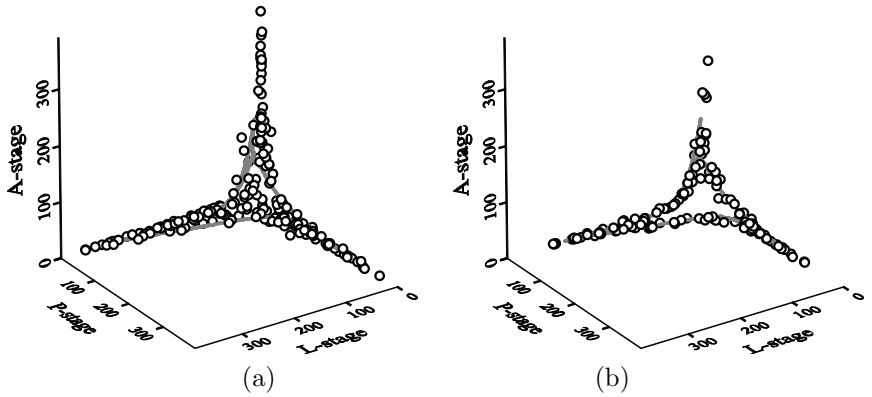

(a) (b)

FIGURE 29. (a) The data from one replicate (open circles) of the chaos treatment $c_{pa} = 0.35$ is plotted together with the continuous state space chaotic attractor predicted by the LPA model (in gray). This experiment was conducted in 20g of medium, i.e., $V = 1$ in the LPA model. A follow-up experiment in 60g ($V = 3$) produced the data shown in (b).

the LPA model in the larger habitat by comparing the variances of the one-step residuals from both habitats. This variance decreased from 36.64 in $V = 1$ to 16.45 in $V = 3$, illustrating that the deterministic LPA model had considerably less error in its one-step predictions in the larger habitat.

In summary, in this lecture we considered methods that connect population data with matrix models, and with the theory presented in Lectures 1 and 2, by making use of stochastic versions of deterministic models. Case studies involving experimental cultures of flour beetles illustrate how one can use a parameterized model to design experimental protocols for the study dynamic bifurcations and in particular a route-to-chaos. That study led to new insights into the analysis of complex dynamics in a biological population: how deterministic attractors alone are not sufficient to explain observed dynamic patterns, even in highly controlled circumstances; how a stochastic mix of transients, attractors and unstable invariant sets can provide an adequate description of real data; how discrete state space lattice effects might play a role in observed patterns; and how habitat size plays a significant role in the expression of deterministic dynamic patterns.

EXERCISES

Exercise 14. Consider the environmental stochastic Ricker model

$$x(t+1) = bx(t)e^{-cx(t)}e^{E(t)},\ b > 0,\ c > 0$$

where $E(t)$ is a normal random variable with mean 0 and variance $v > 0$. Given a set $y(0), y(1), \cdots, y(q)$ of $q+1$ observations, find algebraic formulas for the maximum likelihood estimates of b, c and v.

Exercise 15. In a simple population survivorship model we saw that the variance in the random number of survivors in one unit of time under demographic stochasticity was proportional to the population size n, while under environmental stochasticity it is proportional to n^2. For demographic stochasticity the variance was approximately stabilized by means of the transformation $g(n) = \sqrt{n}$, while

under environmental stochasticity it was approximately stabilized by the transformation $g(n) = \ln n$. Suppose we characterize the variability in the presence of both types of stochasticity as a linear combination of n and n^2, i. e., $v(n) = k_1 n + k_2 n^2$. Calculate the variance stabilizing transformation $g(n)$. Choose the arbitrary constants involved in the calculation so that in the formula gives $\ln n$ when $k_1 \to 0$ and $\sqrt{n}$ when $k_2 \to 0$.

LECTURE 4

Periodically Fluctuating Environments

An interesting experiment involving *T. castaneum* was reported by D. Jillson in [**38**]. In this experiment the habitat volume V was not held fixed in time, but was periodically fluctuated. Jillson used various periodic schedules for V, but one particular schedule caused an unexpected result. All periodic schedules for V were designed to have an average equal to the habitat size in standard, non-fluctuating cultures, namely, the volume occupied by 20g of medium ($V = 1$ in the LPA model (3.11)). In those cultures in which Jillson oscillated the medium with period 2 (between 8g and 32g), the beetle populations markedly increased in numbers. This was not true for schedules involving other periods.

One reason Jillson's result was surprising is that it contradicted a tenet held at the time that fluctuations in habitat size should be deleterious to a population. By this is meant that the population's average abundance would be less in a fluctuating habitat than in it would be in a habitat held constant at the average of the fluctuations [**54**]. This tenet was based on properties of the logistic differential equation with a non-constant carrying capacity. It is also implied by the discrete logistic equation, as we can see by the following. Consider the discrete logistic equation (1.2)

$$x(t+1) = b\frac{1}{1+(b-1)\frac{1}{K}x(t)}x(t), \quad b > 1.$$

If the inherent growth rate b is greater than 1, then all solutions with $x(0) > 0$ tend to the carrying capacity $K > 0$. If the carrying capacity fluctuates periodically, i.e., if $K = K(t)$ is a p-periodic sequence, then

$$x(t+1) = b\frac{1}{1+(b-1)\frac{1}{K(t)}x(t)}x(t), \quad b > 1, \quad K(t+p) = K(t) > 0. \tag{4.1}$$

This p-periodically forced, discrete logistic equation still has the trivial (extinction) equilibrium $x = 0$, but no longer has a positive equilibrium (carrying capacity). Instead all solutions with $x(0) > 0$ tend to a positive p-cycle with an average less than that of $K(t)$.

To see this for $p = 2$, notice that the population density $y(t) = x(2t)$ monitored at even time steps satisfies the equation (obtained from the composition of the right hand side with itself)

$$y(t+1) = b^2\frac{1}{1+(b-1)\left(\frac{K(1)+bK(0)}{K(0)K(1)}\right)y(t)}y(t).$$

All solutions of this autonomous discrete logistic equation with $y(0) = x(0) > 0$ tend to the positive equilibrium, i.e.

$$\lim_{t\to+\infty} y(t) = (b+1)\,\frac{K(0)K(1)}{K(1)+bK(0)}.$$

A similar argument shows that that the population density $w(t) = x(2t+1)$ sampled at odd times tends to the positive equilibrium of

$$w(t+1) = b^2 \frac{1}{1+(b-1)\left(\frac{K(0)+bK(1)}{K(0)K(1)}\right)y(t)}w(t),$$

that is

$$\lim{}_{t\to+\infty} w(t) = (b+1)\,\frac{K(0)K(1)}{K(0)+bK(1)}.$$

It follows that all solutions of the 2-periodic logistic (4.1) with $x(0) > 0$ tend to the 2-cycle solution that oscillates between the two values

$$x(0) = (b+1)\,\frac{K(0)K(1)}{K(1)+bK(0)}, \qquad x(1) = (b+1)\,\frac{K(0)K(1)}{K(0)+bK(1)}.$$

The average of this 2-cycle

$$\frac{1}{2}\left(x(0)+x(1)\right) = (b+1)^2\,\frac{K(0)K(1)}{\left(K(1)+bK(0)\right)\left(K(0)+bK(1)\right)}\,\frac{K(0)+K(1)}{2}$$

is strictly less than the average of the carrying capacity $\left(K(0)+K(1)\right)/2$ if $K(t)$ is not constant, i.e., if $K(0) \neq K(1)$, since the inequality

$$(b+1)^2\,\frac{K(0)K(1)}{\left(K(1)+bK(0)\right)\left(K(0)+bK(1)\right)} < 1$$

is equivalent to $0 < \left(K(1)-K(0)\right)^2$. It follows, for a discrete logistically growing population in a habitat with a period $p = 2$ fluctuating carrying capacity, that the average asymptotic population size is less than the average of the carrying capacity.

In fact, it has been proved for all periods p that if $b > 1$ then all solutions of the p-periodic logistic (4.1) with $x(0) > 0$ tend to a positive p-cycle whose average is less than that of $K(t)$ (if $K(t)$ is not constant) [**25, 42**]. Such cycles are called *attenuant* [**30**]. Attenuant cycles have been studied in other models as well [**6, 30, 43, 44**].

It follows that Jillson's experimental observation cannot be explained by the periodically forced logistic equation (4.1). However, attenuance is not a universal property of periodically forced population models. Under some circumstances the opposite can occur, i.e., the average of an attracting p-cycle can exceed that of the carrying capacity, a property called *resonance* [**2**]. Since Jillson's experiment was carried out with populations of *T. castaneum* in periodically fluctuating volumes of culture medium, perhaps we can find an explanation using the LPA model (3.11). To do so, however, would involve letting the model parameter V fluctuate. For example, for Jillson's period 2 protocol we have

$$V = V_0\left(1+\alpha(-1)^t\right)$$

where the average and the relative amplitude are $V_0 = 1$ (the volume occupied by the standard 20g of medium) and $\alpha = 3/5$. Such a change in the LPA model makes the model non-autonomous, specifically, periodically forced with period 2.

The modeling methodology and results in Lectures 1 and 2 involve time autonomous matrix models. The entries in the fertility and transition matrices can change in time only through a dependence on the state variables and not an explicit dependence on t. Such autonomous models are not appropriate if, for example, a vital rate or a environmental parameter does not remain constant in time. This is the case for the LPA model with $V = V_0\,(1 + \alpha(-1)^t)$.

Before addressing the "Jillson effect", I give a brief overview of how to generalize the equilibrium theory for autonomous matrix models in Lectures 1 and 2 to a theory of periodic cycles for periodically forced matrix models.

It is necessary to begin with some preliminary facts about periodically forced linear matrix models. Let $Z \triangleq \{0, 1, 2, \cdots\}$ denote the non-negative integers. The set $S_{m,p}$ of p-periodic sequences in R^m $(1 \leq p \in Z)$ is a Hilbert space under the inner product $\langle x, y\rangle \triangleq \Sigma_{t=0}^{p-1} x^*(t)y(t)$ for x and $y \in S_{m,p}$. Let $S_{m,p}^+$ denote the set of positive p-periodic sequences in $S_{m,p}$, i.e., sequences for which $x(t) > 0$ for all $t \in Z$.

Consider the linear matrix equation

$$x(t+1) = P(t)x(t) + h(t), \quad t \in Z \tag{4.2}$$

where $h \in S_{m,p}$ and $P(t)$ is a p-periodic matrix: $P(t+p) = P(t)$, $t \in Z$. Of interest is the existence of p-periodic solutions of this equation. Solutions of (4.2) are provided by the (variation of parameters) formula

$$x(t) = \begin{cases} X(t,0)x(0) + \sum_{i=0}^{t-1} X(t,i+1)h(i) & \text{for } t = 1, 2, \cdots \\ x(0) & \text{for } t = 0 \end{cases} \tag{4.3}$$

where for $s \in Z$

$$X(t,s) \triangleq \begin{cases} P(t-1)P(t-2)\cdots P(s+1)P(s) & \text{for } t = s+1, s+2, \cdots \\ I & \text{for } t = s \end{cases}$$

is the *fundamental solution matrix* [**24**]. It is straightforward to see that a solution is p-periodic if and only if $x(0) = x(p)$, i.e., if and only if $x(0)$ solves the equation

$$(I - X(p,0))\,x(0) = \textstyle\sum_{i=0}^{p-1} X(t,i+1)h(i). \tag{4.4}$$

If the associated homogeneous system

$$(I - X(p,0))\,x(0) = 0$$

has no nontrivial solution, that is to say if the homogeneous matrix equation

$$x(t+1) = P(t)x(t) \tag{4.5}$$

has no nontrivial p-periodic solution, then there is a unique solution

$$x(0) = (I - X(p,0))^{-1} \textstyle\sum_{i=0}^{p-1} X(t,i+1)h(i)$$

of the periodicity condition (4.4) and therefore a unique p-periodic solution of (4.2). This solution is given by the formula

$$x(t) = X(t,0)\,(I - X(p,0))^{-1} \textstyle\sum_{i=0}^{p-1} X(t,i+1)h(i) + \sum_{i=0}^{t-1} X(t,i+1)h(i). \tag{4.6}$$

The assumption that the homogeneous equation (4.5) has no nontrivial p-periodic solution is equivalent to the nonsingularity of the matrix $I - X(p,0)$, i.e., that $\lambda = 1$ is not an eigenvalue of $X(p,0)$.

If, on the other hand, the homogeneous equation (4.5) has nontrivial p-periodic solutions, i.e., if 1 is an eigenvalue of $X(p,0)$, then equation (4.4) has a solution if and only if the right hand side is orthogonal to the kernel of the transpose, that is,

$$l\sum_{i=0}^{p-1} X(t,i+1)h(i) = 0 \tag{4.7}$$

for all left eigenvectors l of $X(p,0)$ associated with eigenvalue 1.

If 1 is not an eigenvalue of $X(p,0)$, then we can rewrite the formula for the unique p-periodic solution (4.6) as

$$x(t) = \sum_{i=0}^{p-1} G(t,i)h(i)$$

where

$$G(t,i) = \begin{cases} \left(I - X(p,0)\right)^{-1} X(p,i+1) + X(t,i+1) & \text{for } 0 \le i < t \\ \left(I - X(p,0)\right)^{-1} X(p,i+1) & \text{for } 0 \le t \le i \le p-i \end{cases}$$

is a *Green's function*. This formula defines a solution operator

$$G : S_{m,p} \to S_{m,p}$$

which is linear and bounded (and therefore compact, since $S_{m,p}$ is finite dimensional). For $h \in S_{m,p}$, $x = Gh$ is the unique p-periodic solution of the nonhomogeneous, linear matrix equation (4.2).

The first goal is to establish generalizations of the bifurcation Theorems 2.1 and 2.3 that apply to periodically forced matrix equations. Consider a periodically forced version of the nonlinear matrix equation (2.7)

$$x(t+1) = \left(A(t) + \mu B(t) + H(t,\mu,x(t))\right) x(t) \tag{4.8}$$

where μ is a real parameter. Here $A(t)$ and $B(t)$ are p-periodic matrices and the components h_{ij} of the matrix $H(t,\mu,x) = (h_{ij}(t,\mu,x))$ are p-periodic in t, are k times differentiable, and are higher order in x near $x = 0$, that is[1]

$$\begin{gathered} h_{ij} \in C^k\left(Z \times R^1 \times R^m \to R^1\right) \text{ for some } k \in Z \\ |h_{ij}(t,\mu,x)| = O\left(|x|\right) \text{ near } x = 0 \\ h_{ij}(t+p,\cdot,\cdot) = h_{ij}(t,\cdot,\cdot). \end{gathered} \tag{4.9}$$

Consider the linear equation (the linearization of (4.8) at $x = 0$):

$$x(t+1) = \left(A(t) + \mu B(t)\right) x(t). \tag{4.10}$$

A real number μ_c is a *characteristic value* if (4.10), with $\mu = \mu_c$, has a nontrivial p-periodic solution $x \in S_{m,p}$. Let $X_\mu(t,x)$ denote the fundamental matrix of (4.10). A characteristic value is *simple* if $\dim \ker\left(I - X_{\mu_c}(p,0)\right) = 1$, i.e., 1 is an eigenvalue of $X_{\mu_c}(p,0)$ with (geometric) multiplicity 1. This means there is only one independent nontrivial p-periodic solution.

Suppose $\mu = 0$ is not a characteristic value of (4.10) and let G be the Green's function of $x(t+1) = A(t)x(t)$. Solving the periodically forced, nonlinear matrix equation (4.8) for a p-periodic solution $x \in S_{m,p}$ is equivalent to solving the equation

$$x = \mu L x + g(\mu, x) \tag{4.11}$$

where $L \triangleq GB$ is a linear operator and $g : R^1 \times S_{m,p} \to S_{m,p}$, defined by $g(\mu,x) \triangleq GH(t,\mu,x)x$, is $O\left(|x|^2\right)$ near $x = 0$ in $S_{m,p}$.

[1] $|x| \triangleq \langle x, x\rangle^{1/2}$.

Define $\mathcal{S}$ to be the set of all nontrivial p-periodic solution pairs $(\mu, x) \in R \times S_{m,p}$, $x \neq 0$, of (4.11) (equivalently (4.8)). If $(\mu_c, 0) \in \bar{\mathcal{S}}$ (the closure of $\mathcal{S}$), then $(\mu_c, 0)$ is a bifurcation point. A solution pair (μ, x) is *positive* if $x(t)$ for all t (i.e., if $x \in S^+_{m,p}$).

A necessary condition that $(\mu_c, 0)$ is a bifurcation point is that μ_c be a characteristic value of L (a reciprocal of a nonzero eigenvalue), that is to say, $x = \mu_c L x$ for some $0 \neq x \in S_{m,p}$. By definition, a characteristic value of the linear operator L is a characteristic value of (4.10). If μ_c is a characteristic value of L, a *characteristic solution* x is a nontrivial p-periodic solution of the linear equation (4.10), namely, $x = X_{\mu_c}(t, 0)v_0$ where v_0 is a right eigenvector of $X_{\mu_c}(p, 0)$ associated with eigenvalue 1.

The following theorem results from the well-known global bifurcation theorems of Rabinowitz applied to the operator equation (4.11) [**39, 61**].

Theorem 4.1. *In the matrix equation (4.8) assume A and B are p-periodic matrices and $H = (h_{ij})$ satisfies (4.9). Suppose*

(1) $\mu = 0$ is not a characteristic value of the linearization (4.10);

(2) μ_c is a simple characteristic value of (4.10) for which there is an associated positive characteristic p-periodic solution[2]*.*

Then there exists a continuum $\mathcal{C}^+$ in $\bar{\mathcal{S}}$ that contains the bifurcation point $(\mu_c, 0)$ and satisfies one of the following alternatives:

(a) $\mathcal{C}^+ / \{(\mu_c, 0)\}$ contains only positive p-periodic solution pairs (μ, x) for which $\mu > 0$ and $\mathcal{C}^+$ is unbounded (in $R \times S^+_{m,p}$);

(b) $\mathcal{C}^+ / \{(\mu_c, 0)\}$ contains a nontrivial, non-negative p-periodic solution pair (μ^*, x^*) for which $x^*(t) \geq 0$ has a 0 component at some time t;[3]

(c) $\mathcal{C}^+ / \{(\mu_c, 0)\}$ contains a point $(\mu_c^*, 0)$ where $\mu_c^* \neq \mu_c$ is a characteristic value of (4.10) associated with a non-negative characteristic p-periodic solution.[4]

Alternative (b) says that the continuum of nontrivial equilibria bifurcating from $(\mu_c, 0)$ leaves the positive cone. Often in applications one can rule this alternative out by showing that no nontrivial p-periodic solution can lie on the boundary of the positive cone; that is to say, in many applications one can show that

(4.12) if $x(t) \geq 0$ solves (4.8) then either $x \equiv 0$ or $x(t) > 0$ for all t.

Alternative (c) says that the continuum of nontrivial equilibria bifurcating at the characteristic value μ_c also bifurcates from another characteristic value $\mu_c^* \neq \mu_c$ of (4.10) that is associated with a non-negative characteristic vector. This alternative is ruled out, of course, if no other characteristic value of L is associated with a non-negative characteristic vector (as is the case, for example, when the Perron-Frobenius Theorem applies).

Theorem 4.2. [**7**]*In the matrix equation (4.8) assume A and B are p-periodic matrices and $H = (h_{ij})$ satisfies (4.9). Assume*

(1) $\mu = 0$ is not a characteristic value of the linearization (4.10);

(2) μ_c is a simple characteristic value of (4.10) for which there is an associated positive characteristic p-periodic solution;

---

[2]That is, $X_{\mu_c}(p, 0)$ has eigenvalue 1 and an associated positive eigenvector $v_0 > 0$.

[3]That is to say, x^* lies on the boundary of the positive cone $S^+_{m,p}$.

[4]That is to say, $X_{\mu_c^*}(p, 0)$ has eigenvalue 1 and an associated non-negative eigenvector $v_0^* \geq 0$.

(3) (4.10) has no other characteristic value with a non-negative p-periodic solution;

(4) condition (4.12) holds.

Then there exists an unbounded continuum $\mathcal{C}^+$ in $\bar{S}$ such that $\mathcal{C}^+ / \{(\mu_c, 0)\}$ contains only positive p-periodic solution pairs (μ, x) with $\mu > 0$. Moreover, $\mathcal{C}^+$ is unbounded (in $R \times S^+_{m,p}$).

That $\mathcal{C}^+$ is unbounded means that either the set of positive p-cycles associated with $\mathcal{C}^+$ is unbounded or the spectrum $\sigma(\mathcal{C}^+) \triangleq \{\mu : (\mu, x) \in \mathcal{C}^+\}$ is unbounded (or both).

Stability properties of cycles of p-periodic matrix models are defined in terms of the stability properties of fixed points of the $(p-1$ fold) composite of the equation. A solution $x(t)$ of a p-periodic equation $x(t+1) = f(t, x(t))$ (i.e., $f(t, x) = f(t+p, x)$ for all t and x) is a p-cycle if and only if $x(0) = x(p)$, that is to say, if and only if $x(0)$ is an equilibrium (fixed) point of the composite map $f^{(p-1)}(x) \triangleq f(p-1, f(p-2, \ldots, f(1, f(0, x))))$. A p-cycle $x_p(t)$ is *stable* if $x_p(0)$ is a stable equilibrium of the autonomous (composite) equation $y(t+1) = f^{(p-1)}(y(t))$. Similarly, a p-cycle is an attractor if $x_p(0)$ is an attractor of the composite equation, and a p-cycle is asymptotically stable if $x_p(0)$ is an asymptotically stable equilibrium of the composite equation.

The fundamental solution matrix $X(t, s)$ of the linearization (4.10) at $x = 0$ of the nonlinear, periodically forced matrix model (4.8) depends on μ. A subscript indicates this dependence:

$$X_\mu(p, 0) = \prod_{i=1}^{p} \left(A(p-i) + \mu B(p-i)\right). \tag{4.13}$$

A stability analysis of the equilibrium $x = 0$ of (4.8) is possible by means of the linearization principle [**24**]. Define

$$\delta \triangleq l_0 \frac{d}{d\mu} X_\mu\,(p, 0)|_{\mu=\mu_c}\, v_0 \tag{4.14}$$

where l_0 and v_0 are the left and right eigenvalues of $X_{\mu_c}(p, 0)$ normalized so that $l_0 v_0 = 1$. The following theorem gives conditions under which the trivial (extinction) equilibrium $x = 0$ of the nonlinear, periodically forced equation (4.8) loses stability at the bifurcation point in Theorem 4.1.

Theorem 4.3. [**29**]*In the matrix equation (4.8) assume A and B are p-periodic matrices and $H = (h_{ij})$ satisfies (4.9) with $k \geq 1$. Suppose μ_c is a simple characteristic value of (4.10) with the property that 1 is a strictly dominant eigenvalue of $X_{\mu_c}(p, 0)$ and let l_0 and v_0 denote left and right eigenvectors of $X_{\mu_c}(p, 0)$ normalized so that $l_0 v_0 = 1$. Further, suppose 0 is not an eigenvalue of $X_{\mu_c}(p, 0)$.*

If $\delta > 0$ then the trivial solution $x = 0$ of the nonlinear, periodically forced equation (4.8) loses stability as μ increases through μ_{cr}.

If $\delta < 0$ then $x = 0$ gains stability as μ increases through μ_{cr}.

An analysis of the properties of the positive p-cycles near the bifurcation point $(\mu_c, 0)$ guaranteed by Theorem 4.1 is possible by means of a parametrization of the bifurcating branch. To do this we represent the bifurcating positive, p-cycle pairs $(\mu, x(t))$ as functions of a branch parameter ε and calculate the lowest order terms

in the expansions

$$x(t) = x_1(t)\varepsilon + O\left(\varepsilon^2\right) \tag{4.15}$$
$$\mu = \mu_c + \mu_1\varepsilon + O\left(\varepsilon^2\right)$$

(under the assumption that $k \geq 2$ in (4.9)). These expansions provide approximations to the positive p-cycles near the bifurcation point and allow us to make approximations to the Jacobian of the composite and its dominant eigenvalue

$$\lambda = 1 + \varepsilon\lambda_1 + O\left(\varepsilon^2\right),$$

which determines the stability of the cycles. Here $x_1(t)$ is the positive p-cycle solution of the linearization (4.10) with $\mu = \mu_{cr}$, namely

$$x_1(t) = X_{\mu_c}(t, 0)v_0$$

and the positive p-cycles on the branch correspond to $\varepsilon > 0$.

To calculate the coefficients in (4.15) we substitute these expansions into the nonlinear equation (4.8) and equate coefficients of like powers of ε from both sides of the resulting expressions. This leads to linear matrix equations from which, with the aid of the orthogonality condition (4.7), we can calculate formulas for μ_1 and λ_1.The results are as follows [**29**].

Define $\gamma_{ij}(t)$ to be the gradient of h_{ij} with respect to x evaluated at $(\mu, x) = (\mu_c, 0)$:

$$\gamma_{ij}(t) \triangleq \nabla_x h_{ij}(t, \mu, x)|_{(\mu,x)=(\mu_c,0)}$$

and define the scalars

$$d_{ij}(t) \triangleq \gamma^*_{ij}(t)x_1(t).$$

Form the matrix $D(t) = (d_{ij}(t))$ and define

$$\kappa \triangleq -l_0 \textstyle\sum_{t=0}^{p-1} X_{\mu_c}(p, t+1)D(t)X_{\mu_c}(t, 0)v_0.$$

Then it turns out

$$\mu_1 = \frac{1}{2}\frac{\kappa}{\delta}, \qquad \lambda_1 = -\frac{1}{2}\kappa \tag{4.16}$$

where δ is given by (4.14). Note that the bifurcation is supercritical if $\mu_1 > 0$ and subcritical if $\mu_1 < 0$. The dominant eigenvalue λ is less than 1 (for $\varepsilon > 0$ small) if $\mu_1 > 0$ and greater than 1 if $\mu_1 < 0$.

The bifurcation at $\mu = \mu_c$ described in Theorem 4.1 is called stable if the p-periodic solutions from the positive solutions pairs near the bifurcation point $(\mu, x) = (\mu_c, 0)$ are (locally asymptotically) stable. If these positive periodic solutions are unstable, then the bifurcation is unstable.

Theorem 4.4. [**29**] *In addition to the assumptions in Theorem 4.3 assume $H = (h_{ij})$ satisfies (4.9) with $k \geq 2$ and that $\kappa \neq 0$.*

Suppose $\delta > 0$, i.e., the trivial (extinction) equilibrium $x = 0$ loses stability as μ increases through μ_c. Then for μ sufficiently close to μ_c the bifurcation of positive p-cycles is supercritical and stable if $\kappa > 0$ and is subcritical and unstable if $\kappa < 0$.

Suppose $\delta < 0$, i.e., the trivial (extinction) equilibrium $x = 0$ loses stability as μ decreases through μ_c. Then for μ sufficiently close to μ_c the bifurcation of positive p-cycles is supercritical and stable if $\kappa < 0$ and is subcritical and unstable if $\kappa > 0$.

Theorems 4.1, 4.3 and 4.4 are generalizations to periodically forced equations of Theorems 2.1, 1.7, and 2.3 for autonomous equations. They provide some general conditions under which a periodic matrix equation has a positive p-cycle and conditions under which it is stable or unstable. The expansions (4.15) also provide a way to study the properties of the p-cycles (averages, amplitudes, phases, etc.), at least near the bifurcation point. If need be we can also calculate (by the same procedure described above) the expansion of the p-cycle to higher order in ε :

$$x(t) = x_1(t)\varepsilon + x_2(t)\varepsilon^2 + O\left(\varepsilon^3\right).$$

Example 4.5. *The matrix model*

$$\begin{pmatrix} J(t+1) \\ A(t+1) \end{pmatrix} = \begin{pmatrix} 0 & b\frac{1}{1+A(t)} \\ \tau_{21} & \tau_{22} \end{pmatrix} \begin{pmatrix} J(t) \\ A(t) \end{pmatrix}$$

is a variant of the discrete logistic model in which a juvenile stage J is included. With constant coefficients b (inherent juvenile recruitment rate per adult), τ_{21} (juvenile survivorship) and τ_{22} (adult survivorship), the model is autonomous and a (global) continuum of positive equilibria bifurcates from the critical value $b_c = (1-\tau_{22})/\tau_{21}$ (or equivalently at the critical value 1 of the inherent net reproductive number $n = b\tau_{21}/(1-\tau_{22})$).

Suppose instead that the recruitment rate b oscillates periodically with period 2. Suppose this oscillation has mean μ and amplitude α so that

$$b = \mu\left(1 + \alpha\,(-1)^t\right), \qquad 0 \le \alpha < 1.$$

The model takes the form (4.8) with

$$A(t) = \begin{pmatrix} 0 & 0 \\ \tau_{21} & \tau_{22} \end{pmatrix}, \qquad B(t) = \begin{pmatrix} 0 & 1+\alpha(-1)^t) \\ 0 & 0 \end{pmatrix}$$
$$H = \begin{pmatrix} 0 & -\mu(1+\alpha(-1)^t)\frac{A}{1+A} \\ 0 & 0 \end{pmatrix}.$$

From (4.13) we find

$$\begin{aligned} X_\mu(2,0) &= \begin{pmatrix} 0 & \mu(1+\alpha) \\ \tau_{21} & \tau_{22} \end{pmatrix} \begin{pmatrix} 0 & \mu(1-\alpha) \\ \tau_{21} & \tau_{22} \end{pmatrix} \\ &= \begin{pmatrix} \tau_{21}\mu\,(1+\alpha) & \tau_{22}\mu\,(1+\alpha) \\ \tau_{22}\tau_{21} & \tau_{22}^2 + \tau_{21}\mu\,(1-\alpha) \end{pmatrix} \end{aligned}$$

is a positive matrix. Perron's Theorem implies that $X_\mu(2,0)$ has a positive, strictly dominant simple eigenvalue λ with positive right and left eigenvectors $v_0 > 0$ and $l_0 > 0$ and that no other eigenvalue has a non-negative eigenvector [**26, 37**]. *Specifically, the positive eigenvalue is*

$$\lambda = \tau_{21}\mu + \frac{1}{2}\tau_{22}^2 + \frac{1}{2}\sqrt{\tau_{22}^4 + 4\tau_{22}^2\tau_{21}\mu + 4\tau_{21}^2\mu^2\alpha^2}.$$

This eigenvalue equals 1 when the mean birth rate μ equals the critical value

$$\mu_c \triangleq \frac{1 - \sqrt{(1-\alpha^2)\,\tau_{22}^2 + \alpha^2}}{\tau_{21}\,(1-\alpha^2)}.$$

From (4.14) we calculate

$$\delta = l_0 \frac{d}{d\mu}\, X_\mu(2,0)|_{\mu=\mu_c}\, v_o = l_0 \begin{pmatrix} \tau_{21}\,(1+\alpha) & \tau_{22}\,(1+\alpha) \\ 0 & \tau_{21}\,(1-\alpha) \end{pmatrix} v_0 > 0.$$

Theorem 4.3 implies that the extinction equilibrium $J = A = 0$ loses stability as the average recruitment rate increases through the critical value μ_c. Theorem 4.2 implies the existence of an unbounded continuum of positive 2-cycles with a spectrum (interval) of positive average recruitment rates $\mu > 0$ that bifurcates from the extinction equilibrium at the critical value μ_c. Further calculations show

$$D(0) = \begin{pmatrix} 0 & -\mu_c(1+\alpha) \\ 0 & 0 \end{pmatrix}, \qquad D(1) = \begin{pmatrix} 0 & -\mu_c(1-\alpha)(\tau_{21}+\tau_{22}) \\ 0 & 0 \end{pmatrix}$$

and

$$\begin{aligned} \kappa &= -l_0 \left[(A(1) + \mu_c B(1)) D(0) + D(1) (A(0) + \mu_c B(0)) \right] v_0 \\ &= \frac{2}{3}\tau_{21}\mu_c (1+\alpha) + \frac{1}{3}\mu_c (\tau_{22}+\tau_{21})^2 (1-\alpha). \end{aligned}$$

Since $\kappa > 0$, Theorem 4.4 implies the bifurcation at μ_c is supercritical and stable.

As a numerical example, take $\tau_{21} = \tau_{22} = 1/2$ and $\alpha = 1/10$. Then

$$\mu_c = \frac{10}{99}\left(20 - \sqrt{103}\right) \approx 0.9951$$

and

$$X_{\mu_c}(2,0) = \begin{pmatrix} \frac{1}{2} & \frac{1}{2} \\ \frac{1}{4} & \frac{3}{4} \end{pmatrix}$$

has a dominant eigenvalue 1 with positive eigenvectors

$$v_0 = \begin{pmatrix} 1 \\ 1 \end{pmatrix}, \qquad l_0 = \begin{pmatrix} \frac{1}{3} & \frac{2}{3} \end{pmatrix}$$

that satisfy $l_0 v_0 = 1$. Then $\delta = 2/3$ and $\kappa = 20\left(20 - \sqrt{103}\right)/297 \approx 0.6634$.

It is interesting to note that the bifurcation point μ_c is a decreasing function of the amplitude α. This means that a lower average recruitment rate μ is needed for population survival in the periodically fluctuating habitat than in the constant habitat. In this sense, an oscillatory habitat is advantageous to the population. Although the decrease in μ_c in the numerical example above is not large (from 1 to 0.9951) if the amplitude is changed to $\alpha = 9/10$ the decrease is over 20%, namely from 1 to 0.7788. See Figure 30.

In [**31**] Theorems 4.1, 4.3 and 4.4 are applied to the LPA model with a 2-periodic habitat volume V with average $V_0 = 1$ and amplitude α $(0 < \alpha < 1)$:

$$\begin{aligned} L(t+1) &= bA(t) \exp\left(-\frac{c_{el}}{1+\alpha(-1)^t} L(t) - \frac{c_{ea}}{1+\alpha(-1)^t} A(t) \right) \\ P(t+1) &= (1-\mu_l) L(t) \\ A(t+1) &= P(t) \exp\left(-\frac{c_{pa}}{1+\alpha(-1)^t} A(t) \right) + (1-\mu_a) A(t). \end{aligned} \tag{4.17}$$

With $\mu = b$, this model has the form (4.8) and satisfies the hypotheses of Theorem 4.3 (for any integer k) with

$$X_b(p,0) = \begin{pmatrix} 0 & b & b(1-\mu_a) \\ 0 & 0 & b(1-\mu_l) \\ 1-\mu_l & 1-\mu_a & (1-\mu_a)^2 \end{pmatrix}$$

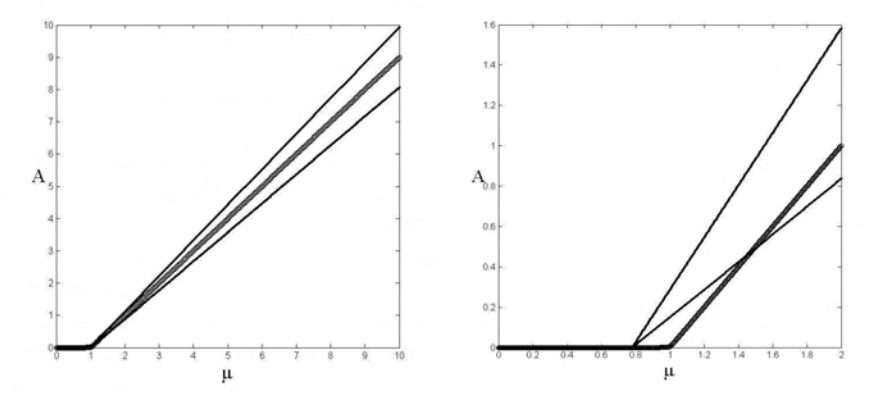

(a) (b)

FIGURE 30. The plots show bifurcation diagrams for the 2-periodic, juvenile-adult logistic model in Example 4.5 with $\tau_{21} = \tau_{22} = 1/2$. The adult component A of the stable, positive 2-cycle is plotted against the average recruitment rate μ. (a) The thin lines are the maximum and minimum of the bifurcating 2-cycles when $\alpha = 1/10$. The thick line is the branch of bifurcating equilibria when $\alpha = 0$. (b) When $\alpha = 9/10$ the bifurcation point μ_c for the 2-cycles is less than it is for the equilibrium case $\alpha = 0$.

and

$$b_c = \frac{\mu_a}{1-\mu_l}.$$

(Equivalently we could use $n = b(1-\mu_l)/\mu_a$ as the bifurcation parameter μ, in keeping with the general equilibrium theory in Lectures 1 and 2, in which case $\mu_c = 1$, but we follow the analysis in [**31**].) The matrix

$$X_{b_c}(2,0) = \begin{pmatrix} 0 & \frac{\mu_a}{1-\mu_l} & \frac{\mu_a}{1-\mu_l}(1-\mu_a) \\ 0 & 0 & \frac{\mu_a}{1-\mu_l}(1-\mu_l) \\ 1-\mu_l & 1-\mu_a & (1-\mu_a)^2 \end{pmatrix}$$

has two complex eigenvalues $\mu_a(\mu_a-2)/2 \pm i\mu_a\sqrt{\mu_a(4-\mu_a)}/2$ of magnitude $\mu_a < 1$ and a dominant eigenvalue 1 with eigenvectors

$$l_0 = \begin{pmatrix} \frac{1-\mu_l}{1+2\mu_a} & \frac{1}{1+2\mu_a} & \frac{1}{1+2\mu_a} \end{pmatrix}, \qquad v_0 = \begin{pmatrix} b_c \\ \mu_a \\ 1 \end{pmatrix}.$$

A calculation shows

$$\delta = l_0 \frac{d}{db} X_b(2,0)|_{b=b_c} v_0 = \frac{2(1-\mu_l)}{1+2\mu_a} > 0$$

and hence Theorem 4.3 implies the extinction equilibrium $x = \mathrm{col}(L,P,A) = \mathrm{col}(0,0,0)$ loses stability as b increases through the critical value b_c. In fact it is shown in [**31**] that the extinction equilibrium $x = 0$ is a global attractor for $b < b_c$ and the periodic LPA model (4.17) is uniformly persistent for $b > b_c$.

It is straightforward to show that if a component of a 2-cycle solution of (4.17) equals 0 at some time t, then all three components equal 0 for all time t, i.e., such

a 2-cycle must in fact be the extinction equilibrium $x = 0$. As a result condition (4.12) holds and Theorem 4.2 implies the existence of an unbounded continuum of positive 2-cycles that bifurcates from $x = 0$ at $b = b_c$. Since $x = 0$ is a global attractor for $b < b_c$ it follows that the bifurcation is supercritical. This, and the stability of the bifurcating branch of positive 2-cycles near b_c, also follows from Theorem 4.4 provided $\kappa \neq 0$. In fact a calculation shows

$$\kappa = \frac{4\mu_a}{(1-\alpha^2)(1+2\mu_a)} > 0$$

which proves the bifurcation is supercritical and stable.

The expansions (4.15) permit some analysis of the bifurcating 2-cycles and, in particular, imply they are attenuant. A calculation of the expansions for both the bifurcating 2-cycles $(L_\alpha(t), P_\alpha(t), A_\alpha(t))$ and the bifurcating equilibria (L_0, P_0, A_0) (Corollary 2.1 and Theorem 2.3) shows this. Let ε_α and ε_0 denote the expansion parameters for the branches respectively. Then [**31**]

$$\begin{aligned}
L_\alpha(t) &= b_c\varepsilon_\alpha + O\left(\varepsilon_\alpha^2\right)(t)\\
P_\alpha(t) &= \mu_a\varepsilon_\alpha + O\left(\varepsilon_\alpha^2\right)(t)\\
A_\alpha(t) &= \varepsilon_\alpha + O\left(\varepsilon_\alpha^2\right)(t)\\
b &= b_c + \left(\frac{b_c\left(c_{ea} + b_c c_{el} + c_{pa}\right)}{1-\alpha^2}\right)\varepsilon_\alpha + O\left(\varepsilon_\alpha^2\right)
\end{aligned}$$

for $\varepsilon_\alpha > 0$ small and

$$\begin{aligned}
L_0 &= b_c\varepsilon_0 + O\left(\varepsilon_0^2\right)\\
P_0 &= \mu_a\varepsilon_0 + O\left(\varepsilon_0^2\right)\\
A_0 &= \varepsilon_0 + O\left(\varepsilon_0^2\right)\\
b &= b_c + b_c\left(c_{ea} + b_c c_{el} + c_{pa}\right)\varepsilon_0 + O\left(\varepsilon_0^2\right)
\end{aligned}$$

for $\varepsilon_0 > 0$ small. A comparison of the averages of the 2-cycle with the equilibrium at the same value of b, to first order, requires $\varepsilon_\alpha = (1-\alpha^2)\varepsilon_0$. Then

$$\begin{aligned}
L_0 - \langle L_\alpha(t)\rangle &= \alpha^2 b_c\varepsilon_0 + O\left(\varepsilon_0^2\right) > 0\\
P_0 - \langle P_\alpha(t)\rangle &= \alpha^2\mu_a\varepsilon_0 + O\left(\varepsilon_0^2\right) > 0\\
A_0 - \langle A_\alpha(t)\rangle &= \alpha^2\varepsilon_0 + O\left(\varepsilon_0^2\right) > 0
\end{aligned}$$

for $\varepsilon_0 > 0$ small. Here $\langle L_\alpha(t)\rangle \triangleq \left(L_\alpha(0) + L_\alpha(1)\right)/2$ denotes the average of the L-stage component of the 2-cycles, etc.

Note that all three life cycle stages are attenuant and, as a consequence, the total population size $L(t) + P(t) + A(t)$ is also attenuant. It follows that near the bifurcation point b_c the bifurcating 2-cycles *cannot* explain the Jillson effect observed in the *T. castaneum* experiment. If resonance is to occur in the periodic LPA model, it must occur for larger values of b.

One approach that has been used to study periodic solutions of periodically forced difference equations utilizes perturbation theory. This approach views a periodic solution as a function of a small parameter appearing in the model equations, which are known to have a solution of a particular type (e.g., an equilibrium or a cycle) when the parameter equals 0. The periodic solutions when the parameter is

small (but not equal to 0) are considered perturbations of this known solution. Taylor expansions with respect to the small parameter lead to useful approximations of the perturbed solutions.

For example, consider the relative amplitude α as a small parameter in the periodic LPA model (4.17). When $\alpha = 0$ the model is autonomous and has (for $b > b_c$) a positive equilibrium. We expect this equilibrium to perturb to a 2-cycle for $\alpha > 0$. Relevant mathematical questions are: does such a perturbed 2-cycle exist? when is it stable? is it resonant or attenuant?

A study of these questions for a general class of difference equations with periodic coefficients appears in [**30**]. Consider the equation $x(t+1) = F(c, x(t))$ in which a coefficient c has been selected to oscillate periodically with an amplitude α around an average which can be taken, without loss in generality, to be 1. Consider the periodically forced equation

$$x(t+1) = F(1 + \alpha\beta(t), x(t)) \tag{4.18}$$

where β is a p-periodic sequence with mean $\langle\beta\rangle = 0$. Assume

$$F : R \times R^m \to R^m \text{ is } k \geq 2 \text{ times continuously differentiable.} \tag{4.19}$$

p-periodic solutions of (4.18) satisfy the operator equation

$$K(\alpha, x) = 0 \tag{4.20}$$

where the operator $K : R \times S_{m,p} \to S_{m,p}$ is defined by

$$K(\alpha, x) \triangleq \{x(t+1) - F(1 + \alpha\beta(t), x(t))\}_{t \in Z} \in S_{m,p}.$$

The Implicit Function Theorem applies to equation (4.20) and yields a solution $(\alpha, x(\alpha))$, $x(\alpha) \in S_{m,p}$, in the neighborhood of a known solution $(0, x(0))$ provided the derivative of K with respect to x at this point is nonsingular. Specifically, suppose the autonomous equation (4.18) when $\alpha = 0$ has an equilibrium $x_0 = F(1, x_0)$. Let $F_x(\alpha, x)$ denote the Jacobian of F with respect to x evaluated at (α, x). Then the Implicit Function Theorem applies to (4.18) at $(\alpha, x) = (0, x_0)$ provided $I - F_x(1, x_0)$ is invertible.

Theorem 4.6. *Consider the p-periodically forced difference equation (4.18) in which β is a p-periodic sequence with mean $\langle\beta\rangle = 0$ and for which (4.19) holds. Assume the equation has an equilibrium when $\alpha = 0$ and that 1 is not an eigenvalue of $F_x(1, x_0)$. Then for each α of sufficiently small magnitude there exists a p-periodic solution $x_\alpha(t)$ of (4.18). The p-cycle $x_\alpha(t)$ is k times continuously differentiable in α and satisfies $\lim_{\alpha \to 0} x_\alpha(t) = x_0$.*

Assume $F_x(1, x_0)$ has no eigenvalue of magnitude equal to 1 (x_0 is hyperbolic). If the equilibrium x_0 is locally asymptotically stable (or unstable), then the p-cycle $x_\alpha(t)$ is locally asymptotically stable (unstable) for $|\alpha|$ sufficiently small.

The assertion about stability in Theorem 4.6 follows from the continuity of the Jacobian of the composites of F and its eigenvalues as functions of α.

If $k \geq 3$ we can write

$$x_\alpha(t) = x_0 + y(t)\alpha + z(t)\alpha^2 + O\left(\alpha^3\right)(t)$$

and calculate the p-periodic coefficients y, z by a substitution of this expansion into equation (4.18). From coefficients of like powers of α we obtain linear difference equations whose solution is in principle straightforward, but in practice is often

tedious (if not intractable), particularly for the coefficients of terms of order two or higher.

Theorem 4.6 applies to the 2-periodic LPA model (4.17), which has a positive equilibrium (L_0, P_0, A_0) when $\alpha = 0$. The α-expansions

$$\begin{aligned} L_\alpha(t) &= L_0 + L_1(t)\alpha + L_2(t)\alpha^2 + O\left(\alpha^3\right)(t) \\ P_\alpha(t) &= P_0 + P_1(t)\alpha + P_2(t)\alpha^2 + O\left(\alpha^3\right)(t) \\ A_\alpha(t) &= A_0 + A_1(t)\alpha + A_2(t)\alpha^2 + O\left(\alpha^3\right)(t) \end{aligned}$$

of the perturbing 2-cycle $(L_\alpha(t), P_\alpha(t), A_\alpha(t))$ are calculated and studied in [**31**]. The results show that the averages of the first order coefficients equal zero and hence

$$\begin{aligned} \langle L_\alpha(t)\rangle - L_0 &= \langle L_2(t)\rangle \alpha^2 + O\left(\alpha^3\right) \\ \langle P_\alpha(t)\rangle - P_0 &= \langle P_2(t)\rangle \alpha^2 + O\left(\alpha^3\right) \\ \langle A_\alpha(t)\rangle - A_0 &= \langle A_2(t)\rangle \alpha^2 + O\left(\alpha^3\right). \end{aligned}$$

The second order coefficients in these α-expansions determine the resonance or attenuance of each stage of the 2-cycle. The calculations necessary to obtain closed form formulas for these coefficients and their averages are intractable. However, conditions are derived in [**31**] sufficient to show that resonance can occur in the periodic LPA model (4.17) in individual life cycle stages and in total population size $T_\alpha(t) = L_\alpha(t) + P_\alpha(t) + A_\alpha(t)$, for sufficiently large $b > 0$ and sufficiently small amplitudes $\alpha > 0$. See Table 1.

For $b > 0$ large and $\alpha > 0$ small
$A_\alpha(t)$ is resonant
Both $L_\alpha(t)$ and $P_\alpha(t)$ are resonant if $\dfrac{\mu_a^2}{1-\mu_a} > 2\dfrac{c_{ea}}{c_{pa}}$
Both $L_\alpha(t)$ and $P_\alpha(t)$ are attenuant if $\dfrac{\mu_a^2}{1-\mu_a} < 2\dfrac{c_{ea}}{c_{pa}}$
Total population size $T_\alpha(t)$ is resonant if $\dfrac{\mu_a^2}{1-\mu_a} > 2\dfrac{c_{ea}}{c_{pa}} - \left(\dfrac{2}{2-\mu_l}\right)\dfrac{c_{el}}{c_{pa}}$
Total population size $T_\alpha(t)$ is attenuant if $\dfrac{\mu_a^2}{1-\mu_a} < 2\dfrac{c_{ea}}{c_{pa}} - \left(\dfrac{2}{2-\mu_l}\right)\dfrac{c_{el}}{c_{pa}}$

TABLE 1.

Maximum likelihood parameter estimates for the 2-periodic LPA model (4.17) obtained from Jillson's data are [**2**]:

$$\begin{aligned} b = 4.445, \quad \mu_l = 4.794 \times 10^{-1}, \quad \mu_a = 1.524 \times 10^{-1} \\ c_{ea} = 5.785 \times 10^{-3}, \quad c_{el} = 5.841 \times 10^{-2}, \quad c_{pa} = 1.053 \times 10^{-2}. \end{aligned} \tag{4.21}$$

and the positive equilibrium of the resulting model is

$$\begin{pmatrix} L_0 \\ P_0 \\ A_0 \end{pmatrix} = \begin{pmatrix} 30.5914 \\ 15.9259 \\ 57.2116 \end{pmatrix}. \tag{4.22}$$

The inequality for a resonant total population size in Table 1 is satisfied (as is the inequality for L and P stage attenuance). However, several points keep this result from providing a satisfactory explanation of Jillson's resonance effect: neither the amplitude $\alpha = 3/5$ used by Jillson is particularly small nor is $b = 4.445$ particularly large. Moreover, the equilibrium is unstable and, as a result, in the application to Jillson's data the 2-cycle perturbing from the equilibrium is unstable.

The equilibrium (4.22) is unstable because one of the eigenvalues (-1.7639, 0.8047, and -0.0718) of the Jacobian at the equilibrium is greater than 1 in magnitude. The stable equilibria bifurcating at $b = b_c \approx 0.29$ destabilize and give rise to a 2-cycle bifurcation at approximately $b = 1.6$. At the estimated parameter value $b = 4.445$ for Jillson's experiment the autonomous ($\alpha = 0$) LPA model (4.17) has a stable 2-cycle that oscillates between the stage vectors

$$\begin{pmatrix} L(0) \\ P(0) \\ A(0) \end{pmatrix} = \begin{pmatrix} 5.037 \times 10^{-5} \\ 138.3 \\ 119.0 \end{pmatrix}, \quad \begin{pmatrix} L(1) \\ P(1) \\ A(1) \end{pmatrix} = \begin{pmatrix} 265.7 \\ 2.622 \times 10^{-5} \\ 140.4 \end{pmatrix}. \tag{4.23}$$

What becomes of this 2-cycle when $\alpha > 0$?

Theorem 4.6 is a special case of a more general theorem proved by Henson [**30**] in which it assumed that the equation (4.18) has, when $\alpha = 0$, a periodic solution $x_0(t)$ of period p. Each phase shift of $x_0(t)$ is also a p-cycle. Denote these phases by

$$x_0^i(t) = x_0(t+i), \quad i = 0, 1, \cdots, p-1.$$

We anticipate that each phase perturbs to a p-cycle solution of (4.18) when $\alpha \neq 0$. Implicit function theorem methods yield the following theorem.

Theorem 4.7. [**30**] *Consider the p-periodically forced difference equation (4.18) in which β is a p-periodic sequence with mean $\langle \beta \rangle = 0$ and for which (4.19) holds. Assume the equation has a p-periodic solution $x_0(t)$ when $\alpha = 0$ and that 1 is not an eigenvalue of $\Pi_{t=p-1}^{0} F_x(1, x_0^0(t))$. Then for each phase $x_0^i(t)$ and each α of sufficiently small magnitude there exists a p-periodic solution $x_\alpha^i(t)$ of (4.18). Each p-cycle $x_\alpha^i(t)$ is k times continuously differentiable in α and satisfies $\lim_{\alpha \to 0} x_\alpha^i(t) = x_0^i(t)$.*

Assume $\Pi_{t=p-1}^{0} F_x(1, x_0^0(t))$ has no eigenvalue of magnitude equal to 1 ($x_0(t)$ is hyperbolic). If the p-periodic solution $x_0(t)$ is locally asymptotically stable (or unstable), then all the p-periodic solutions $x_\alpha^i(t)$ are locally asymptotically stable (unstable) for $|\alpha|$ sufficiently small.

The p-cycles x_α^i are not necessarily phase shifts of one another when $\alpha \neq 0$ (although in some cases this is a possibility). Theorem 4.7 does not require that p be the minimal period of either $x_0(t)$ or $\beta(t)$. If the minimal period of $x_0(t)$ is q and the minimal period of β is r, then Theorem 4.7 can be applied with the common period $p = \text{lcm}(q, r)$. The following theorem addresses the relationships among the phases of the perturbed p-periodic solutions.

Theorem 4.8. [**30**] *In addition to the assumptions of Theorem 4.7 assume*

$$F\left(\eta_1, x_\alpha^i(t)\right) = F\left(\eta_2, x_\alpha^i(t)\right) \Longrightarrow \eta_1 = \eta_2 \tag{4.24}$$

for all t, all $i = 0, 1, \cdots, p-1$, and all sufficiently small $|\alpha|$. Then for $|\alpha|$ small the perturbed p-cycles $x_\alpha^i(t)$ have minimal period $p = \text{lcm}(q, r)$. Moreover, modulo phase shifts, $\gcd(q, r)$ of these perturbed cycles are distinct.

An example given in [**30**] shows (4.24) cannot be dropped from this theorem.

An interesting consequence of Theorem 4.8 is that periodically forcing an equation that has a (non-equilibrium) cycle in general leads to multiple (cyclic) attractors.

With regard to the p-periodic LPA model and Jillson's experiment, Theorems 4.7 and 4.8 with $p = 2$ imply the existence and stability of two distinct 2-cycle solutions that perturb from the two phase shifts of the 2-cycle (4.23). Are either of the perturbed 2-cycles resonant?

In general, the periodic coefficients $y^i(t)$ in the expansions

$$x^i_\alpha(t) = x^i_0(t) + y^i(t)\alpha + O\left(\alpha^2\right) \tag{4.25}$$

of the perturbed p-cycles from Theorem 4.7 determine, to lowest order in the amplitude α, the relationship among the properties of the unperturbed cycle x^i_α (such as cycle average) and those of the perturbed cycle x^i_0. Let $\lceil x \rceil$ denote the sum of the m components of $x \in R^m$. In the population model context in which x is a distribution vector of stage classes $\lceil x \rceil$ is the total population size. The perturbed cycle x^i_α is *resonant (or attenuant) at* $\alpha = 0$ if there exists $\delta > 0$ such that $\left\langle \lceil x^i_\alpha \rceil \right\rangle > \left\langle \lceil x^i_0 \rceil \right\rangle$ $\left(\text{or } \left\langle \lceil x^i_\alpha \rceil \right\rangle < \left\langle \lceil x^i_0 \rceil \right\rangle\right)$ for all $0 < \alpha < \delta$. In [**30**] Henson shows that $\Sigma_{i=0}^{p-1} \lceil y^i \rceil = 0$. Therefore, if $\lceil y^i \rceil \neq 0$ for at least $i = 0, 1, \cdots p-1$, it follows that there must be at least one $\lceil y^i \rceil > 0$ and one $\lceil y^i \rceil < 0$.

Theorem 4.9. [**30**] *Under the assumptions of Theorem 4.7, if there exists at least one* $i = 0, 1, \cdots p-1$ *such that*

$$\lceil y^i \rceil = \left\lceil \left. \frac{d}{d\alpha} x^i_\alpha \right|_{\alpha=0} \right\rceil \neq 0$$

then at least one of the perturbed cycles x^i_α *is resonant at* $\alpha = 0$ *and at least one is attenuant at* $\alpha = 0$.

It is tedious to calculate the expansion (4.25) for the 2-periodic LPA model with parameter values (4.21). However, with the help of an algebraic computer program to carry out the calculations, we find that one of the 2-cycles that perturbs from the 2-cycle (4.23) is resonant while the 2-cycle that perturbs from its phase shift is attenuant. Since both 2-cycles are stable, a population tends to one or the other depending on its initial condition.

This analysis is valid, however, only for small amplitudes α. Are there two stable 2-cycles in Jillson's experiment when $\alpha = 3/5$? Figure 31 shows a numerically calculated bifurcation diagram for the 2-periodic LPA model with parameters (4.21). This diagram shows that the attenuant 2-cycle disappears for $\alpha > 0.45$. This is because the attenuant 2-cycle collides with the unstable 2-cycle that perturbs from the unstable equilibrium in a saddle-node bifurcation at $\alpha = 0.45$. For larger values of α, including $\alpha = 3/5$ that Jillson used, this bifurcation leaves only the stable resonant 2-cycle.

Theorem 4.9 indicates that, in general, the result of periodically forcing an oscillating population is a multiple attractor situation (as in Figure 31(b)). Multiple attractors for the dynamics of a biological population are intriguing. For *Tribolium* the possibility is especially intriguing because there is no reported evidence of multiple attractors in single species cultures, despite over a half century of research utilizing these insects. Moreover, one of the 2-cycles predicted by the 2-periodic

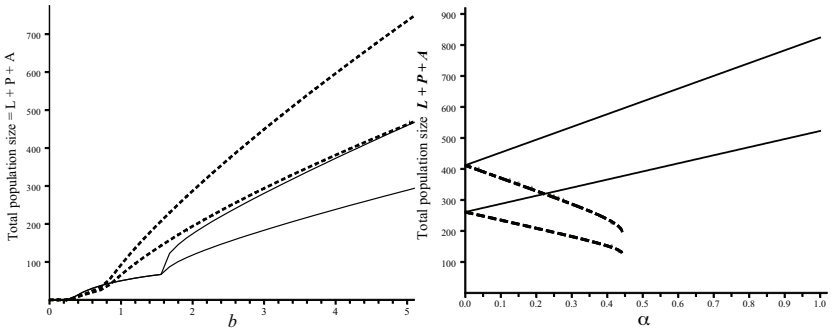

(a) (b)

FIGURE 31. (a) A bifurcation diagram for the 2-periodic LPA model with ML parameters (4.21) is shown using b as the bifurcation parameter. The solid line is for the autonomous case when the amplitude $\alpha = 0$. Notice the period doubling bifurcation at $b \approx 1.6$. The dashed lines are the maxima and minima of 2-cycles for the case $\alpha = 3/5$ used in Jillson's experiment. A close look near the bifurcation point $b_c \approx 0.29$ shows that the bifurcating 2-cycles are attenuant for b near b_c. As b increases they become resonant. The ML estimated value of b for Jillson's experiment is 4.445 where resonance clearly occurs. (b) The solid lines are the maxima and minima of the resonant, perturbed 2-cycles for the 2-periodic LPA model with ML parameters (4.21) as a function of the relative amplitude α of the habitat oscillation. The dashed lines are the maxima and minima of the attenuant, perturbed 2-cycles. These dashed lines disappear at approximately $\alpha = 0.45$ due to a (reverse) saddle-node bifurcation with the 2-cycles that perturb from the unstable equilibrium (not shown). [Reprinted from [**33**], with permission from Springer.]

LPA model (namely the attenuant cycle in Figure 31(b)) has dynamic characteristics that do not seem biologically feasible with regard to the synchronization of the life cycle oscillations with those of the habitat. Will beetle cultures really exhibit multiple attractor dynamics with small amplitude oscillations in habitat volume? Or is this prediction just a spurious prediction of an overly simplified mathematical model?

In [**33**] there appears a report and analysis of an experiment carried out to test the multiple attractor prediction implied by Figure 31(b). The highlights of that analysis are as follows. Replicated cultures of *T. castaneum* were grown in 2-periodic fluctuating habitats with $\alpha = 0.4$ and 0.6 as well as the constant habitat case $\alpha = 0$ (as a control). For the (model predicted) multiple attractor case at $\alpha = 0.4$, one set of cultures (with replicates) initiated in the predicted basin of attraction of the resonant 2-cycle and another set (with replicates) initiated in the predicted basin of the attenuant 2-cycle[5].

Beside resonance and attenuance, notable characteristics of the predicted 2-cycles include larva oscillations that, in the resonance case, are large and out-of-phase with the oscillations in the habitat volume V. In the attenuant case, the oscillations in larvae numbers are suppressed and in-phase with the habitat volume.

[5]The proper phase space in which to view the dynamics is that of the composite map. Fixed points of the composite correspond to 2-cycles and their basins of attraction are those of the 2-cycles.

See Figure 32(a) for the model predicted dynamics of the larval stages. Figure 32(b) shows plots of the larval data from selected experimental replicates for each basin at attraction. These plots exhibit these predicted characteristics of the two different 2-cycle attractors.

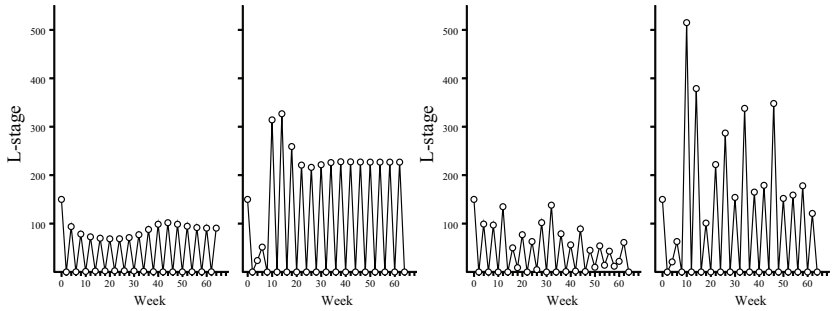

FIGURE 32. (a) The plots show the L-stage of two model orbits that approach the two stable 2-cycles predicted by the 2-periodic LPA model (4.17) in the experiment reported in [**33**]. In that experiment the model parameter values were $b = 6.598$, $\mu_l = 0.2055$, $\mu_a = 0.1000$, $c_{ea} = 0.01000$, $c_{el} = 0.1000$, $c_{pa} = 0.004700$ and $\alpha = 0.4000$. The graph on the left is for the initial condition $(L(0), P(0), A(0)) = (150, 0, 150)$, which lies in the basin of attraction of the attenuate 2-cycle. For this 2-cycle the L-stage oscillates in-phase with the oscillations in habitat volume V. The graph on the right is for the initial condition $(L(0), P(0), A(0)) = (150, 200, 150)$, which lies in the basin of attraction of the resonant 2-cycle. For this 2-cycle the L-stage oscillates out-of-phase with the oscillations in habitat volume V. (b) The plots of the L-stages of one experimental replicate for each initial conditions show the predicted oscillatory characteristics of the two different attractors in (a).

The multi-attractor experiment lasted longer than the 64 weeks shown in Figure 32. Figure 33(a) shows the L-stage of the attenuate 2-cycle data for the 140 weeks of the experiment. There is an startling occurrence: at week 66 the culture "jumps" to the resonant -cycle! A stochastic event apparently caused the population to hop into the basin of attraction of the resonant 2-cycle. This in fact occurred in all replicates started in the basin of attraction of the attenuant 2-cycle. Moreover, the reverse switch from the resonant cycle basin to the attenuant cycle basin never occurred.

It is interesting that a (environmental) stochastic version of the 2-periodic LPA model predicts this "basin jumping" phenomenon; see [**33**]. Thus, although the deterministic model predicts a multiple attractor dynamic, the stochastic version of the model predicts, in effect, a single "attractor". In 50,000 simulations of the stochastic version of the 2-periodic LPA model, with ML parameter estimates obtained from the experiment, all orbits starting from the experimental initial condition $(L(0), P(0), A(0)) = (150, 0, 150)$ lying in the attenuant 2-cycle basin of attraction had moved to the resonant 2-cycle's basin of attraction within 100 times steps. A histogram of the basin jump times appears in Figure 33(b). The mean basin jump

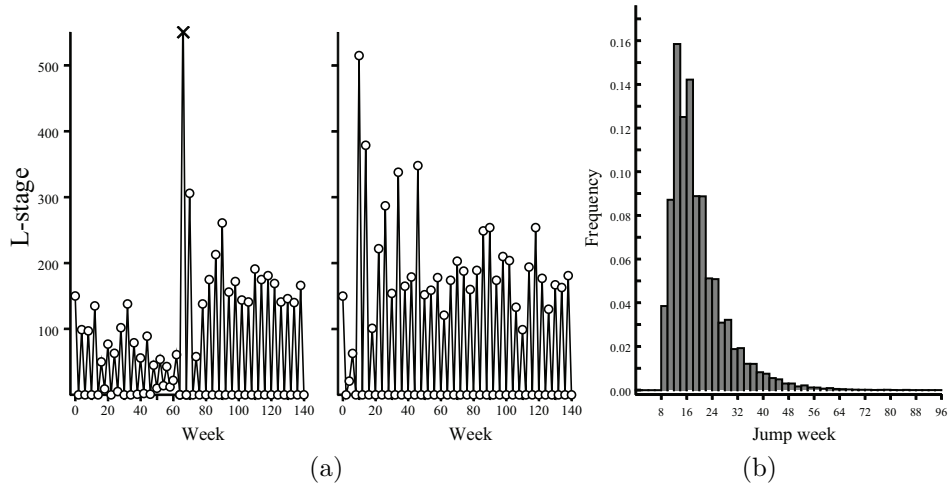

FIGURE 33. (a) The time series data shown in Figure 32(b) for 64 weeks is shown here for 140 weeks. The data appearing in the graph on the left abandons the dynamic pattern of the attenuant 2-cycle at week 66 and takes on that of the resonant 2-cycle. (b) The histogram shows the results of calculating the time at which each of 50,000 simulated orbits of the stochastic 2-periodic LPA model (with ML parameter estimates obtained from the experiment), starting from the initial condition $(L, P, A) = (150, 0, 150)$ lying in the attenuant 2-cycle basin of attraction, jumped into the basin of attraction of the resonant 2-cycles.

time in these simulations was 18.55 time steps. In the experiment, the replicate shown in Figures 31 and 32 is an unusual one in this regard. The other two replicates both jumped basins at week 22, which is quite close to the model predicted mean jump time.

A more detailed experimental study of attractor basin jumping, as well as the role of the unstable saddle 2-cycle that lies on the basin boundary, appears in [**33**]. In that study characteristics of the saddle 2-cycle, and its stable manifold, are also observed in the experimental data.

Thus, we have another example of the importance of stochastic events in data (even those collected from highly controlled experiments). To explain the observed patterns, it is not sufficient to consider deterministic model attractors alone, but transients and unstable invariant sets mixed together by stochasticity. For more on these issues see [**36**].

In summary, this lecture generalized the equilibrium theory presented in Lecture 2 to periodically forced matrix models. The results of an experiment conducted by Jillson [**38**], which exhibited a resonance effect, motivated this generalization. The theory and methods, when applied to a periodically forced version of the LPA model, provided an explanation for Jillson's observation. Furthermore, the study of this experimental result led to further theoretical insights into the effects that periodically fluctuating habitats can have on the dynamics of a population. These insights stimulated new experiments that corroborated some non-intuitive predictions concerning multiple attractors predicted by theoretical models.

EXERCISES

Exercise 16. Using the average recruitment rate μ as the bifurcation parameter, analyze the juvenile-adult model in Example 2.2

$$J(t+1) = cbA(t)e^{-A(t)}J(t) + be^{-A(t)}A(t)$$
$$A(t+1) = \tau_{21}J(t) + \tau_{22}A(t)$$

when the recruitment rate $b = \mu\left(1+\alpha\left(-1\right)^t\right)$ is 2-periodic. How does the bifurcation point μ_c depend on the amplitude α?

Exercise 17. Derive the variation of constants formula 4.3.

Exercise 18. (a) Find a formula for the initial condition $x(0)$ of the 2-cycle solutions of the discrete logistic

$$x(t+1) = b(t)\frac{1}{1+x(t)}x(t)$$

when $b(t)$ is a positive 2-periodic sequence. (b) Repeat (a) when $b(t)$ is 3-periodic. (c) By induction, repeat (a) when $b(t)$ is p-periodic.

Exercise 19. (a) By definition, a stable p-cycle $x_p(t)$ of a p-periodic equation $x(t+1) = f(t, x(t))$, $x_p(0)$ is a stable fixed point of the autonomous composite equation $y(t+1) = f^{(p-1)}(y(t)) \triangleq f(p-1, f(p-2, \ldots, f(1, f(0, x))))$. Show that this implies for each $\varepsilon > 0$ there exists a $\delta > 0$ such that $|x(0) - x_c(0)| < \delta$ implies $\Sigma_{i=t}^{t+p-1}|x(i) - x_c(i)| < \varepsilon$ for all $t \geq 0$. (b) By definition, a p-cycle $x_p(t)$ is an attractor if $x_p(0)$ is an attractor of the composite equation. Show that this implies there exists a $\delta > 0$ such that $|x(0) - x_c(0)| < \delta$ implies $\lim_{t\to+\infty}\Sigma_{i=t}^{t+p-1}|x(i) - x_c(i)| = 0$.

Exercise 20. Consider the scalar ($m = 1$) linear equation $x(t+1) = bx(t) + \tau x(t)$ where the per capita birth rate $b > 0$ and the survivorship rate satisfies $0 \leq \tau < 1$. The extinction equation $x = 0$ is stable if $b > 1 - \tau$ and unstable if $b < 1 - \tau$. The critical bifurcation value of the birth rate is $b_{cr} = 1 - \tau$. Suppose the birth rate oscillates with period 2, relative amplitude α ($0 \leq \alpha < 1$) and mean $b > 0$ and replace b in the equation by $b\left(1+\alpha\left(-1\right)^t\right)$. Find the critical bifurcation value b_c of the mean birth rate b. Treating $b_c = b_c(\alpha)$ as a function of the amplitude α show $b_c(\alpha) > b_c(0) = 1 - \tau$. Interpret this result biologically.

Exercise 21. The extinction equation of the linear, juvenile-adult, semelparous model

$$\begin{pmatrix} J(t+1) \\ A(t+1) \end{pmatrix} = \begin{pmatrix} 0 & b \\ \tau & 0 \end{pmatrix}\begin{pmatrix} J(t) \\ A(t) \end{pmatrix}$$

is stable if $b < 1/\tau$ and is unstable if $b > 1/\tau$. Thus, the critical bifurcation value is $b_c = 1/\tau$. Suppose the birth rate oscillates with period 2 and replace b by $b\left(1+\alpha\left(-1\right)^t\right)$ where b is now the mean birth rate and α is the amplitude ($0 < \alpha < 1$). Find the critical bifurcation value b_c of the mean birth rate b. Treating $b_c = b_c(\alpha)$ as a function of the amplitude α show $b_c(\alpha) < b_c(0) = 1/\tau$. Interpret this result biologically.

LECTURE 5

Competitive Interactions

The general theory of structured population dynamics presented in Lectures 1, 2, and 4, and the case studies in Lecture 3 deal with populations of a single species. Matrix models of the form (1.7) can also describe interactions of two or more structured species when the projection matrix $P = T + F$ of each species depends on the state variables of the other species [**4**]. Classical classifications of ecological interactions, which historically are based on models without structuring, are limited to a small number of basic types: mainly, competition, predation, and mutualism (symbiosis). Structured models, on the other hand, allow for more complicated interactions that take into account changes in the relationships and interactions among species as individuals pass through life cycle stages. For example, two species might compete as juveniles, but as adults one species might become a prey of the other. See [**66**] for biological examples of mixed interactions of these kinds. Matrix models for mixed ecological interactions remain largely unexplored.

Laboratory experiments by G. F. Gause (using paramecia) and T. Park (using flour beetles) helped establish the competitive exclusion principle, which during the first half of the twentieth century was hotly debated. The fundamental concept underlying this principle is that in order to coexist two species must find a way to decrease their competition for resources. Competition can take many forms, ranging from direct confrontations and conflicts among individuals to more indirect struggles for access to resources of limited availability. This principle finds expression in the notions of ecological niche and limiting similarity among species. The principles of competitive exclusion and ecological niche are so dogmatic today that they often are not explicitly stated in ecological studies and are instead implicitly assumed in force. It is well-known that the famous Lotka-Volterra differential equations played a significant role in the historical development of competition theory and in the formulation of the competitive exclusion principle. It is less well known that discrete time models also played an important role.

In his experimental studies of the competitive exclusion principle, T. Park collaborated with P. H. Leslie and J. C. Gower in formulating a mathematical model for two competing species. To interpret and explain Park's experimental data they used the system of difference equations

$$
\begin{aligned}
x(t+1) &= b_1 \frac{1}{1 + c_{11}x(t) + c_{12}y(t)} x(t) \\
y(t+1) &= b_2 \frac{1}{1 + c_{21}x(t) + c_{22}y(t)} y(t)
\end{aligned}
\tag{5.1}
$$

to account for the dynamics of two competing species. In their application of this *Leslie-Gower competition model* to Park's experimental data, x and y are densities of adults from two different species of *Tribolium*. This model is an extension of

the discrete logistic model and is naturally regarded as the discrete analog of the Lotka-Volterra differential equation model.

The competition model (5.1) has been thoroughly analyzed mathematically (it defines what is called a monotone flow [**64**]) and it turns out that its dynamic possibilities are exactly the same as those of the Lotka-Volterra differential model [**64, 12**]. Only four phase portraits are possible, as shown in Figure 34. The asymptotic dynamics are only equilibrium dynamics. Both species survive (i.e., the positive equilibrium is attracting) if and only if $c_{12}c_{21} < c_{11}c_{22}$, that is to say, if competition between the species, as measured by the product $c_{12}c_{21}$ of the interspecific competition coefficients, is small (relative to intraspecific competition as measured by the product $c_{11}c_{22}$).

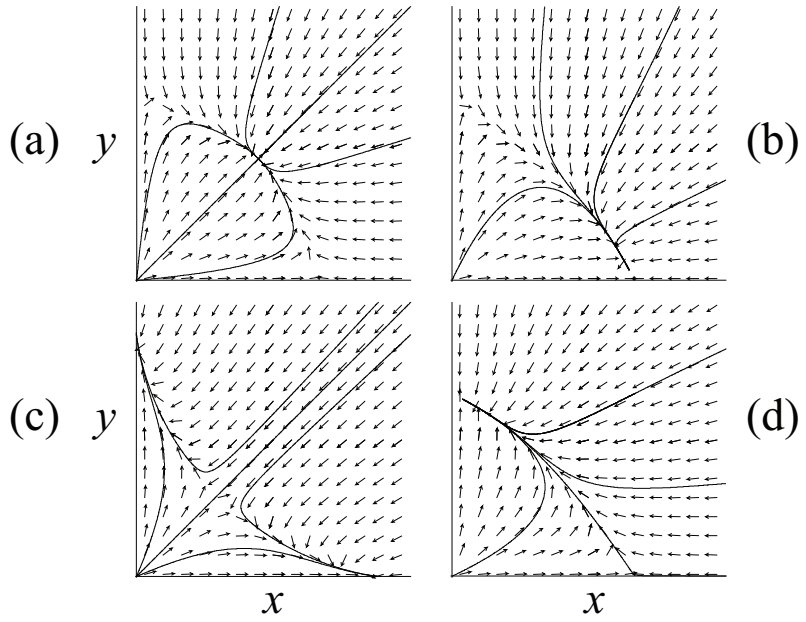

FIGURE 34. The discrete Leslie-Gower competition model (5.1) has the same dynamic possibilities as the classic Lotka-Volterra competition system of differential equations. (a) If interspecific competition is weak then there is a globally attracting positive (coexistence) equilibrium. If one interspecific competition coefficient is sufficiently large, then an exclusion equilibrium on a coordinate axis is globally attracting, as shown in (b) and (d). If both interspecific competition coefficients are sufficiently large, then as shown in (c) competitive exclusion occurs and which species wins depends on initial conditions (except for the stable manifold of the saddle equilibrium). It is this saddle case that played a prominent role in Park's *Tribolium* experiments.

The Leslie-Gower model does not model structured species, despite the fact that it was derived and utilized in the analysis of experiments with insects that have significant life cycle stages (flour beetles). What happens to the competition theory based on the Lotka-Volterra phase portraits in Figure 34 when one or both species are given, say, juvenile stages in the model equations? It is still true that

strong competitive interactions as measured by large competition coefficients will lead to the exclusion of one of the species?

For a study of the Leslie-Gower model when one species of the two species has a juvenile stage in the model see [**12, 13**]. Since (as pointed out by Darwin) competition is most likely strongest among similar species, of more interest would be a Leslie-Gower model extended so as to include juvenile stages for both species:

$$
\begin{aligned}
J(t+1) &= b_A \frac{1}{1+A(t)+c_j j(t)} A(t) \\
A(t+1) &= (1-\mu_J)J(t) + (1-\mu_A)A(t) \\
& \\
j(t+1) &= b_a \frac{1}{1+a(t)+c_J J(t)} a(t) \\
a(t+1) &= (1-\mu_j)j(t) + (1-\mu_a)a(t).
\end{aligned}
\tag{5.2}
$$

In this model the competition between the (upper case and the lower case distinguished) species occurs between the juvenile classes J and j and results in a reduction in juvenile recruitment. The intensity of the interspecific competition is measured by the magnitude of the competition coefficients c_j, $c_J \geq 0$.

In the absences of one species the dynamics of the other species are governed by the juvenile-adult version

$$
\begin{aligned}
x_1(t+1) &= b \frac{1}{1+x_2(t)} x_2(t) \\
x_2(t+1) &= (1-\mu_1)x_1(t) + (1-\mu_2)x_2(t)
\end{aligned}
\tag{5.3}
$$

of the discrete logistic equation. This equation has a locally asymptotically stable positive equilibrium

$$
\begin{pmatrix} x_1 \\ x_2 \end{pmatrix} \triangleq \begin{pmatrix} \frac{(1-\mu_1)b-\mu_2}{1-\mu_1} \\ \frac{(1-\mu_1)b-\mu_2}{\mu_2} \end{pmatrix}
$$

provided the inherent net reproductive number exceeds 1: that is,

$$
\frac{b(1-\mu_1)}{\mu_2} > 1.
$$

Therefore, both species of the competition model (5.2) have, in the absence of the other species, stable positive equilibria

$$
\begin{pmatrix} J_e^0 \\ A_e^0 \end{pmatrix} \triangleq \begin{pmatrix} \frac{\mu_A}{1-\mu_J}\left(n_J^0 - 1\right) \\ n_J^0 - 1 \end{pmatrix}, \qquad \begin{pmatrix} j_e^0 \\ a_e^0 \end{pmatrix} \triangleq \begin{pmatrix} \frac{\mu_a}{1-\mu_j}\left(n_j^0 - 1\right) \\ n_j^0 - 1 \end{pmatrix}
$$

provided

$$
n_J^0 \triangleq b_A \frac{1-\mu_J}{\mu_A} > 1, \qquad n_j^0 \triangleq b_a \frac{1-\mu_j}{\mu_a} > 1. \tag{5.4}
$$

We assume these two inequalities hold. The quantities n_J^0 and n_j^0 are the inherent net reproductive numbers of the two species in the absence of competition. These

equilibria give rise to the *exclusion equilibria*

$$\begin{pmatrix} J_e^0 \\ A_e^0 \\ 0 \\ 0 \end{pmatrix} \triangleq \begin{pmatrix} \frac{\mu_A}{1-\mu_J}\left(n_J^0 - 1\right) \\ n_J^0 - 1 \\ 0 \\ 0 \end{pmatrix} \tag{5.5}$$

$$\begin{pmatrix} 0 \\ 0 \\ j_e^0 \\ a_e^0 \end{pmatrix} \triangleq \begin{pmatrix} 0 \\ 0 \\ \frac{\mu_a}{1-\mu_j}\left(n_j^0 - 1\right) \\ n_j^0 - 1 \end{pmatrix} \tag{5.6}$$

of the competition model (5.2). If the first of these equilibria is locally asymptotically stable, then the (j, a) species cannot survive (invade the (J, A) species) when starting from small initial numbers. Similarly, if the second of these equilibria is locally asymptotically stable, then the (J, A) species cannot survive (invade the (j, a) species) when starting from small initial numbers.

Conditions for the local stability of the exclusion equilibria (5.5) and (5.6) derive from an investigation of the eigenvalues of the Jacobian of the system (5.2) evaluated at these equilibria. These Jacobians are 4×4 matrices and the analysis seems daunting until we notice that these matrices are block diagonal. For example, the Jacobian at the exclusion equilibrium (5.5) has the form

$$\begin{pmatrix} B_1 & B_2 \\ 0 & B_3 \end{pmatrix}$$

and therefore its eigenvalues are those of the two 2×2 matrices B_1 and B_3. It turns out that B_1 is the Jacobian of the juvenile-adult, logistic (5.3) that governs the dynamics of the (J, A) species in the absence of the (j, a) species. By assumption (5.4) this matrix has eigenvalues of magnitude less than 1. Therefore, the stability of the exclusion equilibrium of the competitive system is determined by the eigenvalues of the matrix

$$B_3 = \begin{pmatrix} 0 & b_a \frac{1}{1+c_J J_e^0} \\ 1-\mu_j & 1-\mu_a \end{pmatrix}.$$

The eigenvalues of this matrix have magnitude less than 1 if (and only if)

$$n_j \triangleq b_a \frac{1-\mu_j}{\mu_a} \frac{1}{1+c_J J_e^0} < 1.$$

The number n_j is the inherent net reproductive number of species (j, a) when species (J, A) is at its inherent equilibrium (J_e^0, A_e^0). If $n_j > 1$ the exclusion equilibrium is unstable, which suggests that the species (j, a) will not go extinct and can successfully invade the species (J, A).

The loss of stability of the exclusion equilibrium is consistent with a transcritical bifurcation at $n_j = 1$ from the exclusion equilibrium (5.5). In this example, we can verify this bifurcation by algebraically solving the equilibrium equations

$$\begin{aligned} J &= b_A \tfrac{1}{1+A+c_j j} A \\ A &= (1-\mu_J)J + (1-\mu_A)A \\ j &= b_a \tfrac{1}{1+a+c_J J} a \\ a &= (1-\mu_j)j + (1-\mu_a)a \end{aligned}$$

for

$$\begin{pmatrix} J_e \\ A_e \\ j_e \\ a_e \end{pmatrix} = \begin{pmatrix} \left(\left(n_J^0-1\right)\frac{1-\mu_j}{\mu_a} - \left(n_j^0-1\right)c_j\right)\Delta^{-1} \\ \frac{1-\mu_J}{\mu_A}\left(\left(n_J^0-1\right)\frac{1-\mu_j}{\mu_a} - \left(n_j^0-1\right)c_j\right)\Delta^{-1} \\ \left(n_j-1\right)\frac{n_j^0}{n_j}\frac{1-\mu_J}{\mu_A}\Delta^{-1} \\ \left(n_j-1\right)\frac{n_j^0}{n_j}\frac{1-\mu_j}{\mu_a}\frac{1-\mu_J}{\mu_A}\Delta^{-1} \end{pmatrix} \tag{5.7}$$

where

$$\Delta \triangleq \frac{1-\mu_J}{\mu_A}\frac{1-\mu_j}{\mu_a} - c_j c_J.$$

The j_e and a_e components of this equilibrium vanish when $n_j = 1$, at which point a calculation shows $J_e = J_e^0$ and $A_e = A_e^0$. In other words, this equilibrium bifurcates from the exclusion equilibrium (5.5) at $n_j = 1$. For n_j near 1, the components J_e and A_e remain positive while the sign of the j_e and a_e components is the same as the sign of $(n_j - 1)/\Delta$. Thus, a supercritical bifurcation of positive equilibria (coexistence equilibria) occurs if $\Delta > 0$ and a subcritical bifurcation occurs if $\Delta < 0$. The inequality $\Delta > 0$ means that competition is weak in the sense that the competition coefficients are small enough; $\Delta < 0$ means competition is strong.

The exclusion equilibrium (5.5) loses stability as n_j increases through 1. It follows by the exchange of stability property of transcritical bifurcations (see [**4**]) that the coexistence equilibria are stable when they bifurcate supercritically ($\Delta > 0$) and unstable when they bifurcate subcritically ($\Delta < 0$). Thus, at low population levels the species (j, a) can successfully invade species (J, A) if the competition between the species is not strong and if the inherent net reproductive number of (j, a) at the equilibrium level of (J, A) exceeds 1.

The model scenario is symmetric and analogous conclusions hold for the invasion of (j, a) by (J, A).

The analysis of the juvenile-adult, Leslie-Gower model (5.2) illustrates general theorems that guarantee the bifurcation of a coexistence equilibria from the equilibrium of a resident as an appropriate parameter varies. For example, consider two matrix models of the form

$$\begin{aligned} x(t+1) &= \left(F_1(x(t), y(t)) + T_1(x(t), y(t))\right) y(t) \\ y(t+1) &= \left(F_2(x(t), y(t)) + T_2(x(t), y(t))\right) y(t) \end{aligned} \tag{5.8}$$

in which F_i and T_i are the fertility and transition matrices of two species x and y. The two species do not necessarily have the same number of classes (i.e., x is an m_1-dimensional vector, y is an m_2-dimensional vector and it is allowed that $m_1 \neq m_2$). Consider y as the resident species in a habitat and assume it has a stable equilibrium $y_e > 0$ in the absence of species x. For notational convenience define

$$P(x, y) \triangleq F_2(x, y) + T_2(x, y)$$

Then the equilibrium y_e satisfies the equation

$$y = P(0, y)y.$$

The equilibrium equations for the interacting system (5.8) are

$$x = (F_1(x,y) + T_1(x,y))\, y$$
$$y = P(x,y)y.$$

Under sufficient smoothness assumptions (say, P is $k \geq 1$ times continuously differentiable in x and y) the Implicit Function Theorem applies to the second equilibrium equation and results in a solution $y = \xi(x)$, $\xi(0) = y_e$, provided $I - P_y(0, y_e)$ is nonsingular (here P_y is the Jacobian of P with respect to y). This solution $\xi(x)$ is defined for x in a neighborhood of $0 \in R^{m_1}$ and is k times continuously differentiable in x. A substitution of $\xi(x)$ into the first equilibrium equation yields the algebraic matrix equation

$$x = (F(x) + T(x))\, x$$

for x where $F(x) \triangleq F_1(x, \xi(x))$ and $T(x) \triangleq T_1(x, \xi(x))$ are smooth functions in a neighborhood of $x = 0$. We can apply the bifurcation methods of Lectures 1 and 2 to this equation. To do this write $F(x) = n\Phi(x)$ where n is the inherent net reproductive of species x when species y is at equilibrium y_e. Provided the necessary assumptions on F and T hold, the methods and results of Lectures 1 and 2 imply the bifurcation of a branch of positive equilibria $(x, y(x))$ near $(0, y_e)$ at $n = 1$. With this approach there is a proviso, however. The implicit function theorem provides only a local solution $y(x)$, i.e., a solution for x near 0, and as a result we obtain only a local bifurcation at $n = 1$ (a bifurcating branch whose existence is guaranteed only near the bifurcation points $(0, y_e)$). For details relating the direction of bifurcation and stability properties of the bifurcating branch for multi-species matrix models see [**4**].

This equilibrium bifurcation result applies to the general two species matrix model (5.8). In specific applications, one often has in mind a model of a specific type of interaction based on classical classifications: for example, a competition or predator-prey model. However, the general bifurcation result applies to models that describe any kinds of interaction, including mixed types such as those mentioned above.

On the other hand, for one important class of matrix models it is possible to devise a classification scheme, based on the classical types of interactions, in terms of each species' net reproductive number. Suppose that the dependencies of the fertility and transition matrices for both models depend on two weighted population sizes

$$p_1(t) = \sum_{i=1}^{m_1} \omega_i x_i(t), \quad p_2(t) = \sum_{i=1}^{m_2} \chi_i y_i(t)$$

($\omega_i, \chi_i \geq 0$, $\Sigma_i \omega_i \neq 0$), so that (5.8) becomes

$$x(t+1) = (F_1(p_1(t), p_2(t)) + T_1(p_1(t), p_2(t)))\, x(t)$$
$$y(t+1) = (F_2(p_1(t), p_2(t)) + T_2(p_1(t), p_2(t)))\, y(t). \tag{5.9}$$

Under assumptions (2.2) the species have net reproductive numbers $n_1 = n_1(p_1, p_2)$ and $n_2 = n_2(p_1, p_2)$ that depend on p_1 and p_2. Both reproductive numbers equal 1

at an equilibrium

$$n_1(p_1, p_2) = 1$$
$$n_2(p_1, p_2) = 1$$

where p_1 and p_2 are the weighted population sizes at equilibrium.

Let n be the *inherent* net reproductive number of species y at the *extinction* equilibrium $p_1 = p_1^e > 0$, $p_2 = 0$ and write $n_2(p_1, p_2) = n\nu_2(p_1, p_2)$ where $\nu\,(p_1^e, 0) = 1$. Then along the branch of equilibria bifurcating from this extinction equilibrium we have the identities

$$n_1(p_1, p_2) = 1$$
$$n\nu_2(p_1, p_2) = 1.$$

From these invariants along the bifurcating continuum of positive equilibria, we can calculate conditions that determine the direction of bifurcation (i.e., whether $n > 1$ or $n < 1$ near the bifurcation point). When the Implicit Function Theorem is applied to the first equation, we obtain $p_1 = p_1(p_2)$, $p_1(0) = p_1^e$, provided the partial derivative $\partial n_1/\partial p_2$ evaluated at $(p_1, p_2) = (p_1^e, 0)$ is nonzero. Denote this derivative by $\partial_2 n_1^0 \neq 0$. Then the second invariant near bifurcation becomes

$$n\nu_2(p_1(p_2), p_2) = 1. \tag{5.10}$$

The bifurcation will be supercritical if $\nu_2(p_1(p_2), p_2)$ is decreasing in p_2 at $p_2 = 0$ and will be subcritical if it is increasing. For example, the bifurcation is supercritical (stable) if

$$\partial_1 \nu_1^0 p_1'(0) + \partial_2 \nu_2^0 < 0$$

which, since $p_1'(0) = -\partial_2 n_1^0/\partial_1 n_1^0$ (by implicit differentiation of (5.10)), is the same as

$$\det M > 0, \quad M \doteq \begin{bmatrix} \partial_1 n_1^0 & \partial_2 n_1^0 \\ \partial_1 n_2^0 & \partial_2 n_2^0 \end{bmatrix}.$$

If $\det M < 0$, then the bifurcation is subcritical (unstable).

Using the net reproductive numbers for the model (5.9) we can define competition and predator-prey interactions according to the inequalities:

$$\begin{array}{lll} \text{predator-prey:} & \partial_2 n_1(p_1, p_2) > 0, & \partial_1 n_2(p_1, p_2) < 0 \\ \text{competition:} & \partial_2 n_1(p_1, p_2) < 0, & \partial_1 n_2(p_1, p_2) < 0 \end{array}$$

If each population has self density regulation, then

$$\partial_1 n_1(p_1, p_2) < 0, \quad \partial_2 n_2(p_1, p_2) < 0.$$

Under this assumption, $\det M > 0$ for a predator-prey interaction and the bifurcation is supercritical (stable). For a competitive interaction the bifurcation is supercritical (species y can invade the resident x) if

$$\det M = \partial_1 n_1^0 \partial_2 n_2^0 - \partial_2 n_1^0 \partial_1 n_2^0 > 0$$

i.e., interspecific competition is weaker that intraspecific competition as measured by the products $\partial_2 n_1^0 \partial_1 n_2^0$ and $\partial_1 n_1^0 \partial_2 n_2^0$ respectively. The bifurcation is subcritical (species y cannot invade the resident x) if the reverse inequality holds, i.e., if interspecific competition is strong.

While this analysis provides a nice classification scheme for models of the type (5.9), not all two species matrix models are of this type. The competition model (5.2), for example, is not.

Historically competition theory is almost exclusively an equilibrium theory. For structured populations, however, the possibility of non-equilibrium dynamics is high and we are led to wonder in what way and to what extent the competitive exclusion principle (founded on equilibrium dynamics) holds true in non-equilibrium scenarios.

As a tractable example, consider the juvenile-adult competition model (5.2) when adult survivorships are equal to 0 :

$$\begin{aligned} J(t+1) &= b_A \frac{1}{1 + A(t) + c_j j(t)} A(t) \\ A(t+1) &= (1-\mu_J) J(t) \end{aligned}$$

(5.11)

$$\begin{aligned} j(t+1) &= b_a \frac{1}{1 + a(t) + c_J J(t)} a(t) \\ a(t+1) &= (1-\mu_j) j(t). \end{aligned}$$

Biologically this model concerns two competing semelparous populations (both populations in model (5.2) are iteroparous when μ_A and $\mu_a < 1$). It was shown above that the exclusion equilibrium (5.5) is locally stable if $n_j < 1$. This inequality is equivalent to

$$c_J > (1-\mu_J)\, \frac{n_j^0 - 1}{n_J^0 - 1}.$$

Thus, if the interspecific competition coefficient c_J is sufficiently large, then species (j, a) cannot invade species (J, A) when starting at low population density. By a symmetric analysis the exclusion equilibrium (5.6) is locally stable if

$$c_j > (1-\mu_j)\, \frac{n_J^0 - 1}{n_j^0 - 1}.$$

If the interspecific competition coefficient c_j is sufficiently large, then species (J, A) cannot invade species (j, a) when starting at low population density.

It follows that if both competition coefficients are large, then both exclusion equilibrium are locally stable. Moreover, in this case the coexistence equilibrium (5.7) is positive. These facts are commensurate with the saddle case in the Leslie-Gower (Lotka-Volterra) competition scheme shown in Figure 34(c). It is proved in [**14**] that the coexistence equilibrium (5.7) is a saddle in this case.

Unlike the Leslie-Gower model (and the Lotka-Volterra differential model), however, equilibrium dynamics are not the whole story for the juvenile-adult competition model (5.11).

The single species, semelparous juvenile-adult model

$$\begin{aligned} x_1(t+1) &= b \frac{1}{1 + x_2(t)} x_2(t) \\ x_2(t+1) &= (1-\mu_1) x_1(t) \end{aligned} \tag{5.12}$$

has a non-negative 2-cycle

$$\begin{pmatrix} x_1(0) \\ x_2(0) \end{pmatrix} = \begin{pmatrix} 0 \\ b(1-\mu_1)-1 \end{pmatrix}, \quad \begin{pmatrix} x_1(0) \\ x_2(0) \end{pmatrix} = \begin{pmatrix} \frac{b(1-\mu_1)-1}{1-\mu_1} \\ 0 \end{pmatrix}$$

when the inherent net reproductive number $b(1-\mu_1)$ exceeds 1. This cycle is called *synchronous* because the juvenile and adult stages are synchronized so as to never appear together (the generations are non-overlapping) [**8, 9**]. This cycle gives rise to *two exclusion 2-cycles* of the competition model (5.11)

$$\begin{pmatrix} J(0) \\ A(0) \\ j(0) \\ a(0) \end{pmatrix} = \begin{pmatrix} 0 \\ n_J^0 - 1 \\ 0 \\ 0 \end{pmatrix}, \quad \begin{pmatrix} J(1) \\ A(1) \\ j(1) \\ a(1) \end{pmatrix} = \begin{pmatrix} \frac{n_J^0-1}{1-\mu_J} \\ 0 \\ 0 \\ 0 \end{pmatrix}$$

(5.13)

$$\begin{pmatrix} J(0) \\ A(0) \\ j(0) \\ a(0) \end{pmatrix} = \begin{pmatrix} 0 \\ 0 \\ 0 \\ n_j^0 - 1 \end{pmatrix}, \quad \begin{pmatrix} J(1) \\ A(1) \\ j(1) \\ a(1) \end{pmatrix} = \begin{pmatrix} 0 \\ 0 \\ \frac{n_j^0-1}{1-\mu_j} \\ 0 \end{pmatrix}$$

when

$$n_J^0 = b_A\,(1-\mu_J) > 1, \qquad n_j^0 = b_a\,(1-\mu_j) > 1.$$

There are also two *coexistence 2-cycles*

$$\begin{pmatrix} J(0) \\ A(0) \\ j(0) \\ a(0) \end{pmatrix} = \begin{pmatrix} 0 \\ n_J^0 - 1 \\ 0 \\ n_j^0 - 1 \end{pmatrix}, \quad \begin{pmatrix} J(1) \\ A(1) \\ j(1) \\ a(1) \end{pmatrix} = \begin{pmatrix} \frac{n_J^0-1}{1-\mu_J} \\ 0 \\ \frac{n_j^0-1}{1-\mu_j} \\ 0 \end{pmatrix} \tag{5.14}$$

$$\begin{pmatrix} J(0) \\ A(0) \\ j(0) \\ a(0) \end{pmatrix} = \begin{pmatrix} 0 \\ \frac{\left(n_J^0-1\right)c_J - c_j(n_j^0-1)(1-\mu_J)}{c_J - c_j(1-\mu_j)(1-\mu_J)} \\ (1-\mu_j)\,\frac{\left(n_J^0-1\right)c_J - c_j(n_j^0-1)(1-\mu_J)}{c_J - c_j(1-\mu_j)(1-\mu_J)} \\ 0 \end{pmatrix}$$

(5.15)

$$\begin{pmatrix} J(1) \\ A(1) \\ j(1) \\ a(1) \end{pmatrix} = \begin{pmatrix} \frac{1}{1-\mu_J}\,\frac{\left(n_J^0-1\right)c_J - c_j(n_j^0-1)(1-\mu_J)}{c_J - c_j(1-\mu_j)(1-\mu_J)} \\ 0 \\ 0 \\ (1-\mu_J)\,(1-\mu_j)\,\frac{\left(n_J^0-1\right)c_J - c_j(n_j^0-1)(1-\mu_J)}{c_J - c_j(1-\mu_j)(1-\mu_J)} \end{pmatrix}.$$

By the linearization principle we can study the stability of a 2-cycle by examining the eigenvalues of the Jacobian of the composite map (which turns out to equal the product of the Jacobians of the map evaluated at $t = 0$ and $t = 1$). A computer algebra program makes tractable such a stability analysis of the 2-cycles (5.13), (5.14) and (5.15). The results imply that all 2-cycles are unstable, except the

coexistence 2-cycle (5.14) which is stable if the competition coefficients c_J and c_j are sufficiently *large*, specifically if the competition coefficients satisfy the inequalities

$$c_J > (1-\mu_J)\,\frac{n_j^0-1}{n_J^0-1}, \qquad c_j > (1-\mu_j)\,\frac{n_J^0-1}{n_j^0-1}. \tag{5.16}$$

Note that these are precisely the inequalities that imply both exclusion equilibria are stable. If one of the inequalities is reversed the 2-cycle is unstable.

Thus, in model (5.11) coexistence is possible in a non-equilibrium (2-cycle) way when interspecific competition is strong enough. When inequalities (5.16) hold there are three locally stable attractors, the two exclusion equilibria and a coexistence 2-cycle. See Figure 35.

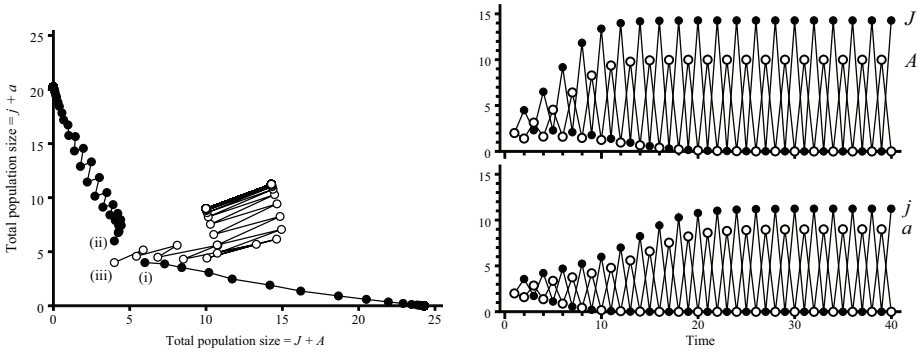

FIGURE 35. (a) The total population sizes of three orbits of the semelparous juvenile-adult, Leslie-Gower model (5.11) with different initial conditions that lead to three different asymptotic outcomes. The model parameters are $c_j = c_J = 2$, $\mu_J = 0.3$, $\mu_j = 0.2$, $n_J = 11$, $n_j = 10$ ($b_A = 110/7 \approx 15.71, b = 100/8 \approx 12.50$). Initial conditions (i) $(J, A, j, a) = (4, 2, 2, 2)$ and (ii) $(J, A, j, a) = (2, 2, 4, 2)$ lead to competitive exclusion, with species (J, A) winning in the first case and (j, a) winning in the second case. Initial condition (iii) $(J, A, j, a) = (2, 2, 2, 2)$ leads to coexistence in a 2-cycle. (b) The coexistence 2-cycle is synchronous in that the juvenile and adult stages do not overlap.

In this model the fact that increased competition intensity can lead to coexistence seemingly goes against the competitive exclusion principle, which asserts interspecific competition must be avoided if two species are to coexist. In the case of the competition model (5.11) there is a reconciliation, however. Note that when oscillating according to the coexistence 2-cycle (5.14) the two species actually avoid competition altogether because of the synchrony of the oscillations in the life cycle stages. In this way the two species coexist even when the intensity of (potential) competition is high.

Another interesting observation concerning the competition model (5.11) is that the avoidance 2-cycle is available for all parameter values, including those for which there is a stable coexistence equilibrium. This fact does not support a competition principle that asserts species strive (or are selected) to avoid competition. In this case, the species "choose" to compete at equilibrium rather than avoid competition altogether in a 2-cycle.

The competition model (5.11) is only a "toy" model. However, one bit of evidence for non-equilibrium coexistence under increased competitive intensity occurs in *Tribolium* species. In T. Park's famous competition experiments, one example of two species coexistence unexpectedly occurred and a speculative explanation based on a competition version of the LPA model (3.11) is given by Edmunds et al. [**23**]. Their explanation is based on the existence of robust coexistence 2-cycles when realistic parameter values are used and interspecific cannibalistic coefficients sufficiently large. It is suggestive that Park in fact reported increased cannibalistic voracity in his experiments. The competition LPA model is a $m = 6$ dimensional system for which extensive analysis is intractable (although a basic theory, particularly of the exclusion equilibria, is worked out in [**22**]). Numerical studies show, however, that the model can exhibit very exotic dynamics and coexistence non-equilibrium attractors (even multiple coexistence attractors).

Although derived in application to a specific experimental system, the LPA model is a rather generic, three life cycle stage model, not uncommon in biological species (especially insects). A competition theory based on that model is far richer than that derived from the limited equilibrium dynamic possibilities of Lotka-Volterra type models. To what extent these complicated dynamics necessitates a modification of classical competition tenets, or to what extent they can be reconciled with classical theory, remains an open question.

EXERCISES

Exercise 22. The system

$$\begin{aligned} J(t+1) &= b_1 \frac{1}{1 + A(t) + c_1 y(t)} A(t) \\ A(t+1) &= \tau J(t) \\ y(t+1) &= b_2 \frac{1}{1 + y(t) + c_2 J(t)} y(t) \\ b_1, b_2, c_1, c_2 > 0, &\qquad 0 < \tau < 1 \end{aligned}$$

is a version of the Leslie-Gower competition model in which one of the species has a juvenile stage. (a) Show the (J, A) species goes extinct if $n \triangleq \tau b_1 < 1$ and that the y species goes extinct if $b_2 < 1$. (b) Assume $b_1, b_2 > 1$. Find formulas for the two exclusion equilibria and determine conditions on the competition coefficients c_1 and c_2 under which each is locally asymptotically stable and conditions when each is unstable. Interpret your answers biologically. (c) Find a formula for a synchronous exclusion 2-cycle and determine a conditions on c_2 under which it is locally asymptotically stable and conditions when it is unstable.

Exercise 23. Find all equilibrium of the Leslie-Gower competition model (5.1)

$$\begin{aligned} x(t+1) &= b_1 \frac{1}{1 + c_{11} x(t) + c_{12} y(t)} x(t) \\ y(t+1) &= b_2 \frac{1}{1 + c_{21} x(t) + c_{22} y(t)} y(t). \end{aligned}$$

Show the extinction equilibrium $(x, y) = (0, , 0)$ is globally asymptotically stable if $b_1 < 1$ and $b_2 < 1$. Do a linearization stability analysis of the competitive exclusion equilibria $(x, 0)$ and $(0, y)$ and determine conditions on the competition

coefficients c_{ij} under which they are stable and conditions under which they are unstable. Under what conditions is there a positive (competitive coexistence) equilibrium $(x, y) > 0$? Under those conditions do a linearization stability analysis on the equilibrium and determine conditions on the competition coefficients c_{ij} under which they are stable and conditions under which they are unstable (difficult).

Bibliography

[1] H. Caswell, *Matrix Population Models: Construction, Analysis and Interpretation*, Second Edition, Sinauer Associates, Inc. Publishers, Sunderland, Massachusetts, 2001

[2] R. F. Costantino, J. M. Cushing, B. Dennis, R. A. Desharnais, S. M. Henson, Resonant population cycles in temporally fluctuating habitats, *Bulletin of Mathematical Biology* 60, No. 2 (1998), 247-275

[3] R. F. Costantino, Robert A. Desharnais, J. M. Cushing, Brian Dennis, S. M. Henson, and A. A. King, The flour beetle Tribolium as an effective tool of discovery, *Advances in Ecological Research*, Volume 37, 2005, 101-141

[4] J. M. Cushing, *An Introduction to Structured Population Dynamics*, CBMS-NSF Regional Conference Series in Applied Mathematics, Vol. 71, SIAM, Philadelphia, 1998

[5] J. M. Cushing, The LPA model, *Fields Institute Communications* 43 (2004), 29-552

[6] J. M. Cushing, Oscillatory population growth in periodic environments, *Theoretical Population Biology* 30 (1987), 289-308

[7] J. M. Cushing, Periodically forced nonlinear systems of difference equations, *Journal of Difference Equations and Applications* 3 (1998), 547-561

[8] J. M. Cushing, Cycle chains and the LPA model, *Journal of Difference Equations and Applications* 9, No. 7 (2003), 655-670

[9] J. M. Cushing, Nonlinear Semelparous Leslie Models, *Mathematical Biosciences and Engineering*, 3, No. 1 (2006), 17-36

[10] J. M. Cushing, R. F. Costantino, B. Dennis, R. A. Desharnais, and S. M. Henson, Nonlinear population dynamics: models, experiments, and data, *Journal of Theoretical Biology* 194, No. 1 (1998), 1-9

[11] J. M. Cushing, R. F. Costantino, Brian Dennis, R. A. Desharnais, S. M. Henson, *Chaos in Ecology: Experimental Nonlinear Dynamics*, Theoretical Ecology Series, Academic Press/Elsevier, San Diego, 2003

[12] J. M. Cushing, S. LeVarge, N. Chitnis and S. M. Henson, Some discrete competition models and the competitive exclusion principle, *Journal of Difference Equations and Applications* 10, No. 13-15 (2004), 1139-1151

[13] J. M. Cushing and S. LeVarge, Some Discrete Competition Models and the Principle of Competitive Exclusion, *Proceedings of the 9^{th} International Conference on Difference Equations and Applications*, World Scientific

[14] J. M. Cushing, S. M. Henson and L.-I. Roeger, A competition model for populations with juvenile-adult structure, Journal of Biological Dynamics 1, No. 2 (2007), 201-231

[15] J. M. Cushing and Z. Yicang, The net reproductive value and stability in matrix population models, *Natural Resource Modelling* 8 (1994), 297-333

[16] B. Dennis, Allee effects: population growth, critical density, and the chance of extinction. *Natural Resource Modeling* 3 (1989), 481-538

[17] B. Dennis and M. L. Taper, Density dependence in time series observations of natural populations: estimation and testing, *Ecological Monographs* 64 (1994), 205-224

[18] B. Dennis, R. A. Desharnais, J. M. Cushing and R. F. Costantino, Nonlinear demographic dynamics: mathematical models, statistical methods and biological experiments, *Ecological Monographs* 65, No. 3 (1995), 261-281

[19] B. Dennis, R. A. Desharnais, J. M. Cushing, and R. F. Costantino, Transitions in population dynamics: equilibria to periodic cycles to aperiodic cycles, *Journal of Animal Ecology* 66 (1997), 704-729

[20] B. Dennis, R. A. Desharnais, J. M. Cushing, S. M. Henson, and R. F. Costantino, Estimating chaos and complex dynamics in an insect population, *Ecological Monographs* 71, No. 2 (2001), 277-303

[21] R. A. Desharnais, R. F. Costantino, J. M. Cushing, S. M. Henson, B. Dennis, and A. A. King, Experimental confirmation of the scaling rule for demographic stochasticity, Ecological Letters 9 (2006), 537-547

[22] J. Edmunds, A Study of a Stage-Structured Model of Two Competing Species. Ph.D. dissertation, University of Arizona, Tucson, 2001

[23] J. Edmunds, J. M. Cushing, R. F. Costantino, S. M. Henson, B. Dennis and R. A. Desharnais, Park's *Tribolium* competition experiments: a non-equilibrium species coexistence hypothesis, *Journal of Animal Ecology* 72 (2003), 703-712

[24] S. N. Elaydi, *An Introduction to Difference Equations*, Springer-Verlag, New York, 1996

[25] S. Elaydi and R. J. Sacker, Global stability of periodic orbits of non-autonomous difference equations in population biology and the Cushing/Henson conjectures, *Proceedings of the 8th International Conference of Difference Equations and Applications*, pp. 113-126, Chapman & Hall/CRC, Boca Raton, FL, 2005

[26] F. R. Gantmacher, *The Theory of Matrices*, Volume 2, Chelsea Publishing Company, New York, 1960

[27] J. Guckenheimer and P. Holmes, *Nonlinear Oscillations, Dynamical Systems and Bifurcations of Vector Fields*, Springer-Verlag, Berlin, 1983

[28] M. P. Hassell, J. H. Lawton and R. M. May, Patterns of dynamical behavior in single species populations, *Journal of Animal Ecology* 45 (1976), 471-486

[29] S. M. Henson, Existence and stability of nontrivial periodic solutions of periodically forced discrete dynamical systems, *Journal of Difference Equations and Applications*, 2(1996), 315-331

[30] Multiple attractors and resonance in periodically forced populations models, *Physica D* 140 (2000), 33-49

[31] S. M. Henson and J. M. Cushing, The effect of periodic habitat fluctuations on a nonlinear insect population model, *Journal of Mathematical Biology* 36 (1997), 201-226

[32] S. M. Henson, J. M. Cushing, R. F. Costantino, B. Dennis, and R. A. Desharnais, Phase switching in biological population, *Proceedings of the Royal Society* 265 (22 November 1998), 2229-2234

[33] S. M. Henson, R. F. Costantino, J. M. Cushing, B. Dennis and R. A. Desharnais, Multiple attractors, saddles, and population dynamics in periodic habitats, *Bulletin of Mathematical Biology* 61 (1999), 1121-1149

[34] S. M. Henson, R. F. Costantino, J. M. Cushing, R. A. Desharnais, B. Dennis, and A. A. King, Lattice effects observed in chaotic dynamics of experimental populations, *Science* 294 (19 Oct 2001), 602-605

[35] S. M. Henson, A. A. King, R. F. Costantino, J. M. Cushing, B. Dennis, and R. A. Desharnais, Explaining and predicting patterns in stochastic population systems, *Proceedings of the Royal Society*, London B 270 (2003), 1549-1553

[36] S. M. Henson, J. R. Reilly, S. L. Robertson, M. C. Schu, E. W. Davis and J. M. Cushing, Predicting irregularities in population cycles, *SIAM Journal on Applied Dynamical Systems* 2, No. 2 (2003), 238-253

[37] R. A. Horn and C. R. Johnson, *Matrix Analysis*, Cambridge University Press, Cambridge, 1985

[38] D. Jillson, Insect populations respond to fluctuating environments, *Nature* 288 (1980), 699-700

[39] H. Keilhöfer, *Bifurcation Theory: An Introduction with Applications to PDEs*, Applied Mathematical Sciences 156, Springer, New York, 20041

[40] A. A. King, R. A. Desharnais, S. M. Henson, R. F. Costantino, J. M. Cushing, and B. Dennis, Random perturbations and lattice effects in chaotic population dynamics, *Science* 297, (27 September, 2002), p. 2163

[41] A. A. King, R. F. Costantino, J. M. Cushing, S. M. Henson, R. A. Desharnais, and B. Dennis, Anatomy of a chaotic attractor: subtle model-predicted patterns revealed in population data, *Proceedings of the National Academy of Sciences* 101, No. 1 (2003), 408-413

[42] V. L. Kocic, A note on the nonautonomous Bervton-Holt model, Journal of Difference Equations and Applications 11 (2005), 415-422

[43] Ryusuke Kon, A note on attenuant cycles of population models with periodic carrying capacity, *Journal of Difference Equations and Applications* 10, No. 8 (2004), 791-793
[44] Ryusuke Kon, Attenuant cycles of population models with periodic carrying capacity, *Journal of Difference Equations and Applications*, 11 (2005), 423-430
[45] R. Kon, Y. Saito and Y. Takeuchi, Permanence of single-species stage-structured models, *Journal of Mathematical Biology* 48 (2004), 515-528
[46] L. P. Lefkovitch, The study of population growth in organisms grouped by stage, *Biometrics* 21 (1965), 1-18
[47] P. H. Leslie, On the use of matrices in certain population mathematics, *Biometrika* 33 (1945), 183-212
[48] P. H. Leslie, Some further notes on the use of matrices in population mathematics, *Biometrika* 35 (1948), 213-245
[49] E. G. Lewis, On the generation and growth of a population, *Sankhya* 6 (1942), 93-96
[50] C.-K. Li and H. Schneider, Applications of Perron-Frobenius theory to population dynamics, *Journal of Mathematical Biology* 44 (2002), 450-462
[51] T. Y. Li and J. A. Yorke, Period three implies chaos, *American Mathematical Monthly* 82 (1975), 985-992
[52] R. M. May, Biological populations with nonoverlapping generations: stable points, stable cycles and chaos, *Science* 186 (1974), 645-647
[53] R. M. May, Simple mathematical models with very complicated dynamics, *Nature* 261 (1976), 459-467
[54] R. M. May, *Stability and Complexity in Model Ecosystems*, Princeton Landmarks in Biology, Princeton University Press, Princeton, New Jersey, 2001
[55] J. A. J. Metz and O. Diekmann, *The Dynamics of Physiologically Structured Populations,* Lecture Notes in Biomathematics, Volume 68, Springer-Verlag, Berlin, 1986
[56] L. D. Mueller and A. Joshi, *Stability in Model Populations*, Monographs in Population Biology 31, Princeton University Press, Princeton, New Jersey, 2000
[57] R. Pearl, *The Biology of Population Growth*, Alfred A. Knopf, New York, 1925
[58] J. N. Perry, R. H. Smith, I. P. Woiwod and D. R. Morse, *Chaos in Real Data: the Analysis of Nonlinear Dynamics from Short Ecological Time Series*, Kluwer Academic Publishers, Dordrecht, The Netherlands, 2000
[59] E. C. Pielou, *Mathematical Ecology*, Wiley-Interscience, John Wiley & Sons, New York, 1974
[60] E. C. Pielou, *Population and Community Ecology: Principles and Methods*, Gordon & Breach Science Publishers, New York, 1977
[61] P. H. Rabinowitz, Some global results for nonlinear eigenvalue problems, *Journal of Functional Analysis* 7, No 3 (1971), 487-513
[62] W. E. Ricker, Stock and recruitment, *Journal of the Fisheries Research Board of Canada* 11 (1954), 559-623
[63] R. C. Robinson, *An Introduction to Dynamical Systems: Continuous and Discrete*, Pearson/Prentice Hall, Upper Saddle River, New Jersey, 2004
[64] H. L. Smith, Planar competitive and cooperative difference equations, *Journal of Difference Equations and Applications* 3 (1998), 335-357
[65] H. Tong, *Nonlinear Time Series: A Dynamical System Approach*, Oxford University Press, Oxford, England, 1990
[66] E. E. Werner and J. F. Gilliam, The ontogenetic niche and species interactions in size-structured populations, *Ann. Rev. Ecol. Syst.* 15 (1984), 393-425
[67] S. Wiggins, *Introduction to Applied Nonlinear dynamical Systems and Chaos*, Texts in Applied Mathematics 2, Springer, New York 1990
[68] E. O. Wilson, *The Future of Life*, Alfred A. Knopf, New York, 2002